EXPERIMENTAL STUDIES OF ALKALINE BASALT GENESIS

by

John Douglas Adam

B. Sc. (Hons) (University of New England)

Submitted in Fulfilment of the Requirements
for the Degree of

Doctor of Philosophy

University of Tasmania
Hobart

February, 1989

This thesis contains the results of research done in the geology department of the University of Tasmania between 1984 and 1989. It contains no material which has been submitted for the award of any other degree or diploma in any other university and to the best of my knowledge and belief contains no copy or paraphrase of material previously published or written by another person, except where due reference is made,

John Adam
University of Tasmania
Febuary, 1989.

TABLE OF CONTENTS

LIST OF FIGURES

LIST OF TABLES

ACKNOWLEDEMENTS

Firstly I would like to thank my supervisor Prof. David Green who assisted me with his advice, and by making available to me oportunities that I would not ordinarily have had. Thanks are also due to many other people from the University of Tasmania who assisted me in various ways. They include Keith Harris who instucted me in the use of experimental apparatus, Wieslav Jablonski who assisted with the use of the electron microprobe, Phil. Robinson who assisted with chemical analyses, Simon Stevens who prepared polished thin sections and experimental mounts, John Paget who assisted with the calculation of numerical projections, Kurt Stuwe who reanalysed and checked mineral analyses, Karyl Whelan who assisted with typing, and Joe Stolz and Dave Ellis who assisted with field work. Prof.Green, Joe Stolz, Trevor Falloon, Tony Crawford and Rick Varne are also thanked for their advice and comments on various parts and stages of this thesis. Steven Eggins is thanked both for his friendship and for many discussions on various aspects of this work. Wayne Taylor, Graeme Wheller, Ewan Reid, Father Greg Jordan, Margaret and Malcom Wallace, Nic and Kate Odling, Trish Blenman, Tony and Anne Crawford, June Pongratz, Kurt Stuwe, Trevor and Wendy Falloon, Michael and Sabina Seitz, Richard Wedekind, Sharon Adrichem, Dave and Siau Hwi Huston, Garry Davidson, Mark Barsdell, Christian Ballhaus, Leonie Jones, Penny Green and Peter Cornish are thanked for their help and friendship. Lastly special thanks are due to my parents for their support and encouragement throughout the course of this study.

ABSTRACT

This thesis documents an experimental study of the effects of H_2O, CO_2 and pressure on the compositions of basaltic liquids in equilibrium with garnet, clinopyroxene, orthopyroxene and olivine (garnet lherzolite). The results of this study have been combined with compositional data for natural basalts and used to examine some currently popular theories for the origin of alkaline basalts. For this purpose, the thesis has been divided into two parts.

Part I is a study of liquidus phase relationships at 28 kb in the simplified basaltic system CMAS (CaO-MgO-Al_2O_3-SiO_2). Phase relationships were studied for dry, hydrous and CO_2-bearing systems. In the dry system garnet, diopside, enstatite and forsterite, were found to co-exist with a liquid of the approximate composition 50% SiO_2, 16% Al_2O_3, 25% MgO, 9% CaO. Increasing pressure results in an expansion of the garnet liquidus volume and thereby causes liquids in equilibrium with garnet lherzolite to increase in CaO/Al_2O_3. The effect of pressure on the enstatite-forsterite cotectic is, however, relatively small. With the addition of 20 wt.% H_2O, the enstatite and forsterite liquidus volumes are greatly expanded relative to those of clinopyroxene and garnet. As a result of this, H_2O-rich liquids in equilibrium with garnet lherzolite are more $CaAl_2O_4$-rich, and less magnesian, than those produced under dry conditions. Addition of CO_2 produces a large expansion of the garnet and enstatite liquidus volumes. This causes CO_2-rich liquids in equilibrium with garnet lherzolite to be SiO_2-poor and have high CaO/Al_2O_3.

The simple-system liquid trends can be compared with the compositional trends of primitive alkaline basalts from southeastern Australia, central Europe, Hawaii, and the Canary Islands. Although the two sets of data cannot be directly superimposed, the primitive alkaline basalts show the same sense of variation as do liquids produced in the simple system by partial melting of garnet lherzolite in the presence of variable concentrations of CO_2. When the effects of the additional components TiO_2, FeO, P_2O_5, alkalis and H_2O (found in natural systems) are considered, the peridotite-melting trends become more closely matched with the compositional range of the natural basalts. The effect of pressure on the

orthopyroxene-olivine cotectic is also increased; with increasing pressure during partial melting of natural garnet lherzolites, liquids become more SiO_2-poor. Both variation in pressure and variation in CO_2 concentrations during partial melting of garnet lherzolite appear to be capable of producing the compositional range of the natural alkaline basalts. Additional information is needed to decide in individual cases which of the two mechanisms, if either, offers the more likely explanation.

Part II is a case study of a small group of basalts from the Oatlands district of Tasmania. The basalts are of Oligocene age and include olivine tholeiite, alklali olivine basalt, nepheline basanite, transitional nephelinite, and olivine melilitite compositions. Experimental data, combined with independent evididence for primary volatile concentrations in basalt magmas, indicate that the primary magmas of these basalts probably formed in equilibrium with lherzolite and garnet lherzolite residues at pressures between 10 and 50 kb.

Calculated concentrations of minor and trace elements in the basalts source are consistent with a source that was enriched in H_2O, CO_2, K_2O, P_2O_5, FeO, Ba, Sr, Nb and LREE relative to the bulk composition of the mantle. Deep mantle plume and heterogeneous mantle models appear to be inconsistent with the distribution of Cainozoic basalts in Tasmania and other parts of eastern Australia. Experimental and petrological data are consistent with a relatively shallow (lower lithospheric/upper asthenospheric) location for the source prior to the beginning of volcanism; isotopic data indicate that this would need to have become enriched in LREE (and presumably in other incompatible elements as well) at some time following a previous and much longer history of LREE depletion.

Because of similarities between the calculated source compositions and those of metasomatized Cr-diopside xenoliths from southeastern Australia, it is possible that the basalts' source region was enriched in incompatible elements by processes similar to those which affected the lherzolite xenoliths. However, differences between the calculated source compositions and those of the metasomatized xenoliths (particularly in TiO_2) suggest that the basalts' source was unlikely to have been depleted and refractory

lithosphere that was subsequently re-enriched in incompatible elements. This factor, in combination with the high pressures of origin (40-50 kb) inferred for some of the basalts, is consistent with an asthenospheric derivation for the source region.

PART I

DRY, HYDROUS AND CO_2-BEARING LIQUIDUS PHASE RELATIONSHIPS IN THE CMAS SYSTEM AT 28 kb, AND THEIR BEARING ON THE ORIGIN OF ALKALINE BASALTS

1.1 INTRODUCTION

The components of the CMAS system, SiO_2, Al_2O_3, MgO and CaO, comprise about 70-85 wt% of most basalts and >90 wt% of most peridotites. Because of this, the CMAS system has often been studied as a simple analogue for more complex basaltic and peridotitic systems (e.g., O'Hara & Yoder, 1967; Davis & Schairer, 1965; Kushiro, 1968; Sen & Presnall, 1984; Chen & Presnall, 1975; Presnall et al., 1979). Most of these studies have been of two and three component joins. This approach has been used to determine the nature of liquids formed over a range of conditions by melting of peridotite. The most direct determinations of liquid compositions in equilibrium with peridotite are those of Presnall et al. (1979). Presnall et al. (1979) used phase relationships and multiple bulk compositions to estimate compositions of liquids in equilibrium with residual plagioclase and spinel lherzolites. They also analysed quenched glasses and coexisting mineral phases at pressures from 1 atm to 20 kb. Although unable to directly analyse quenched glasses, Davis & Schairer (1965) closely bracketed the liquid composition in equilibrium with simplified garnet lherzolite at 40kb.

The effects of H_2O and CO_2 on liquidus phase relationships in the CMAS system have been investigated over a range of pressures by Kushiro (1968, 1969 and 1972) and Eggler (1978). Experiments were performed for the present study with the intention of examining the effects of H_2O and CO_2 on liquidus phase relationships in the CMAS system at 28kb. At this pressure equilibrium between garnet lherzolite and liquid occurs. The experiments fill a gap between the 20kb data of Presnall et al. (1979) and the 40kb results of Davis & Schairer (1965). A comparison of the effects of H_2O, CO_2, and pressure on the compositions of liquids in equilibrium with simplified garnet lherzolite can also be made.

1.2 EXPERIMENTAL METHODS

Experiments were performed principally on compositions within the pseudo-ternary system SiO_2-$CaAl_2O_4$-Mg_2SiO_4 (Fig. 1). This plane contains the phases or components anorthite, Ca-Tschermaks silicate, enstatite, grossular-pyrope solid solution ($CaMg_2Al_2Si_3O_{12}$), olivine and quartz. Additional peridotite phases include diopside and spinel. To locate invariant points at which liquid, olivine, orthopyroxene, clinopyroxene and garnet coexist, a number of compositions between diopside and the SiO_2-$CaAl_2O_4$-Mg_2SiO_4 plane were also examined. Because of the tendency for liquids to quench to crystalline material instead of glass, phase boundaries were bracketed between compositional points.

Starting materials were SiO_2, H_2O, $CaCO_3$, high purity natural magnesite, and sintered oxide mixtures of Ca-Tschermak's silicate, anorthite, enstatite and forsterite composition. Mixtures of these were contained in welded Pt capsules and run in solid-media piston-cylinder apparatus of the type described by Boyd & England (1960). Furnace assemblies were of 1/2" diameter with talc/pyrex or salt/pyrex sleeves. A -10% pressure correction was made when talc outer sleeve assemblies were used. Pressures are considered to have been within 1kb of 28kb. Temperatures were measured with a $Pt/Pt_{90}Rh_{10}$ thermocouple placed within 0.5 mm of the sample capsule and are considered accurate to within $\pm$ 10°C.

Approximately 20 wt.% H_2O was added to H_2O-bearing mixtures using a graduated microsyringe. Nearly all the H_2O-bearing experiments produced small glass spherules. Similar glass spherules and glassy overgrowths on crystals were interpreted by Kushiro et al. (1968) to have been precipitated from a vapour phase during quenching. This interpretation is consistent with the work of Hodges (1974) who used phase relationships to determine a solubility of approximately 20 wt.% H_2O in liquid diopside at 30 kb. Eggler & Rosenhauer (1978), however, used the same technique to determine a solubility of approximately 30 wt.%. Solubility measurements on more aluminous compositions, such as those used during this study, have not yet been made. It is difficult to decide, therefore, whether the H_2O-bearing experiments performed during this study were H_2O-saturated or not. However, nearly all of the H_2O-bearing experiments

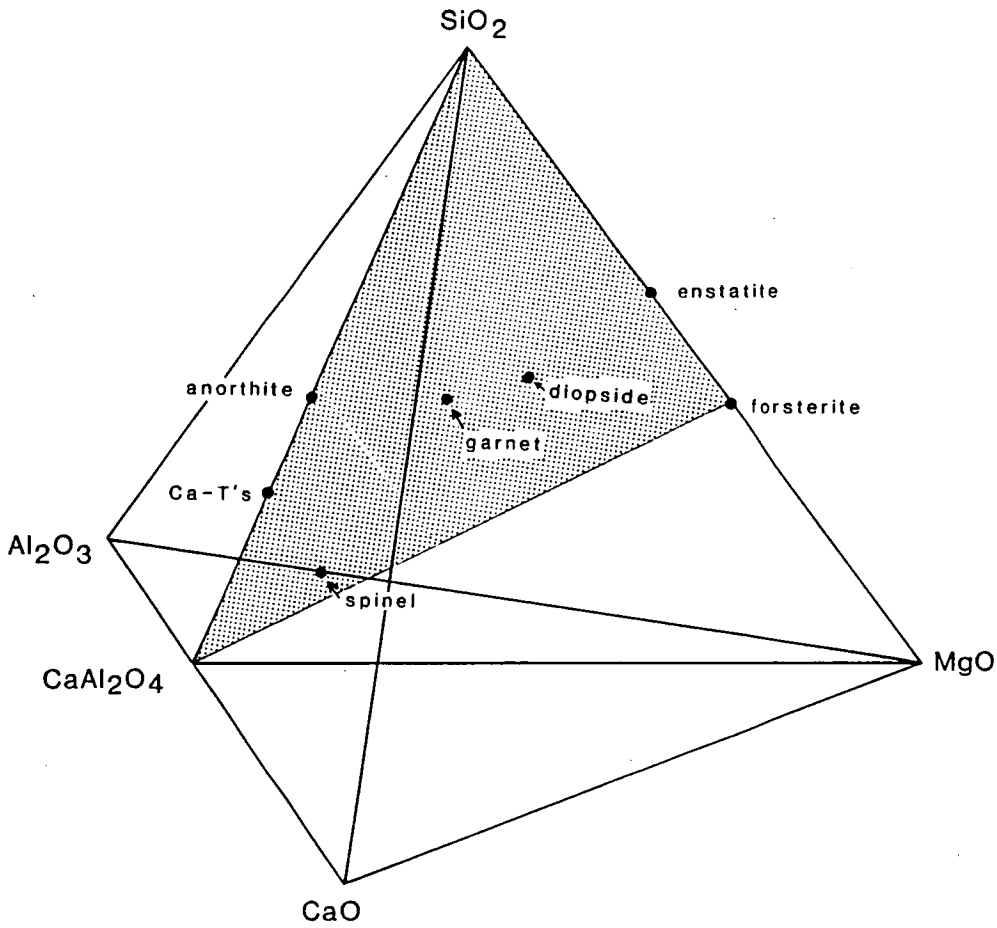

Fig. 1 The quaternary system CaO-MgO-Al_2O_3-SiO_2 and the psuedo-ternary system $CaAl_2O_4$-SiO_2-Mg_2SiO_4 (shaded). Contained within the $CaAl_2O_4$-SiO_2-Mg_2SiO_4 system are the phases/components Ca-Tschermaks silicate (Ca-T's), anorthite, the garnet solid solution $CaMg_2Al_2Si_3O_{12}$, enstatite, forsterite and quartz. Additional phases that may be present include spinel and diopside.

contained 20±1 wt.% H_2O. Regardless of whether H_2O saturation occurred or not, the phase relation determined remain valid for compositions containing 20 wt.% H_2O or less (less if vapour saturation occurred).

Most of the CO_2-bearing samples contained 8-11 Wt% CO_2. Magnesite and $CaCO_3$ were used as sources of CO_2. A number of experiments containing CO_2 produced vesicular charges that are interpreted to have contained a vapour phase (notably T-1875, Table 4). In spite of this, vapour saturation is considered to have occurred during only some and not all of the CO_2-containing experiments. Small amounts of graphite were produced during many of the experiments with CO_2 present, possibly indicating partial reduction by the migration of H_2 through the capsule walls. Graphite formation was prevented by drying starting mixtures at 300°C, and by surrounding the inner sample-bearing capsule by a haematite/magnetite buffer within a double capsule assemblage.

The identification of primary liquidus phases was sometimes made difficult by the formation of secondary pyroxene crystals during quenching. Because of this, optical identifications were usually confirmed with the use of an electron microprobe. The Wells' (1977) two-pyroxene thermometer and the Nickel & Green (1985) enstatite-garnet barometer, applied to analyses of coexisting primary pyroxenes and garnets, produced estimates of temperature and pressure that were within 50°C and 1kb of the actual run conditions (for a listing of mineral analyses see Table 18 of appendix 1). Pyroxenes formed during quenching could usually be distinguished by their high and variable Al_2O_3 contents.

1.3 EXPERIMENTAL RESULTS

The results of experiments on the dry, H_2O-bearing and CO_2-bearing CMAS systems are shown diagramatically in Figs. 2,3 and 5. The results and conditions of individual experiments, together with the compositions used, are listed in Tables 1-4. In the dry system, there is no liquidus phase field for diopside within the compositional plane SiO_2-$CaAl_2O_4$-Mg_2SiO_4 (Fig. 2). The composition of the liquid in equilibrium with the four-phase garnet lherzolite assemblage can be closely bracketed, however, by combining the data

Fig. 2. Liquidus phase relations in the compositional plane SiO_2-$CaAl_2O_4$-Mg_2SiO_4 at 28kb, both dry and with 20 wt.% H_2O added. The dry enststite-forsterite eutectic on the SiO_2-Mg_2SiO_4 join was obtained by extrapolation from the data of Chen and Presnall (1975). Abbreviations are as follows C = corundum, Gt = garnet, Sp = spinel, En = enstatite, and Fo = forsterite.

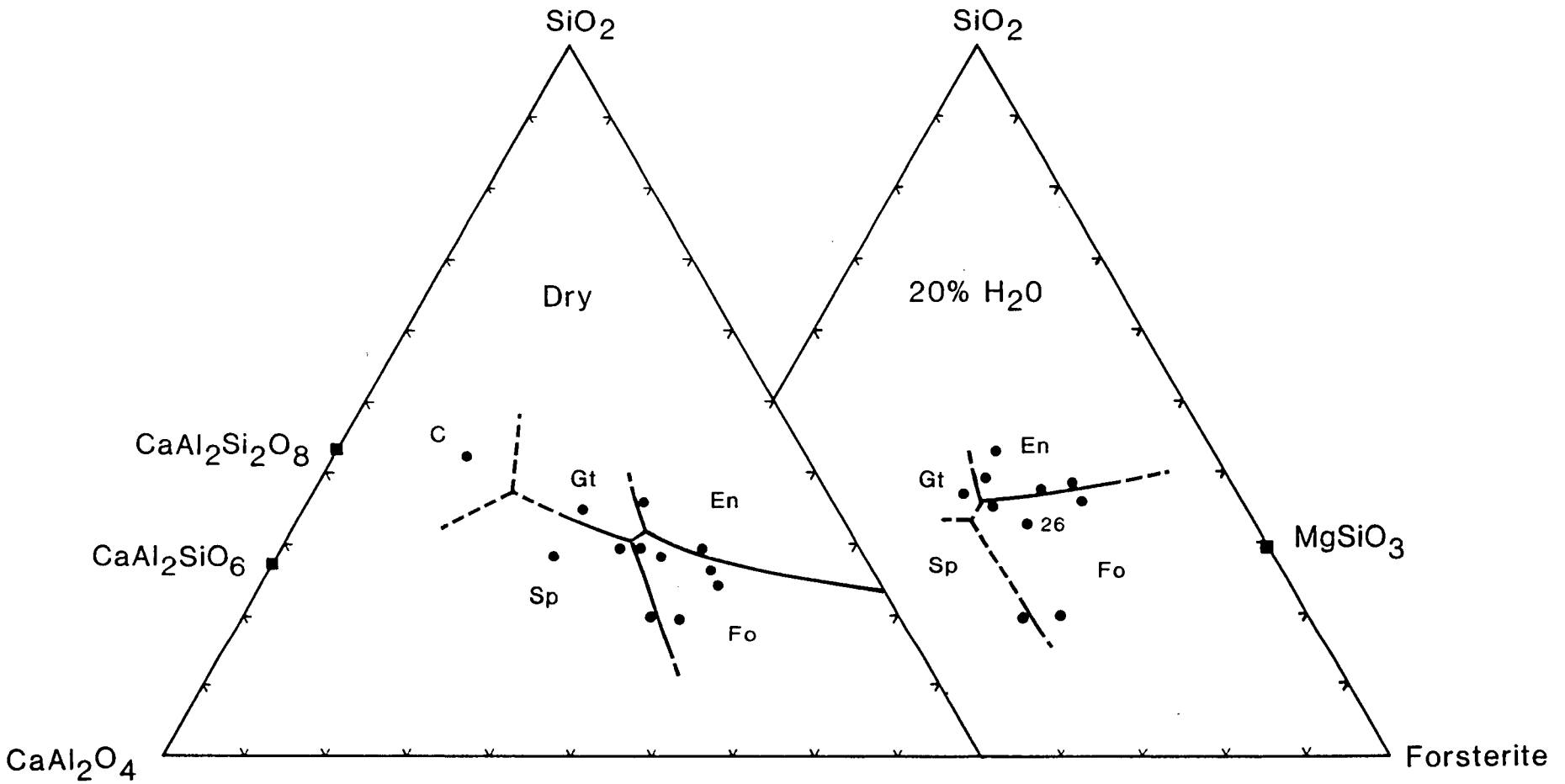
SiO2
SiO2
Dry
20% H2O
CaAl2Si2O8
CaAl2SiO6
CaAl2O4
C
Gt
En
Sp
Fo
Gt
En
26
Sp
Fo
MgSiO3
Forsterite

Weight %

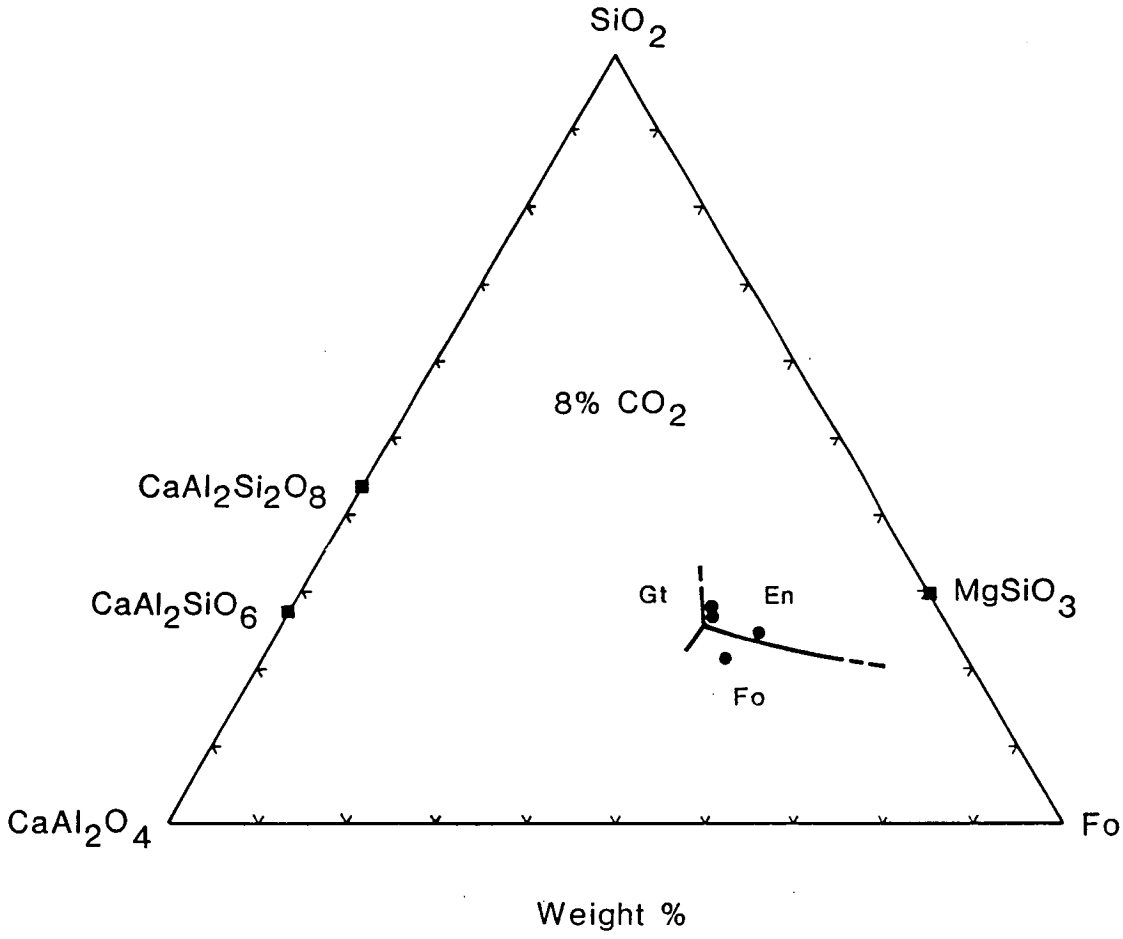

Fig. 3. Liquidus phase relationships in the compositional plane SiO_2-$CaAl_2O_4$-Mg_2SiO_4 at 28kb and with 8 wt.% CO_2 added. Abbreviations as in Fig. 1.

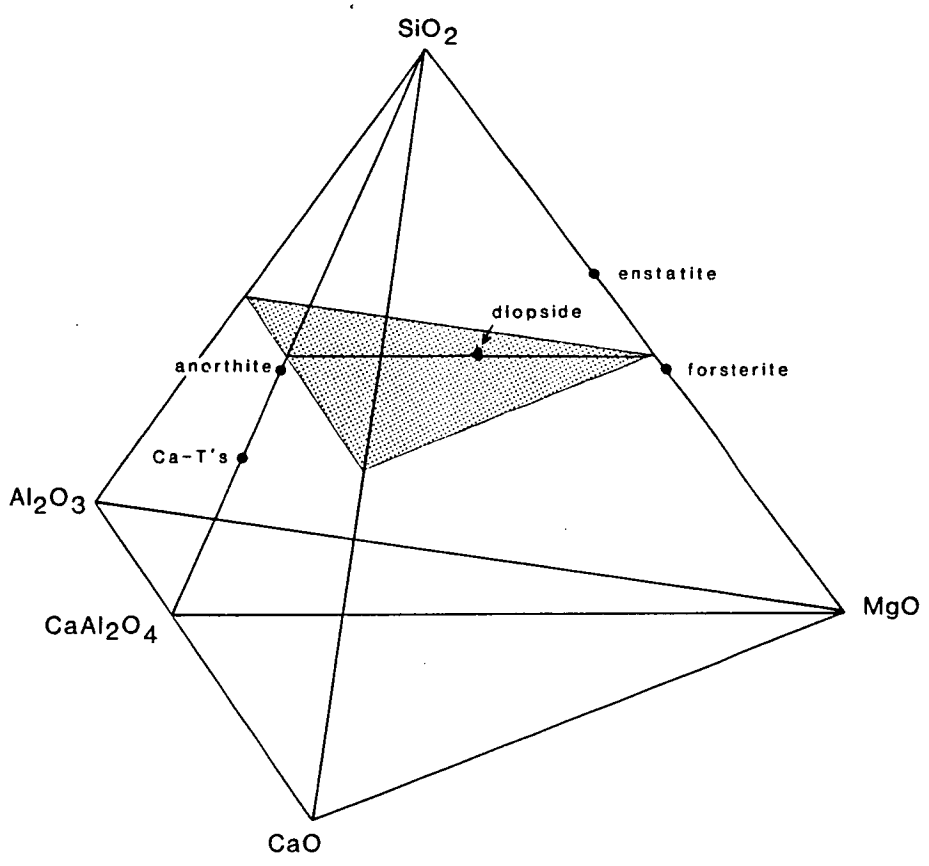

Fig. 4. The system $CaO-MgO-Al_2O_3-SiO_2$ and the compositional plane $CaO-Al_2O_3-MgO$-45 wt.% SiO_2 (shaded; see Fig. 5)

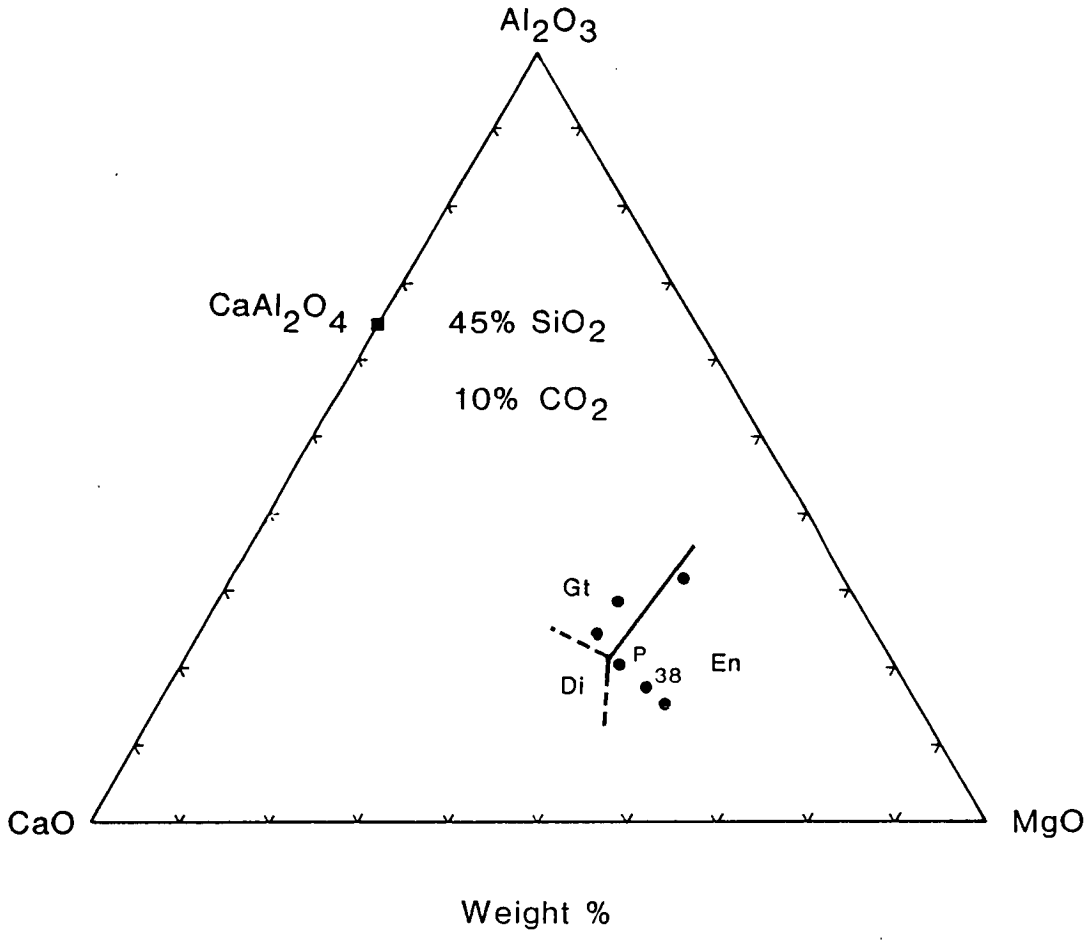

Fig. 5. Liquidus phase relationships at 28kb in the compositional plane CaO-Al_2O_3-MgO with 45 wt.% SiO_2 and 10 wt.% CO_2. Abbreviations as in Fig. 1.

TABLE 1.

RESULTS OF DRY EXPERIMENTS

RUN#	COMP.	T°C	RESULTS	DURATION(MINS)
T-1550	1	1650	Sp+Gl+Q-xtals	15
T-1553	3	1550	Sp+Gl+Q-xtals	25
T-1561	4	1600	Opx+Gl+Q-xtals	16
T-1563	4	1650	Gl+Q-xtals	10
T-1567	5	1600	Ol+Gl+Q-xtals	15
T-1569	5	1650	Ol+Gl+Q-xtals	15
T-1597	7	1620	Ol+Opx?+Q-xtals+Gl	15
T-1615	8	1600	Q-xtals+Gl	16
T-1621	8	1550	Sp(trace)+Q-xtals+Gl	15
T-1692	8	1520	Gt+Q-xtals	18
T-1696	11	1660	Ol+Q-xtals	22
T-1698	11	1630	Ol+Q-xtals	20
T-1702	9	1570	Ol+Q-xtals	20
T-1705	12	1550	Q-xtals+Gl	23
T-1710	12	1510	Corundum+Gl	20
T-1718	8	1540	Gt+Q-xtals	21
T-1719	13	1650	Sp+Ol(minor)+Q-xtals	20
T-1729	14	1540	Q-xtals+Gl	22
T-1733	14	1500	Gt+Q-xtals	22
T-1742	9	1550	Ol+Q-xtals+Gl	20
T-1743	9	1520	Ol+Gt+Sp+Q-xtals+Gl	20
T-1748	9	1490	Gt>>Ol+Sp+Q-xtals	20
T-1751	7	1640	Ol+Q-xtals	20
T-1773	16	1550	Ol+Q-xtals	20
T-1776	16	1520	Gt+Sp+Ol?+Q-xtals	20
T-1803	7	1530	Gt+Ol+Sp(V.minor)+Q-xtals	25
T-1919	29	1570	Opx+Q-xtals	25

Sp = spinel, Gt = garnet, Cpx = diopside, Opx = enstatite
Ol = forsterite, Gl = glass, Q-xtals = quench crystals

TABLE 2.

RESULTS OF CO_2-BEARING EXPERIMENTS

RUN#	COMP.	T°C	RESULT	DURATION (mins)
T-1864	11	1550	Q-xtals+Gl	19
T-1867	11	1500	Ol(minor)+Qch crystals+Gl	19
T-1868	11	1450	Ol+Sp+Q-xtals small degree of crystallization	15
T-1873	5	1500	possible minor primary Opx+ Q-xtals+Gl	25
T-1871	11	1400	Ol+Gt+minor Opx?+Q-xtals	15
T-1875	5	1450	Ol+minor Opx small degree of crystallization	15
T-1930	30	1450	Opx+Gt+Q-xtals	20
T-1935	30	1500	Opx+Q-xtals	20
T-1945	30	1475	Opx+Q-xtals	20
T-1961	32	1450	Opx+Q-xtals	20
T-1962	32	1420	Opx+Gt+Q-xtals	15
T-1991	35	1350	Gt>>Opx+Q-xtals	20
T-1997	35	1390	Q-xtals+Gl	20
T-2000	36	1350	Opx(minor)+Q-xtals+Gl	20
T-2002	36	1310	Gt+Cpx+Opx+Q-xtals	25
T-2004	36	1330	Gt+Cpx+Opx+Q-xtals	25
T-2008	37	1340	Ol+Q-xtals	25
T-2011	38	1340	Ol+Cpx+Opx+Q-xtals	20
T-2013	38	1320	Gt+Opx+Cpx+Q-xtals	26
T-2015	38	1330	Gt+Opx+Cpx+Q-xtals+Gl	25
T-2141	41	1360	Gt+Opx+quench	25
T-2143	40	1250	Gt+Opx+Di+Q-xtals+Gl	145
T-2146	41	1380	Q-xtals+Gl	145
T-2237	40	1100	Gt+Opx+Cpx+Ol?+Dol?	420
T-2239	40	1150	Gt+Opx+Cpx+Ol?+Q-xtals	360

Sp = spinel, Gt = garnet, Cpx = diopside, Opx = enstatite Ol = forsterite, Dol = dolomite, Gl = glass, Q-xtals = quench crystals

TABLE 3.

RESULTS OF WATER-BEARING EXPERIMENTS

RUN#	COMP.	T°C	RESULT	wt% H_2O	DURATION (mins)
T-1790	17	1180	Opx+Q-xtals	20	60
T-1793	17	1220	Q-xtals+Gl	21	30
T-1794	17	1200	Opx+Q-xtals+Gl	21.5	32
T-1798	18	1200	Ol+Opx+Q-xtals+Gl	18.5	31
T-1800	20	1220	Gl+Q-xtals	20.5	32
T-1802	20	1170	Gl+Q-xtals	19	22
T-1805	20	1120	Opx+Gt+Q-xtals+Gl	20	20
T-1808	20	1090	Opx+Q-xtals+Gl	20	25
T-1813	22	1070	Gt+Opx+Q-xtals+Gl	19.5	38
T-1834	25	1050	Gt+Opx+Q-xtals+Gl	19	32
T-1836	25	1100	Gt+Opx+Q-xtals+Gl	20.5	67
T-1837	25	1150	Opx+Q-xtals+Gl	20	120
T-1839	22	1120	Gt+Opx+Q-xtals (close to liquidus)	17	120
T-1841	26	1150	Ol+Q-xtals+Gl	20	130
T-1843	26	1100	Ol+Gt(minor)+Q-xtals (close to liquidus)	20	120
T-1844	26	1050	Opx+Gt+Q-xtals+Gl	20	120
T-1849	27	1100	Cpx+Ol+Gt+Q-xtals	19.5	120
T-1854	27	1140	Ol+Q-xtals+Gl (close to liquidus)	18.5	120
T-1949	14	1140	Ol+Q-xtals	19	35
T-1957	13	1200	Ol+Gl+Q-xtals	18	65
T-1964	33	1200	Sp+Ol+Q-xtals (close to liquidus)	19.5	50
T-2145	42	1140	Gt+Opx?+Q-xtals+Gl	20	60

Sp = spinel, Gt = garnet, Cpx = diopside, Opx = enstatite
Ol = forsterite, Gl = glass, Q-xtals = quench crystals

TABLE 4.

COMPOSITIONS OF STARTING MIXTURES

MIX	1.	3.	4.	5.	7.	8.	9.	11.
SiO_2	43.13	43.42	51.52	47.39	49.50	47.69	48.31	42.5
Al_2O_3	23.98	28.18	12.38	12.73	12.62	18.15	15.95	17.1
MgO	19.21	12.20	29.09	32.67	31.35	24.03	27.08	31.0
CaO	13.67	16.19	7.00	7.20	6.50	10.12	8.65	9.4
MIX	11.	12.	13.	14.	16.	17.	18.	20.
SiO_2	42.5	49.33	41.35	50.00	48.33	56.47	55.43	56.23
Al_2O_3	17.1	26.77	19.35	19.68	16.99	12.10	11.93	16.77
MgO	31.0	6.83	28.65	19.50	25.33	24.53	25.83	17.76
CaO	9.4	14.72	10.65	10.82	9.35	6.90	6.81	9.22
MIX	22.	25.	26.	27.	29.	33.	42.	
SiO_2	52.84	54.00	49.97	48.59	53.02	38.97	49.80	
Al_2O_3	18.52	15.16	17.25	16.72	14.50	22.27	21.48	
MgO	18.00	22.18	22.85	22.06	24.62	26.03	11.82	
CaO	10.64	8.67	9.93	12.63	7.86	12.73	16.90	

TABLE 4. (cont.)

CO_2-BEARING MIXES

MIX	5.	11.	30.	32.	35.	36.	37.	38.
SiO_2	43.61	39.77	42.3	42.9	41.76	40.37	40.42	40.84
Al_2O_3	12.98	16.02	14.61	13.9	14.05	9.96	7.60	8.39
MgO	28.25	27.37	24.58	24.4	21.74	24.03	26.12	24.89
CaO	7.13	8.82	8.34	9.2	13.59	15.32	14.30	14.97
CO_2	8.0	8.0	10.0	9.5	9.5	10.3	11.50	10.9

MIX	40.	41.
SiO_2	42.15	40.05
Al_2O_3	7.69	11.74
MgO	26.50	22.52
CaO	14.56	14.68
CO_2	11.3	11.0

of O'Hara & Yoder (1967) on the diopside-pyrope join (Fig. 6), with results from this study. The diopside-pyrope join intersects the SiO_2-$CaAl_2O_4$-Mg_2SiO_4 plane close to, but slightly below, the garnet-enstatite-forsterite piercing point in Fig. 2. This point (occurring at approximately 1540°C) is nearly coincident with the 30 kb garnet-diopside cotectic along the diopside-pyrope join.

Phase relationships with 20 wt.% H_2O added in the SiO_2-$CaAl_2O_4$-Mg_2SiO_4 plane are also shown in Fig. 2. Liquidus temperatures are approximately 500°C lower than those of the dry system. To investigate the CaO-rich side of the $CaAl_2O_4$-SiO_2-Mg_2SiO_4 plane, a single composition was studied near to composition 26 (Fig. 2), but with 9 Wt% diopside added. At 1140°C, this crystallized forsterite only; at 1110°C it crystallized forsterite, garnet and diopside in approximately equal proportions. In the H_2O-bearing system, the garnet-orthopyroxene-olivine cotectic pierces the $CaAl_2O_4$-SiO_2-Mg_2SiO_4 plane (Fig. 2) at approximately 1130°C. Therefore, although not well constrained in compositional space, the diopside phase volume is known to occur within approximately 30°C of the piercing point in the $CaAl_2O_4$-SiO_2-Mg_2SiO_4 plane.

Within the CO_2-bearing system ten compositions were studied. Four of these were used to find the garnet-enstatite-forsterite piercing point in the SiO_2-$CaAl_2O_4$-Mg_2SiO_4 plane (Fig. 3). Five others were made up within a second plane of constant (45 Wt%) SiO_2 content (Figs. 4 & 5). At point P (composition 36, Table 4) in Fig. 5, enstatite is the liquidus phase at 1350°C, followed by garnet and diopside at 1330°C. Forsterite, enstatite and diopside crystallize from the neighbouring composition, 38, at 1340°C. It appears, therefore, that a five-phase point in the CO_2-bearing system occurs slightly to the $CaAl_2O_4$-rich side of P at 1340-1350°C. Below 1340°C both forsterite and diopside are resorbed into the liquid, and enstatite and garnet are precipitated; this represents a continuation of the vapour absent reaction

$$MgSiO_3 + CaMg(CO_3)_2 = CaMgSi_2O_6 + Mg_2SiO_4 + \text{liquid} \qquad (1)$$

estimated by Eggler (1978, p. 321, Fig. 14) to occur at approximately 1230°C at 28 kb. With decreasing temperature, at temperatures above those of dolomite breakdown, CO_2 is incorporated

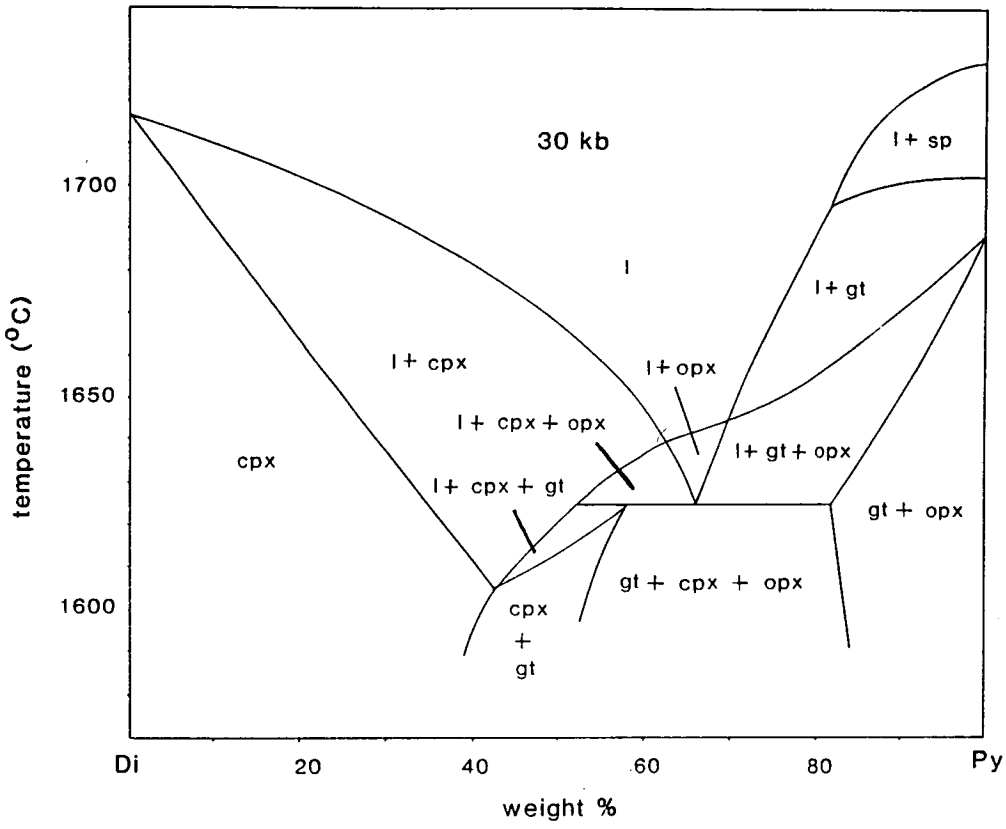

Fig. 6. Phase relationships for the system diopside-pyrope at 30 kb (after O'Hara & Yoder, 1967). Abbreviations include Di = diopside, Py = pyrope, cpx = clinopyroxene, opx = orthopyroxene, gt = garnet, sp = spinel, l = liquid.

into a liquid of increasingly carbonatitic character until the vapour saturated dolomite peridotite solidus is reached at about 1150°C (see results for composition 40, Table 2; and Eggler, 1978).

The presence of dolomite in reaction (1) indicates that the phase relationships discussed for Fig. 5 are relevant to conditions above those of the carbonation reaction

$$CaMgSiO_6 + Mg_2SiO_4 + 2CO_2 = 2MgSiO_3 + CaMg(CO_3)_2$$

Because of this, liquids near the 28 kb dolomite peridotite solidus will be carbonatitic in character (Wyllie & Haung, 1975; Eggler, 1978), and the liquidus phase relationships shown in Fig. 5 will be valid only for liquids containing 10-12 wt.% CO_2.

1.4 DISCUSSION

1.4.1 The Effect of H_2O on the Pyroxene-Forsterite Cotectic

Kushiro (1972) showed that at high pressures, H_2O greatly expands the olivine liquidus phase field relative to those of pyroxenes. However, the magnitude of this effect appears to be compositionally dependent. In Fig. 7 it is shown that the separation between the dry and wet enstatite-forsterite cotectics is decreased with increasing $CaAl_2O_4$ content of the liquid. Between the dry and H_2O-saturated garnet-enstatite-forsterite piercing points there is little difference in SiO_2 concentrations.

1.4.2 Comparison between the Effects of Pressure, H_2O and CO_2

The data of Presnall et al. (1979), together with results from this study and that of Davis & Schairer (1965), are used in Figs. 8 & 9 to show the trend of liquid compositions in equilibrium with simplified plagioclase, spinel and garnet lherzolites between 1 atm and 40kb. The liquid compositions display distinct trends depending on whether equilibrated with plagioclase, spinel or garnet lherzolite. Increasing pressure increases CaO/Al_2O_3 and MgO, and decreases SiO_2 in liquids equilibrated with simplified plagioclase lherzolite. Variation in the liquid compositions formed by melting spinel lherzolite is largely the result of the forsterite content of

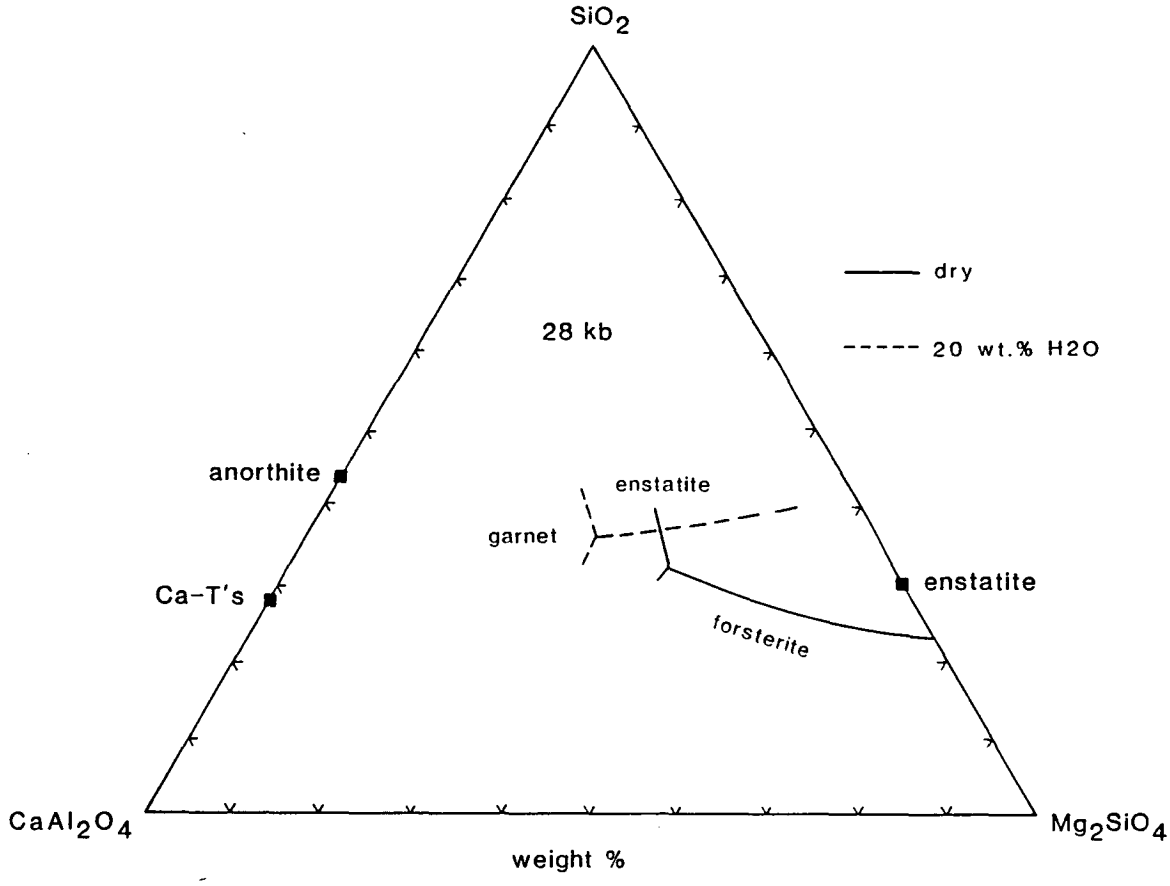

Fig. 7. Dry and H_2O- bearing liquidus phase relationships in the $CaAl_2O_4$-SiO_2-Mg_2SiO_4 system at 28 kb.

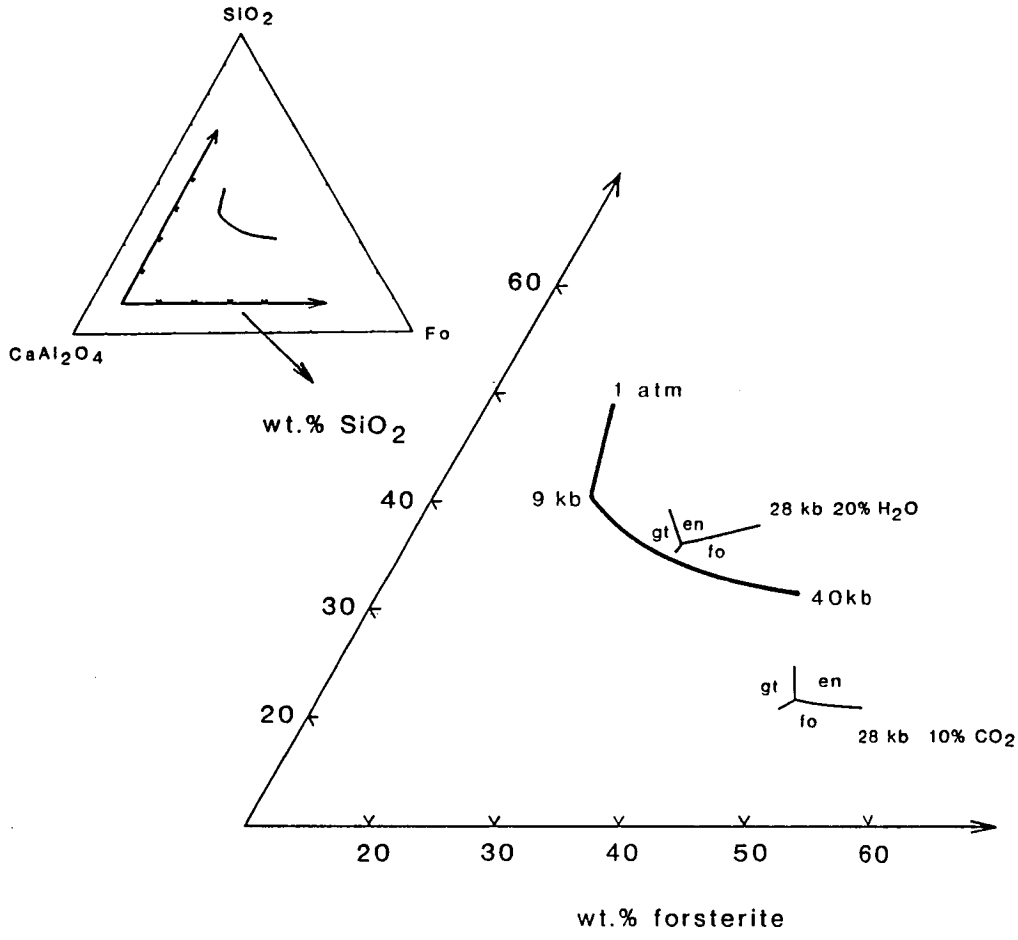

Fig. 8. Compositions of liquids in equilibrium with plagioclase, spinel, and garnet-lherzolite in the CMAS system at pressures from 1 atm. to 40 kb (heavy curved line). Projection is from $CaSiO_3$ onto the plane $CaAl_2O_4$-SiO_2-Mg_2SiO_4.

From this projection the 28 kb and 40 kb compositions appear superimposed. Data for 1 atm to 20 kb are from Presnall et al. (1978). The 40 kb data are from Davis & Schairer (1964). Also shown are the compositions of simple system liquids containing 20 wt.% H_2O and 10 wt.% CO_2 in equilibrium with garnet lherzolite at 28 kb.

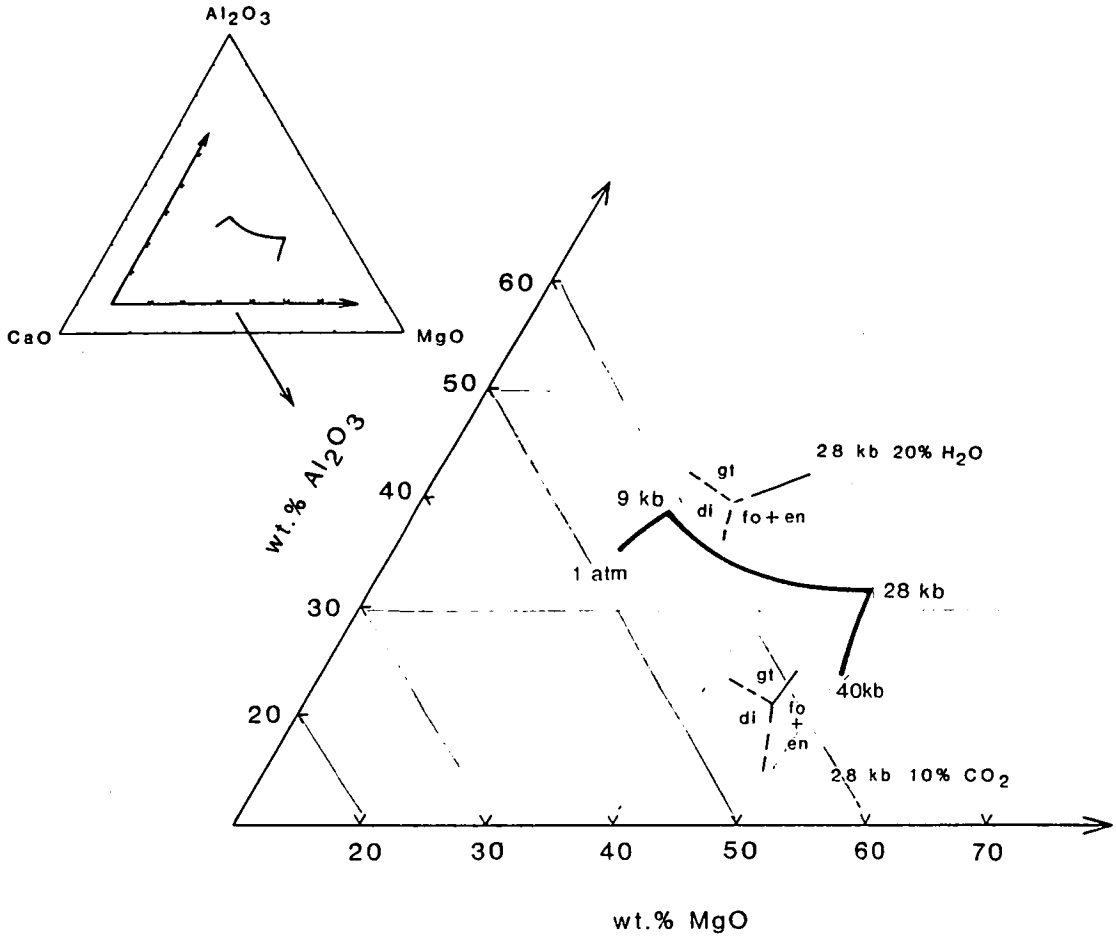

Fig. 9. Compositions of liquids in equilibrium with plagioclase, spinel, and garnet-lherzolite in the CMAS system at pressures from 1 atm. to 40 kb. Projection is from SiO_2 onto the plane CaO-Al_2O_3-MgO. Also shown are the compositions of simple system liquids containing 20 wt.% H_2O and 10 wt.% CO_2 in equilibrium with garnet lherzolite at 28 kb. Symbols and references are as for Fig. 8.

the liquids increasing with increasing pressure. A minimum in CaO/Al_2O_3 is reached at the spinel to garnet-lherzolite transition (at about 26-27 kb). Thereafter, expansion of the garnet field with increasing pressure produces liquids with increasing CaO/Al_2O_3 and slightly higher MgO. Between 28 and 40 kb, increasing pressure appears to cause little change in the SiO_2 concentrations of liquids in equilibrium with garnet lherzolite.

At 28 kb, the main effect of H_2O is to increase the $CaAl_2Si_2O_8$ content of the liquid in equilibrium with garnet lherzolite without significantly changing its SiO_2 content. Addition of CO_2 results in the expansion of the liquidus phase volume of garnet against that of diopside. In this way it has an effect similar to pressure. It also significantly decreases the SiO_2 content of the liquid in equilibrium with garnet lherzolite.

1.4.3 The Effect of Additional Components Na_2O, K_2O, TiO_2, FeO, and P_2O_5

Natural basalts contain significant concentrations of Na_2O, K_2O, TiO_2, FeO, and P_2O_5. These additional components alter the phase relations of natural basalts from those of the pure CMAS system. Shown in Fig. 10 are liquidus relationships for the $KAlSiO_4$-SiO_2-Mg_2SiO_4, and $NaAlSiO_4$-SiO_2-Mg_2SiO_4 systems at 28 kb (from Foley et al., 1986, and Gupta et al., 1987). In both systems, the enstatite and forsterite fields are greatly expanded relative to their extents in the equivalent $CaAl_2O_4$-SiO_2-Mg_2SiO_4 plane of the CMAS system. Alkali-rich liquids in equilibrium with olivine, orthopyroxene and an aluminous phase, such as feldspar, spinel or garnet, should be less magnesian at a given pressure than liquids poor in alkalis.

Equivalent systems at 28 kb have not been studied for TiO_2, FeO or P_2O_5. Studies of related systems by Bowen & Schairer (1935), MacGregor (1965), and Arculus (1975) have shown, however, that addition of these components causes the liquidus fields of pyroxenes to be expanded against olivine. The 40 kb study of Zharikov & Litvin (1985) on the $diopside_{80}hedenbergite_{20}$-$pyrope_{80}almandine_{20}$ join (Fig. 11), has also shown that addition of iron to the CMAS system results in an expansion of the orthopyroxene liquidus field against

Fig. 10

Dry liquidus phase relationships at 28 kb in the CMAS (SiO_2-$CaAl_2O_4$-Mg_2SiO_4), NMAS (SiO_2-$NaAlSiO_4$-Mg_2SiO_4), and KMAS (SiO_2-$KAlSiO_4$-Mg_2SiO_4) systems. Data for the NMAS system from Gupta et al. (1978) and for the KMAS system from Foley et al. (1986). Abbreviations as in Fig. 2 but including Jd = jadeite, and San = sanidine.

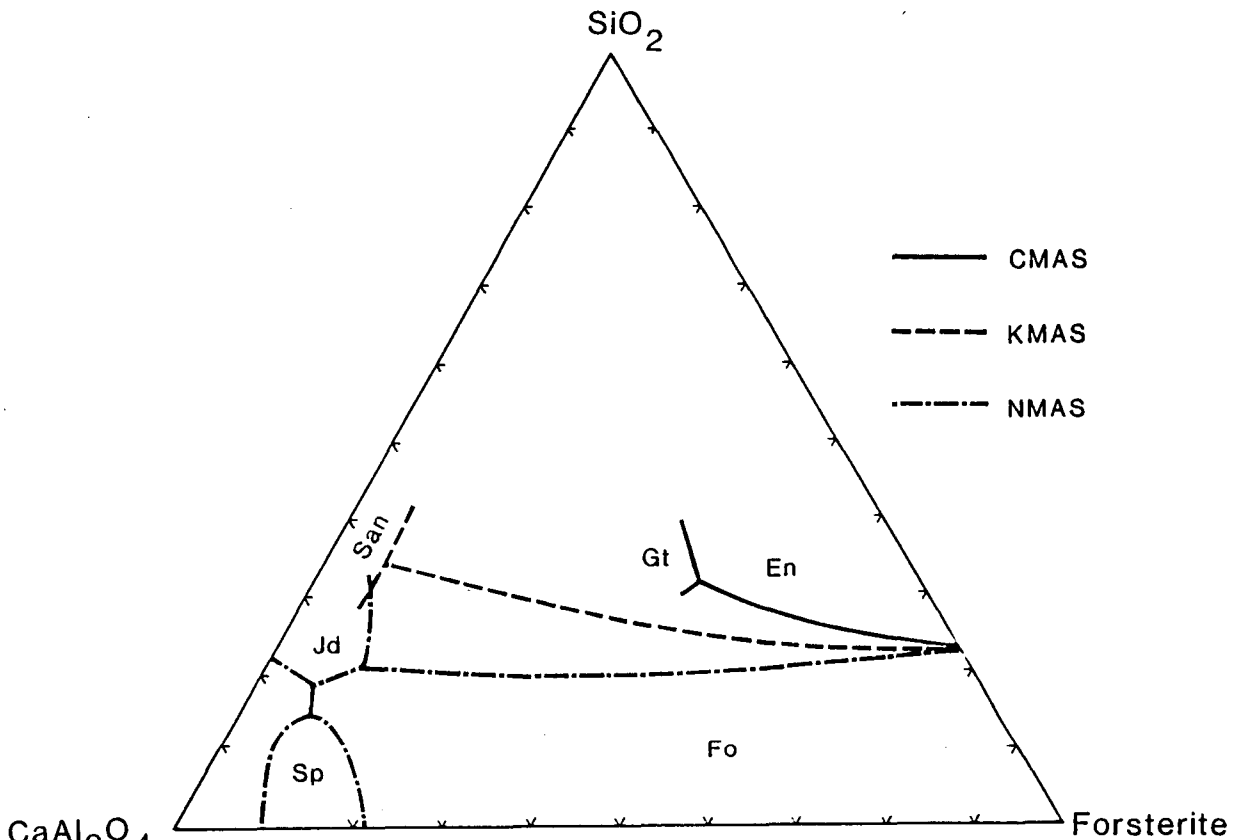
SiO2
CMAS
KMAS
NMAS
San
Gt
En
Jd
Fo
Sp
CaAl2O4
Nepheline
Kalsilite
Forsterite
Weight %

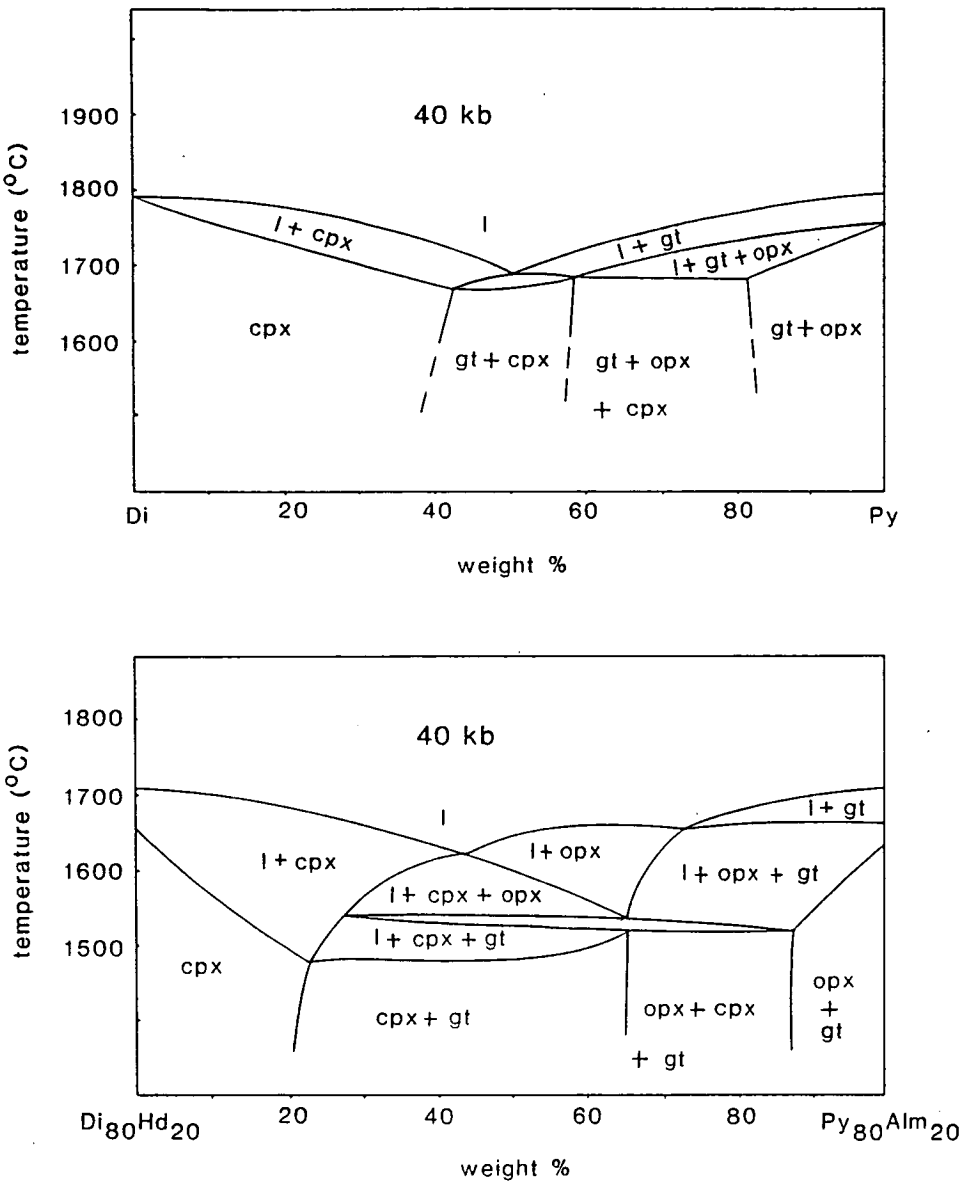

Fig. 11. Comparison between phase relationships in the Fe-free system diopside-pyrope (top) and the Fe-bearing system diopside$_{80}$ hedenbergite$_{20}$-pyrope$_{80}$ almandine$_{20}$ (bottom). Data for the Fe-free system are from Davis (1964). Data for the Fe-bearing system are from Zharikov & Litvin (1985).

garnet and clinopyroxene. In combination, these effects should cause liquids in equilibrium with peridotite to be less mafic and have lower SiO_2 concentrations.

In the CMAS system, increasing pressure apparently causes little decrease in the SiO_2 concentrations of liquids in equilibrium with garnet lherzolite. With the addition of alkalis, the effect of pressure would be more significant. This effect was discussed by Kushiro (1980), who noted that in the $KAlSiO_4$-SiO_2-Mg_2SiO_4, and $NaAlSiO_4$-SiO_2-Mg_2SiO_4 systems, the position of the enstatite-forsterite cotectic becomes more sensitive to pressure, as the alkali content of the liquid increases. Kushiro attributed this effect to the greater compressibility of alkali-rich liquids.

1.4.4 Comparison with Complex or Natural Systems

There is no data set available, for natural peridotite-melting systems, which systematically shows the effects of variation in pressure, degree of melting, and of concentrations of H_2O and CO_2, on the compositions of liquids produced by partial melting of peridotite. To gain a general overview of this subject, it is necessary to combine data from several sources. There is a fairly large amount of information available on the way pressure and degree of melting affect volatile-free liquid compositions produced by partially melting different peridotite compositions (e.g., Jaques & Green, 1980; Stolper, 1980; Takahashi & Kushiro, 1983; Fujii & Scarfe, 1985; Falloon & Green, 1988 ; Falloon et al.,-1988). Most of these data are for pressures below those of garnet lherzolite stability. Additional information on the effects of higher pressures (>25 kb) and of volatile components, comes mainly from high pressure near-liquidus studies of natural alkaline basalts (e.g., Bultitude & Green, 1971; Green, 1973a; Brey & Green, 1977).

The most comprehensive studies to date of volatile-free peridotite melting are probably those of Falloon & Green (1988) and Falloon et al. (1988). These authors studied the effects of pressure, degree of partial melting, and of peridotite starting composition, on the compositions of liquids produced by partially melting peridotite at pressures from 5 to 35 kb. In Fig. 12 are plotted liquid compositions taken from the data of Falloon & Green

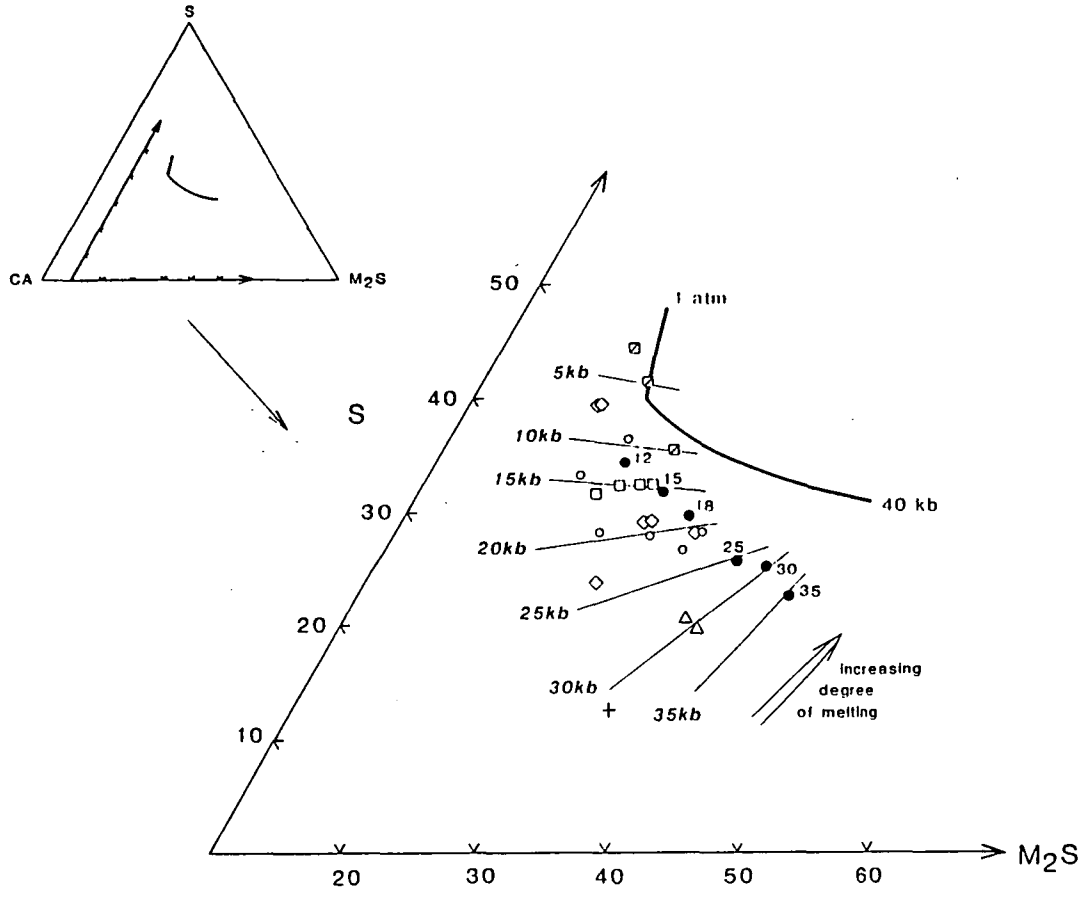

Fig. 12. Liquid compositions formed by partial melting of complex ("natural") peridotites. Shown by the filled circles are liquids produced by 15-33% partial melting of MORB-pyrolite-90 (Falloon & Green, 1988): numbers beside the filled circles indicate, in kb, pressures of formation. Other symbols include: ⊠ = liquids formed by partial melting of Tinaquillo lherzolite (Falloon & Green, 1988); ◇ = liquids formed by partial melting of Hawaiian pyrolite (Falloon et al., 1988); o = liquids formed by partial melting of MORB pyrolite (Falloon & Green, 1988); □ = liquids formed at 10 kb by partial melting of the peridotite SM-2 (Fujii & Scarfe, 1985); △ = liquids formed at 29 kb by partial melting of average north Hessian Depressian lherzolite (Mengel & Green, 1988); + = liquid in equilibrium with garnet, clinopyroxene, orthopyroxene and olivine, formed at 29 kb during experiments on a nepheline basanite from Mt. Leura, Victoria (Green, 1973a).

(1988) and Falloon et al. (1988). These compositions were selected to include only those of liquids equilibrated with olivine + orthopyroxene + clinopyroxene ± plagioclase ± spinel ± garnet. The original analyses were re-cast as CMAS components by following a modified version of the procedure used by O'Hara (1968). This procedure is as follows:

$S = (SiO_2 - 2Na_2O - 2K_2O)\ 60.09$
$A = (Al_2O_3 + Fe_2O_3 + Na_2O + K_2O)\ 101.98$
$M = (MgO + FeO + MnO)\ 40.32$
$C = (CaO + Na_2O + K_2O - 5/3P_2O_5)\ 56.08$
All oxides are in molecular proportions
TiO_2 is ignored

As alternatives to the components CA, S and M_2S shown in Fig. 12, CA may be considered as equal to $CaAl_2O_4$ + $NaAlSiO_4$ (nepheline) + $KAlSiO_4$ (kalsilite), S as SiO_2, and M_2S as olivine. The liquid compositions have been projected from the point CA ($CaSiO_3$). This point was chosen because it gives a nearly edge on projection of the data without casting large 'shadows' from data points removed from the CA-S-M_2S plane (i.e. it does not produce large changes in the relative values of CA, S and M_2S as a function of C/A).

Highlighted in Fig. 12 (by black dots) are liquid compositions produced by between 15% and 33% partial melting of MORB pyrolite-90 at pressures of 12 kb to 35 kb. These compositions contain similar concentrations of TiO_2 and alkalis. They can be compared with the simple (CMAS) system trends for liquids in equilibrium with lherzolite ± plagioclase ± spinel ± garnet (Fig. 12). Although the complex liquid trends are displaced from those of the simple system, it is apparent that pressure effects the complex system similarly to the simple system. With increasing pressure up to 20 kb, liquids in equilibrium with lherzolite decrease in SiO_2 concentration and become increasingly olivine normative. At pressures above 20 kb, liquids continue to increase in normative olivine content with increasing pressure, but there is a decrease in the effect of pressure on SiO_2 content. Unfortunately there is insufficient information on liquid compositions produced at higher pressures (>25 kb), to know how large an effect increasing pressure has on the

CaO/Al_2O_3 ratios and normative olivine contents of complex liquids equilibrated with residual garnet lherzolite.

The general pattern described for liquids produced by similar degrees of melting is upset when the degree of partial melting is varied. This can be seen from the data plotted in Fig. 12. With decrease in the degree of melting at constant pressure, liquids become enriched in alkalis, TiO_2 and P_2O_5, and also become less magnesian. SiO_2 concentrations do not vary greatly with variation in the degree of melting.

Liquids containing much less than 46 wt.% SiO_2 were not produced by the experiments of Falloon & Green (1988), and Falloon et al. (1988). Most analysed melts were relatively low in alkalis, TiO_2 and P_2O_5, and volatile free. To examine the effects of pressures greater than 20 kb on more alkali-rich liquids, it is necessary to consider the results of high pressure near-liquidus studies on natural alkaline basalts, and of peridotite melting studies that were specifically designed to investigate such compositions (e.g., Green, 1973a; Mengel & Green, 1988). When the results of these studies are considered, it can be seen that there is a relatively strong tendency for alkali-rich liquids in equilibrium with lherzolite to decrease in SiO_2 content as pressure increases. This effect appears to become greater as the alkali content of the liquid increases.

The data of Falloon & Green (1988), and Falloon et al. (1988) have been used, together with those of Green (1973a) and Mengel & Green (1988), to plot a series of isobaric cotectics in the CA-S-M_2S plane (Fig. 12). These show variation in the compositions of complex ("natural") liquids in equilibrium with lherzolite at pressures from 5 to 35 kb. In the complementary C-A-M plane the cotectics have not been plotted. This was because they superimpose on one another, as well as on the locus of liquid compositions produced in the CMAS system. Relative to liquids produced in the CMAS system (Fig. 9), the natural system cotectics are shifted slightly towards the CA-rich part of the C-A-M plane. Because there is some variation in the positions of the cotectics with the different starting compositions used by Falloon et al. (1988), Mengel & Green (1988), and Green (1973a) the positioning of the cotectics in Fig. 12 is not precise.

In their general sense of variation they are probably accurate, however, and serve to show the main effects of pressure and increasing alkalis, TiO_2 and P_2O_5 on complex silicate liquids in equilibrium with lherzolite.

There have been a number of comparative studies showing the effects of H_2O and CO_2 on the liquidus phase relationships of natural basalts (e.g., Bultitude & Green, 1968; Green, 1973a; Nicholls & Ringwood, 1973; Merrill & Wyllie, 1975; Stern et al., 1975; Brey & Green, 1977). A more limited number of studies have also been conducted on the effects of H_2O and CO_2 on liquids produced by partially melting peridotite (e.g., Green, 1973b; Nicholls, 1974; Mysen & Boettcher, 1975). After evaluation of the data from these studies, it can be concluded, that in general, natural basaltic systems behave similarly to the simple CMAS system. Detailed predictions of how H_2O and CO_2 concentrations will affect complex ("natural") liquid compositions produced by partially melting peridotite over a range of pressures and temperatures are, however, difficult to make. In particular, some of the effects produced by variations in the concentrations of H_2O and CO_2 may be difficult to distinguish from those produced by variation in pressure. Natural basaltic liquids produced by partially melting peridotite in the presence of an H_2O-rich fluid component should, however, be relatively less mafic and have less normative olivine than equivalent liquids produced by anhydrous melting.

1.4.5 Application to the Problem of Alkaline Basalt Genesis

Partial melting of garnet lherzolite (garnet lherzolite is used here in a mineralogical sense only, rather than as a reference to the nodules found in kimberlite pipes) at high pressures within the mantle is one of the most commonly advocated mechanisms for the production of very SiO_2-poor alkaline basalt magmas (e.g., Green, 1973a; Frey et al., 1978; Clague & Frey, 1982). In numerous geochemical studies, particularly of REE, it has been concluded that garnet lherzolite is a probable residue of alkaline basalt formation (e.g., Frey et al., 1978; Clague & Frey, 1982; Alibert et al., 1983; Chauvel & Jahn, 1984). Experimental studies of natural and simple systems have also shown that volatiles, particularly H_2O and CO_2, may be necessary contributing components during the formation of

alkaline basalt magmas (e.g., Eggler, 1978; Ryabchikov & Green, 1978; Brey & Green, 1977; Mysen & Boettcher, 1975; Bultitude & Green, 1968).

The compositional fields of primitive alkali olivine basalts, basanites, olivine nephelinites, and olivine melilitites from Honolulu, the North Hessian Depression of Germany, the Canary Islands, and Victoria are plotted in Figs. 13 & 14 (using data from Schmincke in von Rad et al., 1982; Irving & Green, 1976; Clague & Frey, 1982; Wedepohl, 1983). The analyses have been selected to include likely primary compositions with 100Mg/(Mg+Fe) = 68.0-70.5, (for Fe_2O_3/FeO = 0.2 by weight) to avoid scatter in the data that may be due to crystal fractionation or crystal accumulation.

Two generalizations can be made about compositional variation in each of the provinces.

(1) There is a continuous range in SiO_2 concentrations from 47% in alkali olivine basalts, to 37% in olivine melilitites. This is accompanied by relatively constant ratios of CaO and alkalis, to MgO and FeO.

(2) With decreasing SiO_2 there is a corresponding increase in CaO relative to Al_2O_3 (Fig. 15).

If it is assumed that the previously described trends are the direct result of peridotite melting to leave a lherzolite $\pm$ spinel $\pm$ garnet residue (rather than products of crystal fractionation, or other secondary processes of magmatic differentiation), then variability in factors such as source composition, degree of melting, pressure of melting, or activities of H_2O and CO_2 during melting, must be invoked to account for them. In Figs. 16 & 17, the compositional fields of primitive alkaline basalts can be compared with those covered by lherzolite cotectics at pressures from 5 to 35 kb. Also plotted for comparison are the compositions of natural alkaline basalts that have had conditions of saturation with lherzolite $\pm$ garnet experimentally determined for them (the compositions are those used in the studies of Green, 1973a; Thompson, 1974; Fujii & Kushiro, 1977; Takahashi, 1980; Adam, unpublished data). Although several of these compositions contained

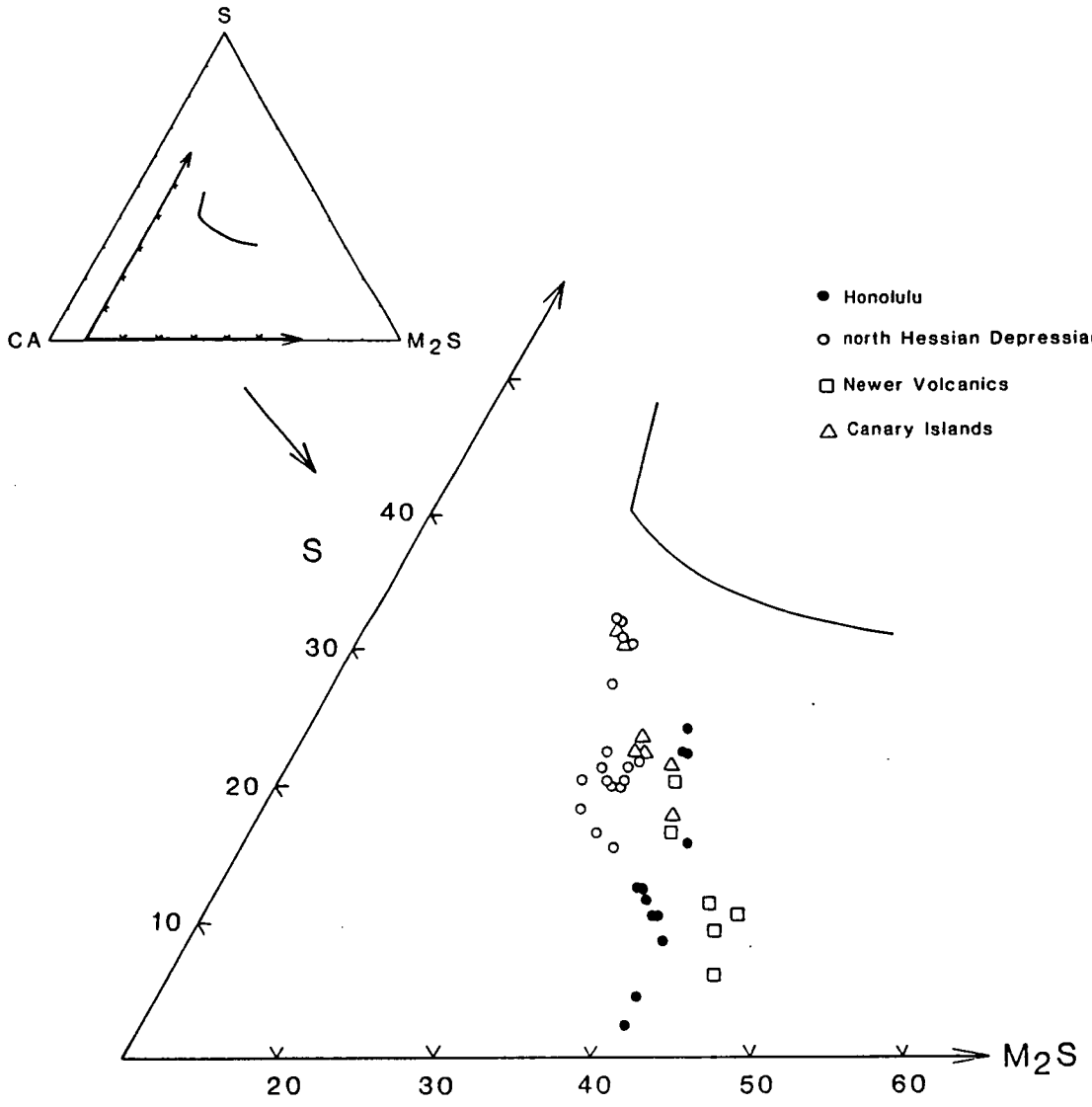

Fig. 13. Primitive alkali olivine basalts, basanites, olivine nephelinites and olivine melilitites (with Mg/(Mg+Fe) = 0.2) from Honolulu (Clague & Frey, 1982), the north Hessian Depressian of Germany (Wedepohl, 1983), the Newer Volcanics of Victoria (Irving & Green, 1976), and the Canary Islands (Schmincke in von Rad et al., 1982) plotted in the plane CA-S-M_2S. For an explanation of the projection and method of recalculating components see text. Shown for reference, by the curved line, is the locus of liquid compositions, between 1 atm and 40 kb, in equilibrium with simplified plagioclase, spinel and garnet lherzolites of the CMAS system (see Fig. 8).

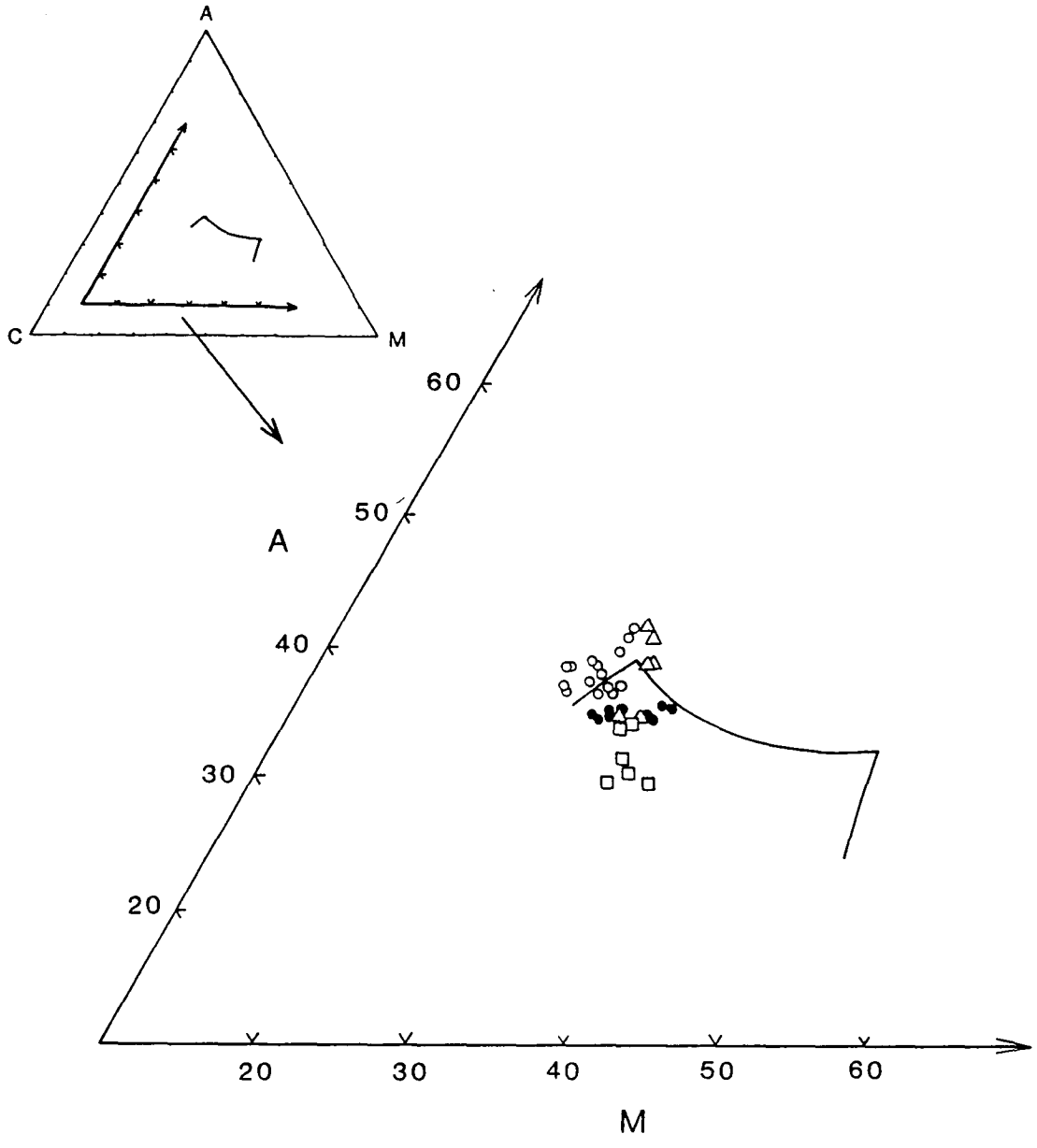

Fig. 14. Primitive alkaline basalts plotted on the plane C-A-M. Projection is from the point S. Shown for reference is the locus of liquid compositions, between 1 atm and 40 kb, in equilibrium with simplified plagioclase, spinel and garnet lherzolites of the CMAS system (see Fig. 9).

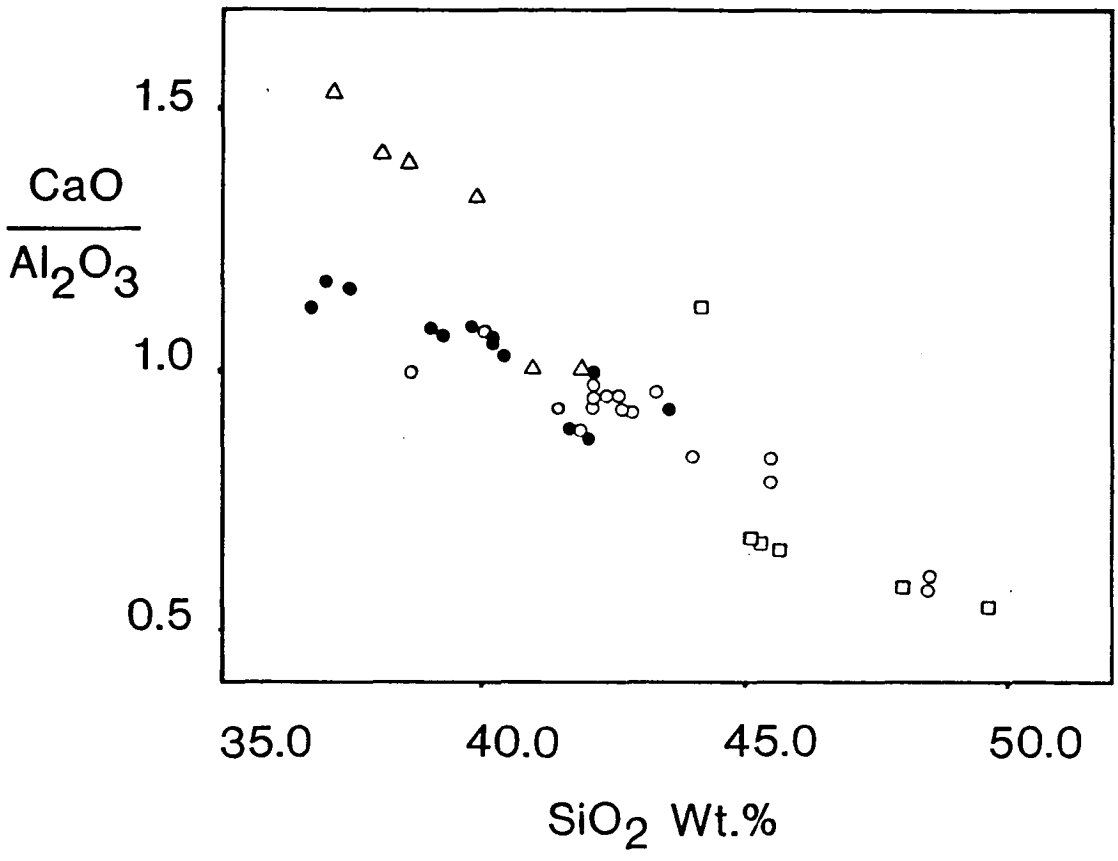

Fig. 15. CaO/Al_2O_3 ratios versus SiO_2 content for primitive alkaline basalts. Triangles show compositions from the Canary Islands (Schmincke in von Rad et al., 1982), squares the Newer Volcanics of Victoria (Irving & Green, 1976), filled circles Honolulu (Clague & Frey, 1982), and open circles the North Hessian Depression (Wedepohl, 1983).

volatiles (with up to 6.5 wt.% combined H_2O and CO_2), none of them contained more than 2 wt.% CO_2 (except that of the Laughing Jack Marsh olivine melilitite, LJM, which contained 7 wt.% CO_2 and 7 wt.% H_2O). It can be seen from Fig. 7, that a major effect of adding H_2O-rich fluids to simple basaltic systems is an expansion of the orthopyroxene phase volume to more CA-rich parts of the CMAS system. It has been suggested earlier, that in natural systems (such as represented by compositions (dots) 26 to 35 in Figs. 16 & 17) the olivine-orthopyroxene cotectic extends to SiO_2-poor compositions (with < 45 wt.% SiO_2) at high pressures. The reason for orthopyroxene appearing as a liquidus phase of some natural basalts, only after H_2O is added to their compositions, can in this context be seen as the result of H_2O expanding the orthopyroxene phase volume against those of garnet and clinopyroxene, rather than an effect on the olivine-orthopyroxene cotectic. The effects of larger concentrations of more CO_2-rich fluids on natural systems can be estimated from results in the simple CMAS system (Figs. 8 & 9) and from the results of the liquidus studies of Brey & Green (1977) on the Laughing Jack Marsh olivine melilitite (see Figs. 16 & 17). In order to achieve garnet lherzolite saturation in the Laughing Jack Marsh olivine melilitite at 30 kb, Brey & Green added 7 wt.% H_2O and 7 wt.% CO_2 to its original composition. In this case, the high CO_2 content of the added volatile component has resulted in the stabilization of orthopyroxene in a very SiO_2-poor basaltic liquid (approximately 38 wt.% SiO_2) at relatively low pressure (30 kb). This reflects the strong control of CO_2 on the position of olivine-orthopyroxene cotectic.

Consideration of the data combined in Fig. 16 shows that both variable pressure and/or activities of CO_2 during peridotite melting could be used to explain the natural range of primitive alkaline basalt compositions. The data available are not sufficient to determine differences that might occur between SiO_2-poor alkaline basalts (e.g. olivine nephelinites and olivine melilitites) produced at high pressures (>> 30 kb), and those produced at intermediate pressures (20-30 kb) in the presence of high CO_2 concentrations. It is possible to say, however, that if CO_2 is a prime factor which determines the very SiO_2-poor compositions of some alkaline basalts, then it must originally have been present in them in quite high concentrations (> 5 wt.%).

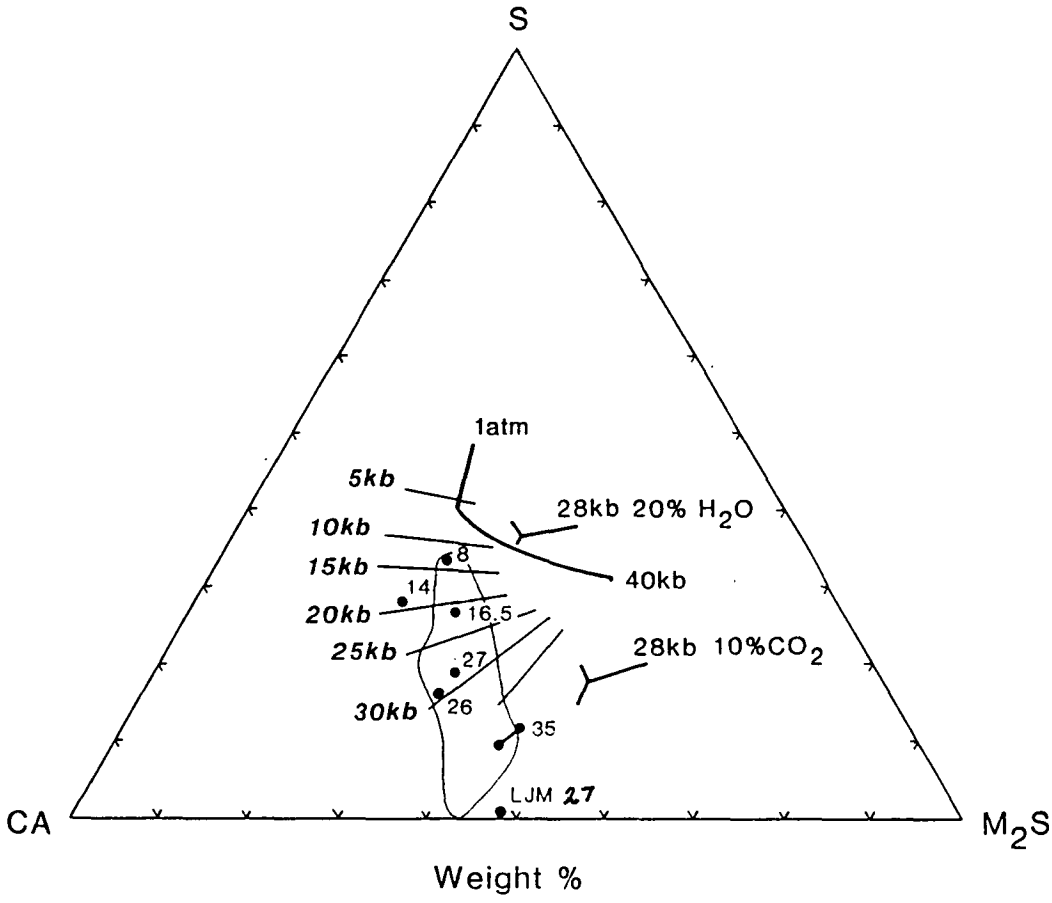

Fig. 16. Compositions of complex ("natural") and simple system liquids in equilibrium with clinopyroxene + orthopyroxene + olivine ± plagioclase ± spinel ± garnet projected from the point CS onto the plane S-CA-M_2S (see text). Isobaric cotectics for complex liquids in equilibrium with lherzolite are shown as a series of straight lines (see Fig. 12). Shown by the heavy curved line is the locus of liquid compositions, between 1 atm. and 40 kb, in equilibrium with simplified plagioclase, spinel and garnet-lherzolite of the CMAS system. Also shown for the CMAS system, are the 28 kb garnet-lherzolite-liquid invariant points for liquids containing 20 wt.% H_2O, and 10 wt.% CO_2. Enclosed by the light curved line is the compositional field of primitive alkaline basalts from the Canary Islands, the Newer basalts of Victoria, Honolulu, and the North Hessian Depression of Germany (see text for references). Dots show the compositions of natural basalts for which conditions of lherzolite ± plagioclase ± garnet have been determined. The dumbell shape represents a composition bracketed between two others, one in equilibrium with garnet + clinopyroxene + olivine, and the other (the 1st composition + 10% enstatite) in equilibrium with orthopyroxene. Small numbers next to the dots and dumbell, indicate in kb, the pressure at which each basalt equilibrated with lherzolite (see text for references). LJM is the Laughing Jack Marsh Olivine melilitite composition studied by Brey & Green (1977).

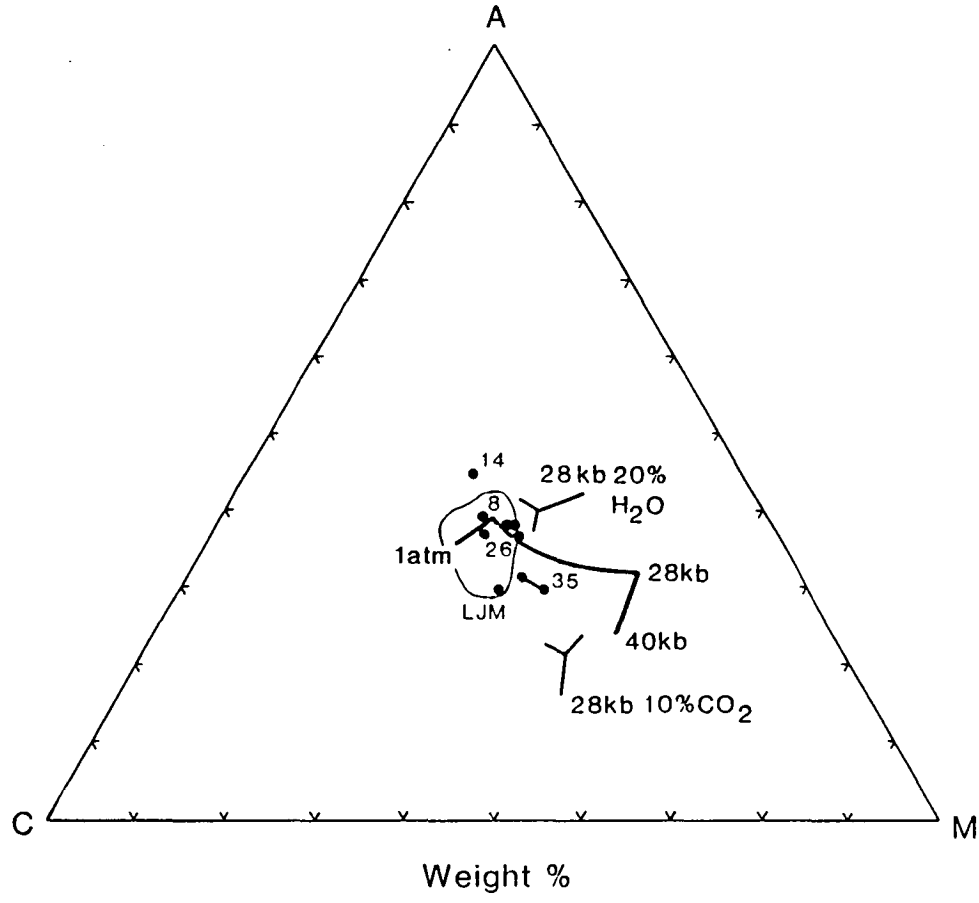

Fig. 17. Compositions of natural and simple system (CMAS) liquids that have been experimentally equilibrated with clinopyroxene + orthopyroxene + olivine ± plagioclase ± spinel ± garnet. Projection is from S. Symbols are as for Fig. 16.

Basaltic glasses quenched under submarine conditions rarely contain more than about 0.5 wt.% CO_2 (Garcia et al., 1978; Harris & Anderson, 1983; Sakai et al., 1984; Byers et al., 1985). Volatile loss from magmas prior to eruption may be responsible in part for these low concentrations (Greenland et al., 1985). Published analyses of submarine glasses are also predominantly of tholeiitic and mildly alkaline samples that are unlikely to have ever contained high volatile concentrations. Subaerially erupted basalts probably lose most of their volatiles during eruption and subsequent crystallization. Because of the low solubility of CO_2 in basalt magmas at pressures less than about 10 kb (Mysen et al. 1975), CO_2-rich magmas which crystallize in subvolcanic dykes should also lose most of their original CO_2 concentrations during emplacement and crystallization. In spite of these expectations, alkaline lamprophyres with compositions similar to those of basanites and nephelinites are often carbonate rich. An average of alkaline lamprophyre compositions compiled by Rock (1977) contained 2.0-2.5 wt.% CO_2. Individual compositions may contain as much as 8 wt.% CO_2 (Barreiro & Cooper, 1987; Goto & Arai, 1987). In contrast, non-lamprophyric alkaline basalt lavas and dykes are typically carbonate poor, rarely containing more than about 2 wt.% CO_2 (see references for Fig. 4). It is possible that SiO_2-poor alkaline basalt magmas (with 45-38 wt.% SiO_2) may be produced both at high pressures (25-50 kb) in the presence of relatively low CO_2-concentrations (< 3 wt.%), and at lower pressures (15-30 kb) in the presence of higher CO_2 concentrations (> 5 wt.%). Petrography, geochemistry, and other relevant geological information, may be needed to decide in individual cases which of the two mechanisms, if either, offers the more likely explanation.

PART II

GEOCHEMISTRY AND EXPERIMENTAL PETROLOGY OF SODIC ALKALINE BASALTS FROM THE OATLANDS DISTRICT OF TASMANIA

2.1 INTRODUCTION

Sodic and mildly-potassic alkaline basalts occur in a variety of geological and tectonic environments worldwide. Although perhaps best known from studies of ocean islands, they are also common in continental intra-plate and some back-arc environments. In relative terms they are a volumetrically minor basalt association. Compared to more voluminous basalt types, however, they are unusually enriched in alkalis and other incompatible components. This, together with the upper mantle xenoliths they frequently contain, has made them a popular subject of study. Individual studies regarding their origin (e.g. O'Hara, 1968; Coombs & Wilkinson, 1969; Bultitude & Green, 1971; Brey & Green, 1974; Mysen & Boettcher, 1975; Sun & Hanson, 1975; Frey et al., 1978) have emphasized to varying degrees the importance of crystal fractionation, source composition, degree of partial melting, residual phases, volatiles (particularly H_2O and CO_2) and physical conditions of origin in determining their compositions.

In the present study, an attempt has been made to use geochemical and experimental data, in combination with other relevant geological information, to obtain information on the processes and conditions which formed a small group of alkaline basalts from the Oatlands district of southeastern Tasmania. The first part of the paper is devoted to describing the field relationships, petrography, mineralogy and chemical composition of these basalts. This is followed by the description of an experimental study, and by a discussion of possible models for the origin of the Oatlands basalts.

2.2 CAINOZOIC VOLCANISM IN THE OATLANDS DISTRICT

The Oatlands district (Fig. 18) forms part of a very much larger Cainozoic basalt province that extends discontinuously along the length of eastern Australia (see Wellman & McDougall, 1974).

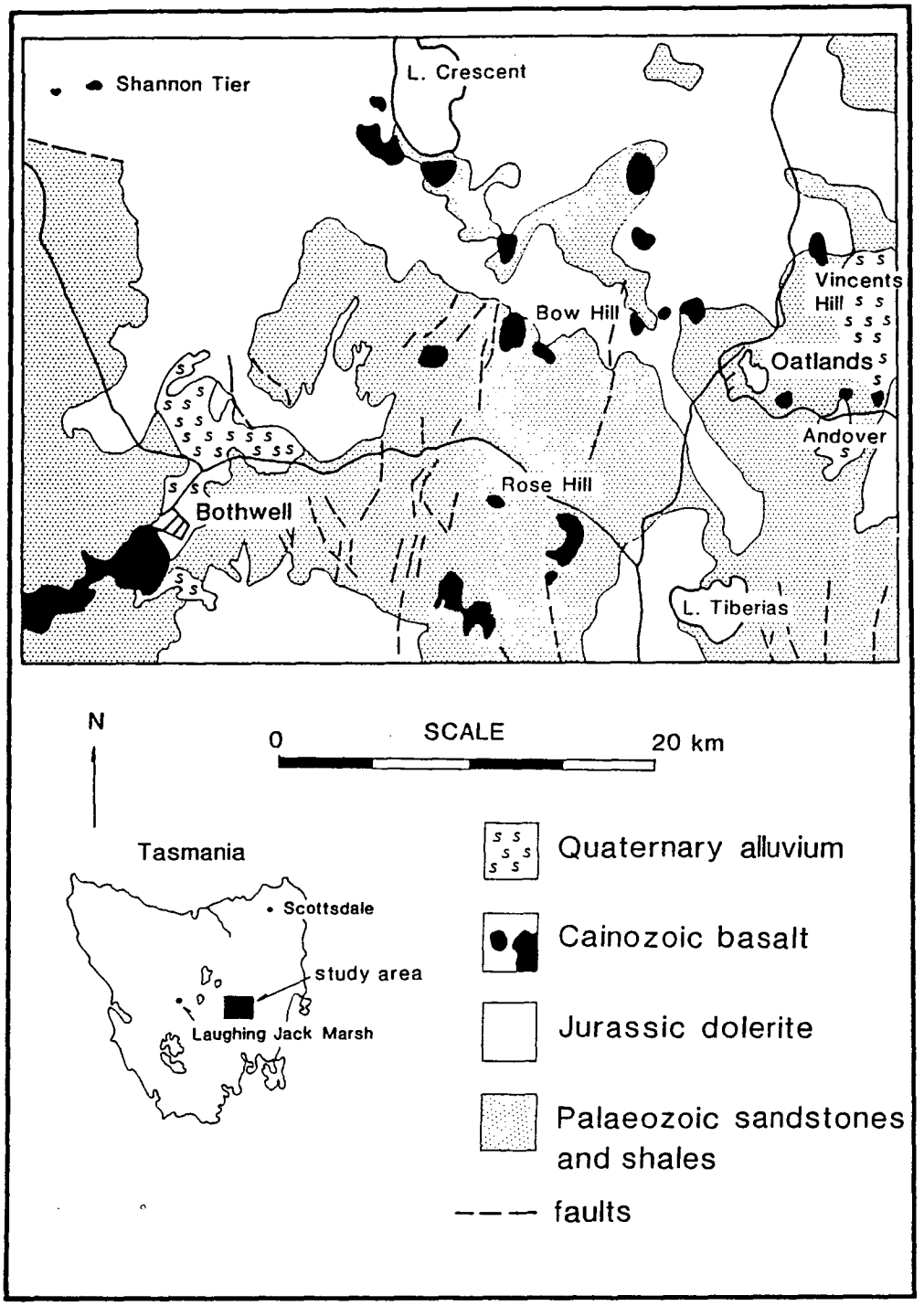

Fig. 18. Geology of the Oatlands district simplified from Gulline & Forsyth (1976), and Sutherland (1984)

Basalts within the district occur mainly as isolated flow remnants and plugs. Diatremes of basaltic breccia also occur. In places an inverted topography has developed where ridge-forming basalt lavas originally flowed down valleys in the ancestral topography (Sutherland, 1984). Volcanic activity within the Oatlands district occurred mainly during the late Oligocene (Sutherland, 1984) and is of similar age to volcanism on the neighbouring Central Plateau and in the Hobart area (Sutherland, 1984; Sutherland et al., 1973).

Upper crustal rocks in the Oatlands district include carbonaceous shales and quartz sandstones of the Permo-Triassic Parmeener Supergroup (see Banks & Clarke, 1987) and Jurassic dolerite. Fragments of these are common as inclusions within the basalts. Faulting within the region is common. Although most of the faulting was produced by wrench tectonics during the late Mesozoic, extensional tectonics are associated with graben formation during the early Tertiary (Berry & Banks, 1985). Continued faulting may have occurred into the late Tertiary (Gunn, 1975). Samples for study were collected from five localities. Descriptions of these and of the collected samples are given in the following section.

2.2.1 Bow Hill

Nepheline basanite (sample UT-70489) and transitional nephelinite (samples UT-70490-91) lavas occur within a series of flows that form two isolated remnants capping Bow Hill. The lavas contain an abundance of small peridotite xenoliths. Included amongst these are rare garnet lherzolite xenoliths (Sutherland et al., 1984). Large (2-5 cm) megacrysts of glassy-black clinopyroxene are also common. Similarly sized megacrysts of spinel and olivine are also present, although they are comparatively rare. In hand specimen the basalts are dark-grey and aphyric, with a blocky fracture. In thin section, microphenocrysts of olivine and clinopyroxene (0.2-0.5 mm) form up to 8% of the basalts' volume. The clinopyroxenes have spongy pale-green cores surrounded by pinkish-brown rims. Euhedral olivine phenocrysts frequently contain melt inclusions, sometimes with fluid bubbles. The phenocrysts occur within a fine groundmass of clinopyroxene, magnetite, apatite, nepheline, alkali feldspar and zeolites. Occasional veins of zeolite, carbonate and clinopyroxene intermesh with the surrounding groundmass and appear to be of late

magmatic origin. Olivine xenocrysts formed by disaggregation of the peridotite inclusions are common. They can be distinguished from phenocrysts by their larger size and irregular form.

2.2.2 Vincents Hill

Analcime basanites at Vincents Hill (samples UT-70493-94) form a sequence of flows some thirty metres in thickness. Petrographically they are similar to the nephelinites at Bow Hill, although they are noticeably richer in zeolite. Segregations and veins of analcime, alkali feldspar and pyroxene are abundant within the basanites. The uppermost flow of the sequence is an alkali olivine basalt (sample UT-70492) which contains small (0.2mm) olivine phenocrysts within a fine groundmass of plagioclase laths, alkali feldspar, clinopyroxene and magnetite.

2.2.3 Andover

Olivine tholeiite (sample UT-70497) containing inclusions of spinel lherzolite occurs approximately nine kilometres ESE of Andover (see Sutherland, 1974). The tholeiite contains about five percent of small euhedral olivine phenocrysts. These are set in a groundmass of plagioclase laths (An_{62}), pinkish-brown clinopyroxene, magnetite, and brown glass.

2.2.4 Rose Hill

Alkali olivine basalt (sample UT-70495) forms a small flow remnant at Rose Hill. This contains small (0.2mm) euhedral olivine phenocrysts within a fine groundmass of plagioclase laths (An_{58}), alkali feldspar, clinopyroxene, magnetite and apatite. Small peridotite inclusions are abundant within the basalt. Less abundant clinopyroxene megacrysts also occur.

2.2.5 Shannon Tier

A number of small olivine melilitite plugs occur at Shannon Tier, approximately twenty two kilometres NNW of Bothwell (Fig. 18). Although geographically this area is more properly regarded as part of the Central Plateau, it has been included in order to extend the

range of basalt compositions considered by this study. At one of the outcrops, from which the analysed sample was taken (sample UT-70496), the melilitite has a very fresh appearance and is associated with a small coarse-grained body of ijolite (see Edwards, 1950; Taylor et al., 1988). Although recognizable spinel lherzolite xenoliths were not found at the outcrop, xenocrysts of magnesian olivine and Cr-rich spinel can be seen in thin section. Small euhedral olivine phenocrysts occur within a groundmass of clinopyroxene, magnetite, olivine, melilite, perovskite, apatite and nepheline.

2.3 MINERALOGY

2.3.1 Phenocrysts

Representative analyses of phenocryst and megacryst phases are given in Table 5. Analyses were performed with a JEOL JXA50A electron microprobe at the University of Tasmania. For most analyses an energy dispersive system was used. Details of techniques and data reduction procedures are given by Ware (1981). Analyses of NiO, MnO and CaO in olivine phenocrysts from a nepheline basanite (UT-70489 from Bow Hill) were performed on the same instrument by wavelength dispersive analysis using techniques and correction routines based on those of Duncumb & Reed (1968). For most elements, the absolute precision of analyses performed by energy dispersive techniques was $\pm$ 0.2 wt.%, whereas that for analyses done by wavelength dispersive techniques was $\pm$ 0.05 wt.%.

Olivine phenocryst cores in the basalts range in Mg# from 87.6 to 67.4 (where Mg# = molecular $100Mg/(Mg + Fe^{+2})$. Maximum measured Mg# values in olivine phenocryst cores increase with increasing host rock Mg#. Within individual samples the forsterite contents of olivine phenocryst cores vary by as much as 8%; in contrast to this, zoning within individual crystals is relatively limited. Olivine phenocrysts in the nepheline basanite UT-70489 from Bow Hill contain from 0.35 to 0.17 wt.% NiO, and 0.12 to 0.25 wt.% MnO (Table 5). The highest NiO and lowest MnO occur in olivine phenocrysts with the highest Mg#.

Table 5. Representative analyses of phenocryst and megacryst phases

	UT-70489			UT-70490		UT-70494		UT-70496	*Bow Hill* Megacrysts				
	Ol	Ol	Cpx	Ol	Cpx	Ol	Cpx	Ol	Cpx	Cpx	Ol	Sp	Sp
SiO_2	40.10	39.62	50.07	38.50	49.42	39.43	48.24	40.04	49.63	49.75	39.42		
TiO_2			1.34		2.01		3.09		1.03	0.95		0.30	0.40
Al_2O_3			4.28		3.45		5.21		8.79	9.02		64.10	61.44
Cr_2O_3			1.23		0.23								
Fe_2O_3			(1.77)[2]		(3.45)[2]		(1.97)[2]		(1.70)[2]	(1.38)[2]		(4.46)[2]	(6.14)[2]
FeO	12.41	13.06	5.13[1]	20.75	6.77[1]	16.56	8.05[1]	12.72	6.15[1]	5.73[1]	17.29	10.72[1]	18.51[1]
MnO	0.15*	0.12*											
NiO	0.30*	0.35*											
MgO	46.90	46.66	14.24	40.63	14.20	43.87	12.08	47.23	14.38	14.51	43.28	20.09	19.15
CaO	0.14*	0.18*	22.77	0.12	23.54	0.14	22.52		18.71	18.76			
Na_2O			0.64		0.38		0.38		1.31	1.29			
oxygens	4	4	6	4	6	4	6	4	6	6	4	4	4
Si	0.997	0.989	1.858	0.993	1.845	0.997	1.809	0.994	1.813	1.813	0.999	0.006	0.008
Ti			0.037		0.056		0.087		0.028	0.026		0.006	0.008
Al			0.187		0.152		0.230		0.378	0.387		1.904	1.867
Cr			0.036		0.007								
Fe^{+3}												0.085	0.118
Fe^{+2}	0.258	0.273	0.159	0.448	0.211	0.349	0.252	0.264	0.188	0.174	0.366	0.232	0.278
Mn	0.003	0.003											
Ni	0.006	0.007											
Mg	1.736	1.735	0.788	1.562	0.791	1.653	0.674	1.747	0.783	0.788	1.635	0.774	0.730
Ca	0.004	0.005	0.905	0.003	0.028	0.002	0.905		0.732	0.732			
Na			0.046		0.028		0.060		0.093	0.091			
sum	2.998	3.011	4.016	3.006	4.032	3.001	4.019	3.006	4.015	4.011	3.000	3.007	3.009
Mg#	87.1	86.4	83.2	77.7	78.9	82.5	72.8	86.9	80.6	81.9	81.7	76.9	70.2

* analysed by wavelength dispersive micro-probe

Ol-olivine, Cpx-clinopyroxene, Sp-spinel

1 FeO = total iron

2 Fe_2O_3 calculated assuming perfect stoichiometry (figures not included in totals)

Clinopyroxene phenocryst cores range from Mg# 83.2 to 72.7 if total iron is expressed as FeO (Table 5). Higher ratios, covering the range of olivine Mg# values, are obtained if ferric iron concentrations are calculated on the basis of assumed stoichiometry. Cr_2O_3 concentrations vary sympathetically with Mg#; the maximum measured concentrations of 0.9 to 1.2 wt.%, measured in phenocrysts from UT-70489, are similar to those in Cr-diopsides from upper mantle xenoliths.

2.3.2 Megacrysts

Although megacrysts occur at all of the localities visited, only examples from Bow Hill were studied. As mentioned previously, the megacrysts at Bow Hill include clinopyroxene, spinel and olivine. One of the olivine megacrysts collected contained inclusions of clinopyroxene. A clinopyroxene megacryst was also found intergrown with spinel. These intergrowth relationships indicate that the megacrysts at Bow Hill probably belong to a genetically related suite. The spinel megacrysts at Bow Hill are mainly hercynite-spinel solid solutions and have Cr_2O_3 concentrations below the detection limits of the microprobe (0.07 wt.%). The O'Neill & Wall (1987) olivine spinel Fe-Mg exchange thermometer suggests crystallization temperatures of 900-1120°C for the olivine and spinel megacrysts.

The clinopyroxene megacrysts have a limited range of Mg# from 79.2 to 81.9 (12 samples). Compositional zoning within megacrysts was not detected. Compared to clinopyroxene phenocrysts in the basanite lavas, the megacryst pyroxenes are richer in Al_2O_3 and Na_2O, and poorer in TiO_2 and CaO. Ferric iron contents, calculated assuming stoichiometry, are similar to those in the phenocrysts.

2.4 MAJOR AND TRACE ELEMENT CHEMISTRY

Whole-rock major and trace element concentrations for nine samples are presented in Tables 6 and 7. Chondrite-normalized plots of rare earth elements and of other trace and minor elements are shown in Figs. 19 and 20. For comparison with the Oatlands samples, analyses of an olivine melilitite from Laughing Jack Marsh, and an

Table 6. Major and minor element analyses of basalts from the Oatlands district

	Bow Hill			Vincents Hill			Rose Hill	Shannon Tier	Andover		Scotts -dale	Laughing Jack Marsh
No.[1]	489	490	491	492	493	494	495	496	497	T14[3]	2854[3]	2927[3]
SiO_2	43.96	42.27	42.30	45.20	42.75	42.76	45.76	36.56	50.02	49.75	39.31	37.79
TiO_2	2.33	2.89	2.94	2.86	3.16	3.19	2.92	2.65	1.92	1.92	3.37	2.69
Al_2O_3	11.36	11.61	11.72	12.36	11.12	10.95	14.02	10.00	13.30	13.35	9.46	9.46
Fe_2O_3[2]	13.05	14.72	14.89	14.56	14.91	14.96	14.86	15.83	12.92	12.90	16.95	14.12
MnO	0.19	0.20	0.20	0.20	0.22	0.22	0.19	0.27	0.18	0.18	0.20	0.24
MgO	12.02	9.92	9.52	8.87	10.37	10.56	8.54	11.71	8.49	8.37	13.91	16.20
CaO	9.38	10.18	10.32	10.06	10.61	10.69	8.33	14.84	9.38	9.80	11.21	13.03
Na_2O	4.20	4.54	4.53	3.71	4.06	3.88	3.10	4.91	2.84	2.85	2.98	3.72
K_2O	2.08	2.21	2.09	1.13	1.45	1.47	1.35	1.72	0.59	0.53	1.53	1.42
P_2O_5	1.43	1.45	1.49	1.05	1.35	1.32	0.93	1.51	0.36	0.35	1.08	1.33
Total	100.00	100.00	100.00	100.00	100.00	100.00	100.00	100.00	100.00	100.00	100.00	100.00
LOI	1.55	1.50	1.52	-0.25	1.47	1.13	1.13	1.00	1.22			
Mg#	68.2	61.6	60.3	59.1	62.3	62.6	57.7	63.7	60.5	61.0	65.8	72.7
Mg# = $100Mg/(Mg+Fe^{+2})$ for $Fe_2O_3/FeO = 0.2$												
or	12.42	13.22	12.49	6.78	8.66	8.79	8.11		3.51	3.2		
ab	7.20	1.14	2.37	18.43	7.28	7.19	24.87		24.31	25.1		
an	6.07	4.82	5.52	13.88	7.95	8.25	20.54	0.19	22.01	22.9	8.1	5.1
ne	15.61	20.45	19.74	7.24	14.88	14.08	0.95	22.79			14.0	17.4
cpx	25.51	29.81	29.70	24.26	29.58	29.72	12.36	12.47	18.44	20.4	25.9	11.7
opx									19.19	19.7		
ol	22.41	18.28	17.67	18.20	19.05	19.34	22.06	29.11	5.07	1.7	28.7	36.0
mt	2.88	3.24	3.28	3.21	3.29	3.30	3.27	3.49	2.90	2.2	3.9	3.1
il	4.48	5.55	5.66	5.49	6.07	6.14	5.60	5.11	3.69	3.8	6.6	5.2
ap	3.41	3.48	3.56	2.50	3.22	3.18	2.23	3.62	0.87	0.9	2.6	3.2
cs								15.17			3.0	11.6
lc								8.04			7.3	6.7

1 University of Tasmania catalogue numbers prefixed by UT-704

2 Fe_2O_3= total iron

3 analyses from Table 2 of Frey et al. (1978)

Norms were calculated assuming $Fe_2O_3/FeO = 0.2$

Table 7. Trace element analyses of basalts from the Oatlands district

	Bow Hill			Vincents Hill			Rose Hill	Shannon Tier	Andover		Scotts -dale	Laughing Jack Marsh
No.[1]	489	490	491	492	493	494	495	496	497	T14*	2854*	2927*
Rb	30	37	36	23	25	26	33	98	12	9	12	29
Sr	1520	1434	1442	903	1213	1233	847	1436	400	373	1250	1440
Ba	727	705	719	392	596	559	440	811	177	125	250	530
Cr	529	360	271	216	316	131	278	222	324	312	410	510
Ni	380	251	204	194	229	226	343	194	212	103	366	458
V	141	148	159	198	198	197	141	236	174	142	194	229
Zn	168	211	178	152	169	170	180	150				
Cu	55	59	50	51	54	51	100	76				
Nb	139	145	145	85	125	123	75	182	26		97	99
Zr	498	513	519	341	522	518	345	317	139	146	320	243
Sc	13	14	13	23	20	22	22	22	27	26	19	24
Y	41	42	41	39	45	43	42	25	26	27	28	31
La	103			63	96			114	19.7	17.6	62.2	75
Ce	194			131	185			202	42.7	44.7	140	160
Pr	21.5			15.5	21.5			23.2	5.5			
Nd	82			61	83			92	24.1	22	57.2	64
Sm	13.5			10.7	13.1			15.6	5.3	5.08	11.9	12.3
Eu	3.78			3.11	3.85			4.29	1.82	1.85	3.9	3.65
Gd	11.4			9.55	11.3			11.8	6.0			
Dy	8.9			8.1	9.2			8.1	5.2			
Er	3.51			3.44	4.23			3.10	2.43			
Yb	1.77			2.28	2.60			2.00	1.62	1.9	1.42	1.80

* analyses from Table 10 of Frey et al. (1978)

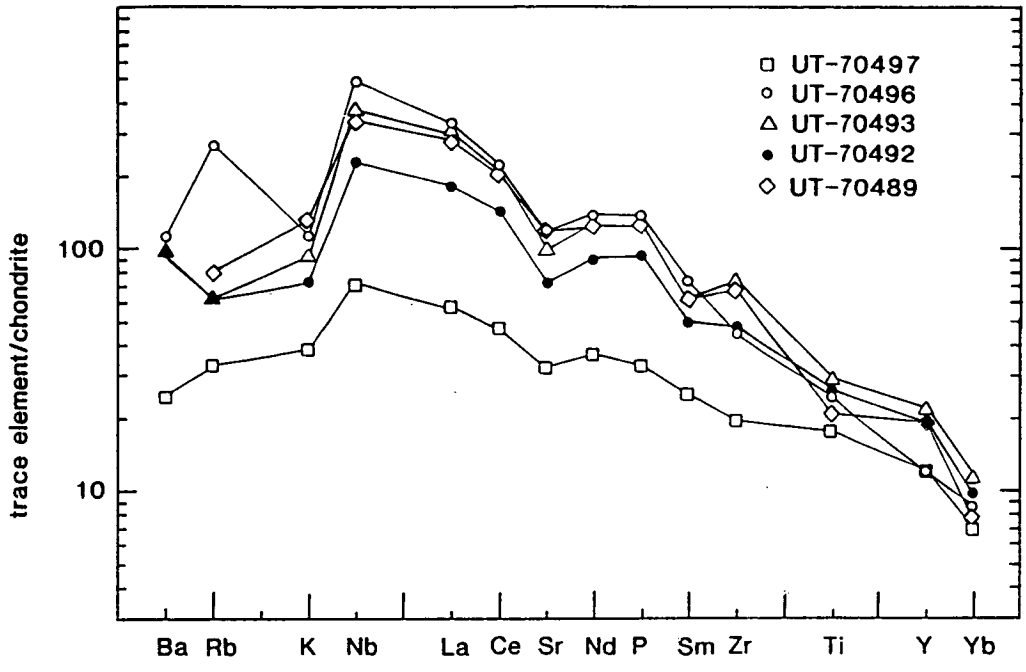

Fig. 19. Chondrite-normalized minor and trace element concentrations in Cainozoic basalts from the Oatlands district. Normalization factors are from Thompson (1982)

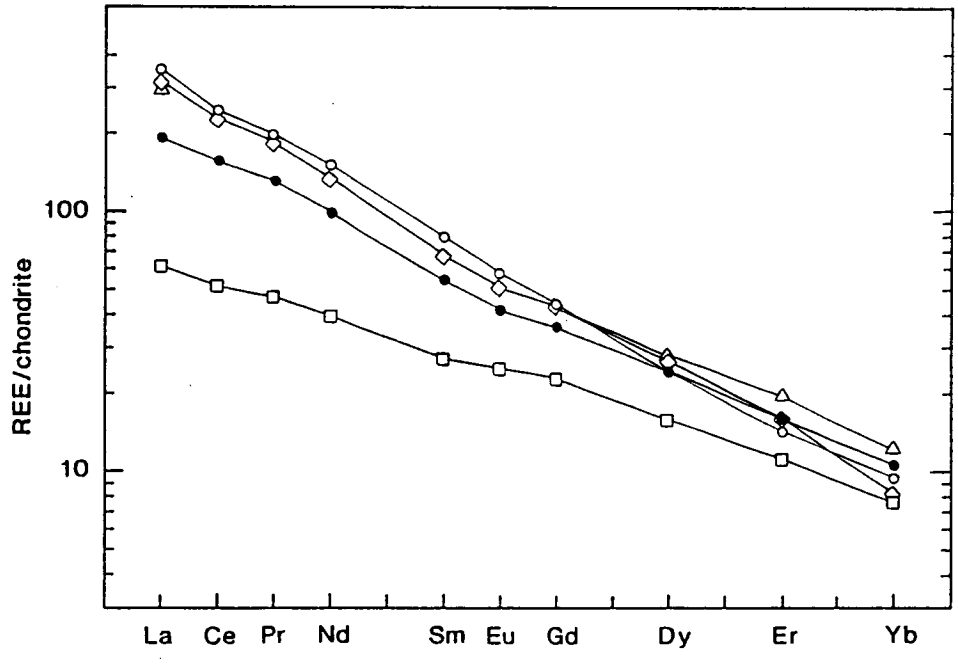

Fig. 20. Chondrite-normalized rare earth element concentrations in Cainozoic basalts from the Oatlands district

olivine nephelinite from Scottsdale [Tables 6 & 7] (see Brey & Green, 1974; Frey et al., 1978) are also given. The analysed samples were selected to include the range of primitive basaltic compositions (from olivine tholeiite to olivine melilitite) present in the Oatlands district. Prior to analysis, samples were first crushed to small chips less than 1 cm in size. Chips free of lherzolite debris were then selected for analysis. Analyses were performed on a Philips PW1410 XRF spectrometer at the University of Tasmania following the methods of Norrish & Chappell (1977). Rare earth element (REE) analyses were obtained by using an ion exchange XRF procedure (Robinson et al., 1986).

Compared to similarly mafic alkaline basalts from other parts of the world, the nepheline basanites and transitional nephelinites in the Oatlands district are unusually rich in alkalis, P_2O_5 and light rare earth elements. In other respects, however, they are little different. In particular, they share some characteristic patterns of inter-element variation. Some of these are shown in Fig. 21. At similar values of Mg#, there is a tendency for CaO, CaO/Al_2O_3, alkalis, P_2O_5 and incompatible trace elements to increase as SiO_2 decreases. These tendencies are most systematically developed in provinces, such as Honolulu and the north Hessian Depression of Germany, where basalts have been erupted within a limited area and period of time (generally less than a few million years).

It can be seen in Fig. 21 that the highly SiO_2-undersaturated basalts from Shannon Tier, Laughing Jack Marsh and Scottsdale have relative concentrations of alkalis, P_2O_5 and SiO_2 that are displaced from the trends of less SiO_2-undersaturated basanites and alkali olivine basalts from the Oatlands district. This feature is in contrast to the elongate and continuous trends that occur between alkaline basalts in provinces such as the north Hessian Depression and Honolulu. Unlike in the latter two provinces, however, Cainozoic volcanism in Tasmania occurred over a relatively large area and period of time (> 30 ma; Sutherland & Wellman, 1986). Episodic volcanism during this time may have produced numerous small volcanic provinces with locally distinct characteristics. Similar provincialism has been found to characterise Cainozoic volcanism in other parts of eastern Australia (Wellman & McDougall, 1974; Price

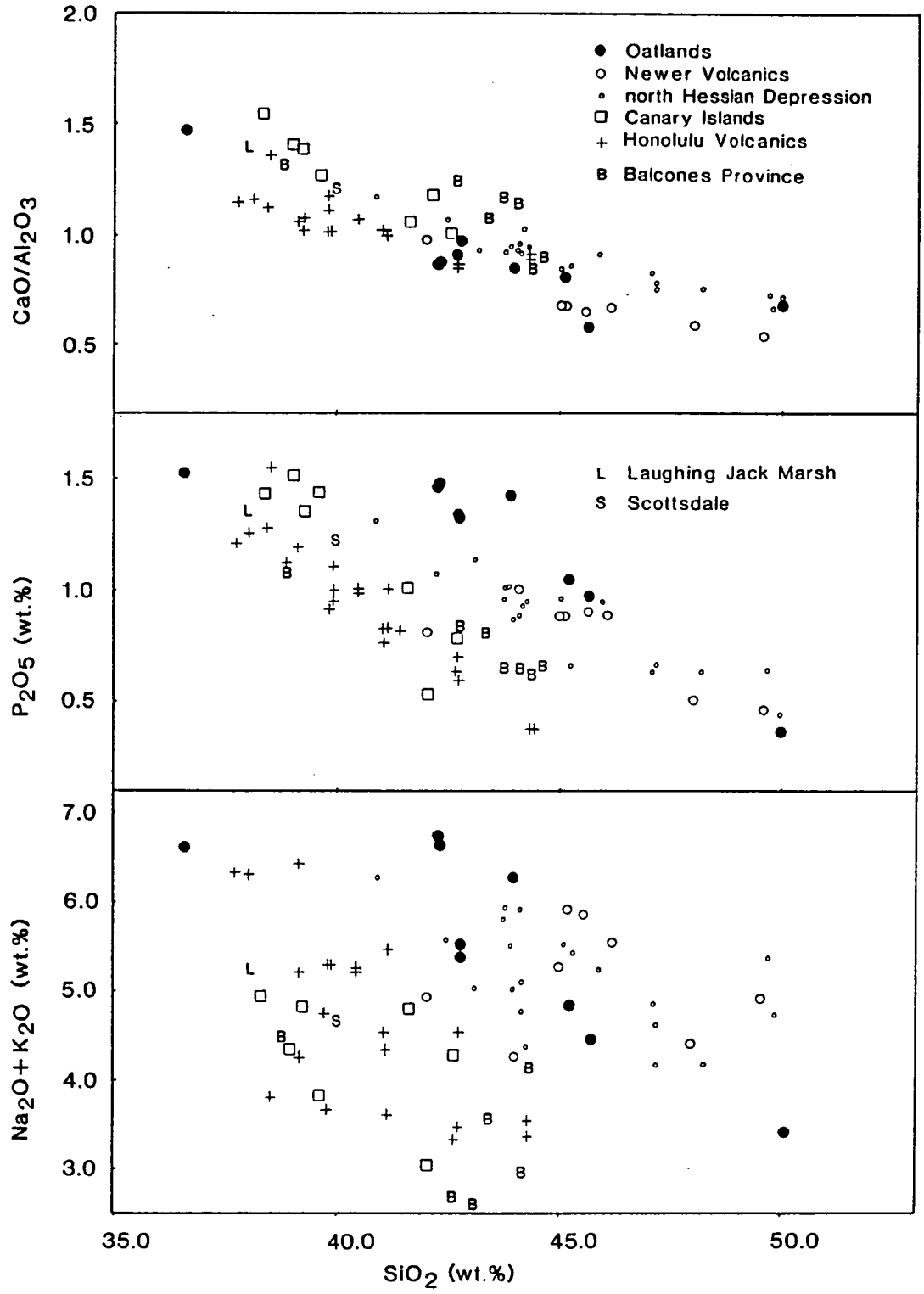

Fig. 21. Inter-element trends in basalts from the Oatlands district and in primitive alkaline basalts from the Newer Volcanics of Victoria , the north Hessian depression of Germany , the Canary Islands , Honolulu , and the Balcones province of Texas . Data sources are Irving and Green (1976), Clague and Frey (1982), Schmincke (in von Rad et al., 1982), Wedepohl (1983), and Barker et al. (1987)

et al., 1988). Basalts in the Oatlands district may therefore represent a local magmatic event distinct from those which formed olivine melilitites on the Central Plateau and olivine nephelinites at Scottsdale.

2.5 CRYSTAL-LIQUID EQUILIBRIA

2.5.1 Phenocrysts

Shown in Fig. 22 is a plot of maximum measured Mg# in olivine phenocrysts against host basalt Mg#. Also plotted for comparison is the maximum Mg# of olivine phenocrysts in the olivine nephelinite (2854) from Scottsdale. Only phenocrysts in UT-70489, UT-70496 and 2854 plot close to the line relating variation of olivine Mg# to changing Mg# of the melt phase, for an olivine/liquid Fe-Mg exchange K_d equal to 0.30 (Roeder and Emslie, 1970). It is possible that olivine phenocrysts in these samples have retained their original liquidus compositions. It would also be likely in this case that the compositions of UT-70489, UT-70496 and 2854 represent close approximations to original liquid compositions. This is made more probable by the relatively low phenocryst concentrations (8 volume % or less) contained by these samples.

2.5.2 Megacrysts

On the basis of petrography, isotopic and other compositional data, and of experimental studies, pyroxene megacrysts found in alkaline basalts have often been considered as the crystallization products, either of the basalts in which they occur, or of closely related magma compositions (Green & Hibberson, 1970; Irving, 1974; Knutson & Green, 1975; Stuckless & Irving, 1976; Liotard et al., 1988). In the case of the Bow Hill clinopyroxene megacrysts, no close compositional match was found with published analyses of experimentally produced liquidus pyroxenes. A good match was found, however, with unpublished analyses of pyroxenes experimentally crystallized from a nepheline mugearite (Irving & Green unpublished data); these are very similar to several of the Bow Hill clinopyroxene megacrysts (Table 5) except for their slightly lower Al_2O_3 concentrations.

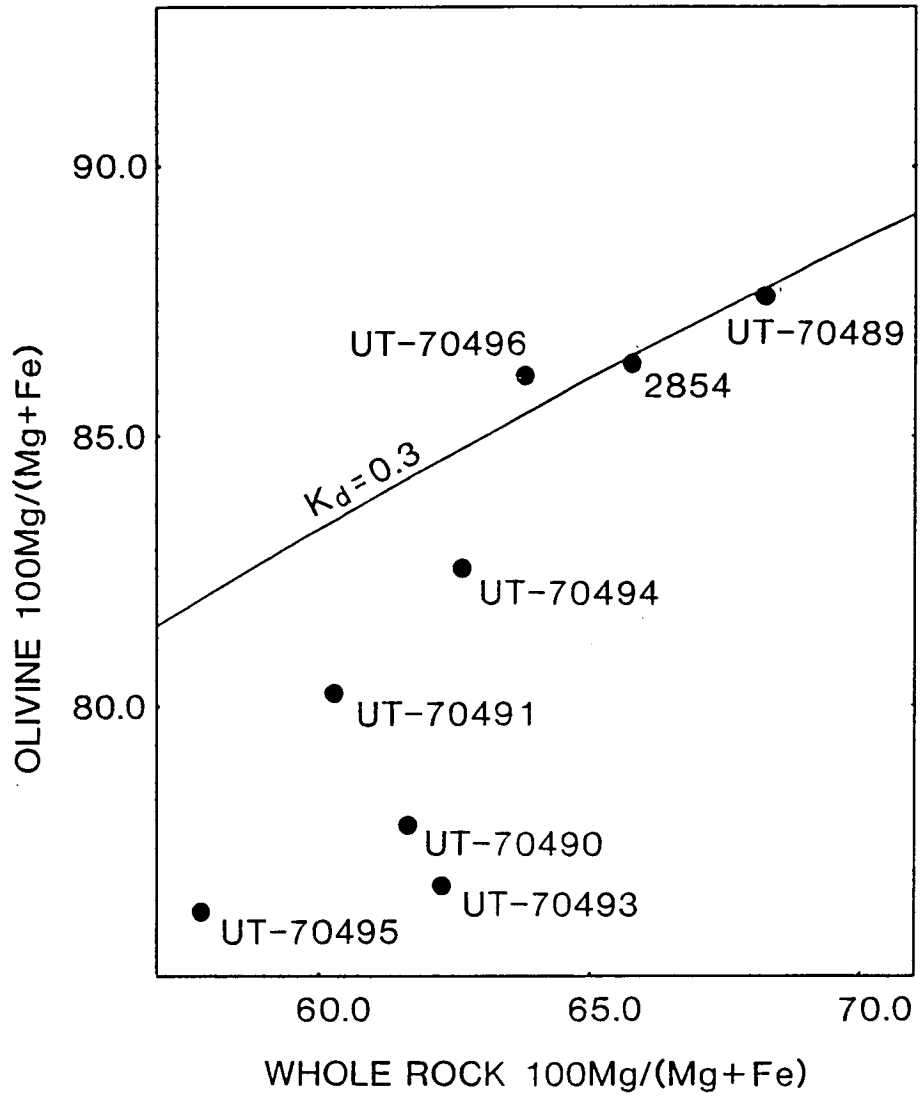

Fig. 22. Variation of maximum measured Mg# of olivine phenocrysts (dots) with Mg# of host basalts. The curve represents the variation of liquidus olivine Mg# with changing Mg# of the melt phase for an olivine/melt Fe-Mg exchange K_d = 0.3 (Roeder and Emslie 1970)

It seems probable, therefore, that the megacrysts at Bow Hill crystallized from an alkaline magma similar in composition to some of the more evolved lavas of the Oatlands district (see Sutherland, 1984). They are unlikely to have crystallized from the relatively Cr-rich basalts in which they were found. This is because the spinel megacrysts found at Bow Hill do not contain detectable Cr, and spinel/melt partition coefficients for Cr are known to be very high (Hill & Roeder, 1974; Maurel & Maurel, 1982).

2.6 CAUSES OF MAJOR AND MINOR ELEMENT VARIATION AMOUNGST THE OATLANDS BASALTS

Except for the Tasmanian basalts, the compositional trends shown in Fig. 21 are for samples that have Mg# within the range 67.0 to 71.0. The interoxide variations shown in Fig. 21 are therefore unlikely to have been produced by crystal fractionation. They are more probably primary features that were produced during melting of peridotite within the basalts source region.

2.6.1 The Effects of Pressure and Variable Degrees of Melting

Experiments on peridotite melting, such as those of Jaques & Green (1980), Takahashi & Kushiro (1983), Fujii & Scarfe (1985), Falloon & Green (1988) and Falloon et al. (1988), have shown that for a particular peridotite composition, concentrations of alkalis and P_2O_5 in the liquid are highest at low degrees of melting and decrease as the degree of melting increases. Experiments on volatile-free systems have also shown that increasing pressure decreases SiO_2 concentrations in liquids in equilibrium with peridotite (Presnall et al., 1978; op. cit.). However, using the comprehensive data of Falloon & Green (1988), and Falloon et al. (1988), there can be found no combination of pressure and temperature, which reproduces the variation in SiO_2, alkalis and P_2O_5 relative to CaO/Al_2O_3 that occurs in the natural alkaline basalts. This may be due to the relatively low pressures and high temperatures (outside those of garnet lherzolite stability) at which most of the Falloon & Green (1988), and Falloon et al. (1988) experiments were conducted.

2.6.2 The Effects of Residual Garnet

Trace element studies, particularly of the REE, have indicated that most highly alkaline basalt magmas probably equilibrated with a garnet-bearing residue during their formation (e.g. Kay & Gast, 1973; Frey et al., 1978; Chauvel & Jahn, 1984). With increasing pressure the liquidus field of garnet is expanded against that of clinopyroxene (see Yoder, 1976 Fig. 85-10). This causes liquids in equilibrium with garnet and clinopyroxene to increase in CaO/Al_2O_3 as pressure increases. A combination of decreasing degree of melting with increasing pressure, during melting to leave a garnet lherzolite residue, might therefore explain most of the major and minor element trends characteristic of natural alkaline basalts. Another possibility is the role that has often been suggested for volatiles, particularly H_2O and CO_2, in the genesis of alkaline magmas (e.g. Bultitude & Green, 1968; Brey & Green, 1974; Mysen & Boettcher, 1975; Eggler, 1978).

2.6.3 The Effects of Volatiles H_2O and CO_2

The volatile-rich nature of alkaline basalt magmas can be inferred from the occurrence in alkaline basalts of volatile-rich phases such as zeolites, micas and carbonates, and from evidence for the frequently explosive nature of their eruptions. Experimental studies of natural and simple systems have also shown that highly silica-undersaturated magmas can be produced by partial melting of peridotite in the presence of significant quantities of CO_2 (Brey & Green, 1974, 1977; Ryabchikov & Green, 1978; Eggler, 1978; Mysen & Boettcher, 1975). Of particular relevance to the basalts at Oatlands are the experiments performed by Brey & Green (1974, 1977) on a natural olivine melilitite from the Central Plateau of Tasmania. Brey & Green found that with 7 wt.% H_2O and 7 wt.% CO_2 added to its composition, the melilitite was in equilibrium with garnet lherzolite at 1160°C and 27 kb.

Considering the high concentrations of incompatible elements such as K, Ba, Sr etc. in alkaline basalts, it would not be surprising if their magmas originally contained correspondingly high concentrations of similarly incompatible volatiles. It is important to know, therefore, how H_2O and CO_2 concentrations vary in basalt

magmas relative to concentrations of other incompatible components, and if they may be exceptionally enriched in alkaline magmas. A useful starting point for a discussion of this matter, is an examination of what direct evidence there is for pre-eruption volatile concentrations in natural basalt magmas.

2.7 VOLATILE CONCENTRATIONS IN BASALT MAGMAS

2.7.1 Submarine Glasses

Submarine basalt glasses have been shown to largely retain their original H_2O concentrations if quenched at depths sufficiently great to maintain volatile solubility in their original magmas (Moore, 1970; Killingley & Muenow, 1975). The exact pressure at which this occurs is dependent upon the magmas composition and volatile content, ranging from about 500 metres for volatile-poor MORB, to greater than 1000 metres for more volatile rich alkalic and tholeiitic basalts from Hawaii. When these effects have been taken into consideration, it has been found that H_2O increases with increase in the concentrations of other incompatible elements such as K and P (Moore, 1970; Moore & Schilling, 1973; Delaney et al., 1978; Byers et al., 1985; Michael, 1988; Dixon et al., 1988). There is, however, a broad range of incompatible element/H_2O ratios.

It was found by Michael (1987), that in submarine glasses from the Pacific Ocean H_2O/K_2O decreases with increase in the incompatible element concentrations of primary basalts. In depleted MORB from the Galapagos spreading centre H_2O/K_2O varies from about 4.0 to 4.5. In contrast, more incompatible-element enriched alkalic and tholeiitic glasses from Loihi Seamount and Kilauea have H_2O/K_2O between approximately 1.0 and 1.5 (Moore, 1965; Muenow et al., 1979; Harris and Anderson, 1983; Byers et al., 1985). This pattern of variation was interpreted by Michael (1987) to indicate that H_2O is more compatible than K_2O during mantle fractionation processes. The compatibility of H_2O was found by Michael to be more similar to those of Ce, Nd, Sr and P. Similar results were obtained by Dixon et al. (1988) who found a close correlation between H_2O and La concentrations in submarine glasses from the Juan de Fuca Ridge and neighbouring seamounts. These results suggest that ratios of H_2O to LREE, Sr or P may be used to estimate the original H_2O

concentrations of subaerially-erupted (and degassed) alkali-rich basaltic magmas.

The weight ratio of $H_2O/(Ce + Nd)$ is approximately 95 $\pm$ 30 for both depleted and enriched Pacific MORB's, and for submarine Hawaiian glasses (Michael, 1987). Higher ratios (of approximately 160) occur in North Atlantic MORB's (Schilling et al., 1985; Poreda et al., 1986). Relative H_2O concentrations may be even higher in some arc and back arc basin basalts. Ratios of H_2O/P_2O_5 in basalt glasses from the East Scotia Sea, Marianas, North Fijii and Lau arc and back-arc basins are several times higher than those found in Pacific and Atlantic Ocean MORB, and in Hawaiian basalts (Garcia et al., 1978; Muenow et al., 1980; Aggrey et al., 1988).

When these data are applied to the problem of H_2O concentrations in the original alkaline basalt magmas of the Oatlands district, it is obvious that only very general constraints can be imposed. If $H_2O/(Ce + Nd)$ ratios in Pacific Ocean MORB's and Hawaiian basalts are used as a standard, then H_2O concentrations of approximately 2.7 $\pm$ 0.8 wt.% can be expected to have occurred in the most incompatible element enriched nepheline basanite and olivine melilitite magmas. Concentrations at least double these can be inferred if comparison is made instead to modern back-arc and arc basalts.

Because of the low solubility of CO_2 in basalt magmas at low pressures (Stolper & Holloway, 1988), primary CO_2 concentrations in basalt magmas are more difficult to determine than are those of H_2O. Ratios of CO_2/H_2O in submarine glasses are usually less than one, and only rarely greater (Delaney et al., 1978; Muenow et al., 1979; Harris & Anderson, 1983; Byers et al., 1985). Because of the low solubility of CO_2, relative to that of H_2O, in basalt magmas at low pressures, measured CO_2/H_2O ratios in basalt glasses are likely to represent minimum values in original magmas.

2.7.2 Volcanic Emissions

Greenland et al. (1984) measured gas emission rates for Kilauea volcano and used these data, in combination with other chemical and geological information, to determine concentrations of

0.32% H_2O, 0.32% CO_2 and 0.09% S in magmas prior to their arrival in a shallow reservoir. Their data showed that analysed submarine glasses from Hawaii must have degassed a substantial proportion of their original CO_2 concentrations prior to eruption. They also indicate that CO_2 concentrations in undegassed basalt magmas may be at least as high as those of H_2O.

2.7.3 CO_2 Concentrations in Alkaline Lamprophyres

Alkaline lamprophyres with compositions similar to those of nepheline basanites and nephelinites are typically carbonate rich and may contain as much as 8 wt.% CO_2 (e.g. Barreiro et al., 1987; Goto & Arai, 1987). Because carbonates are often enriched in late stage segregations within alkaline basalts, it is difficult to know how indicative the exceptionally high CO_2 concentrations sometimes found in alkaline lamprophyres may be of original magmatic values. Regardless of this, concentrations of up to several wt.% CO_2 in alkaline lamprophyre magmas seem highly likely. In contrast to lamprophyres, alkaline basalts from provinces such as eastern Australia and Hawaii are typically carbonate poor, rarely containing more than about 2 wt.% CO_2 (see references for Fig. 21). It may be that volatile concentrations in lamprophyric and non lamprophyric alkaline magmas are different. Alternatively, as suggested by Rock (1977), the more volatile-rich mineralogy of alkaline lamprophyres may simply reflect their different cooling histories.

2.7.4 Constraints from Petrography and Experimental Evidence

An upper limit on probable concentrations of H_2O and CO_2 comes from a consideration of petrographic and experimental evidence. With the 14 wt.% of H_2O and CO_2 used by Brey & Green (1977) to achieve garnet lherzolite saturation in the Laughing Jack Marsh olivine melilitite, the melilitites liquidus temperature is approximately 250°C lower than its dry 1 atm liquidus. If the effects of adiabatic cooling are considered, this temperature difference would be even greater once such a magma was erupted and completely degassed. As a result of this effect, any volatile loss from the melilitite should cause it to begin crystallizing; once completely degassed it would be close to completely crystallized.

These experimental observations are at odds both with the very fine-grained and (more rarely) glassy nature of some melilitites and nephelinites, and with the occurrence of melilitite lavas that are known to have flowed for at least several kilometres (Winchell, 1947; Macdonald & Katsura, 1964).

Subsequent experiments performed for this study have shown that 4.5 wt.% H_2O and 3.5 wt.% CO_2 are incompletely soluble in a nepheline basanite liquid at 10 kb (Adam, unpublished results). It is therefore probable that an olivine melilitite liquid containing 7 wt.% H_2O and 7 wt.% CO_2 would begin exsolving volatiles at pressures considerably greater than 10 kb. Once this occurred, the melilitite would also begin to crystallize. By the time this magma reached the surface it would be phenocryst rich. In contrast to this expectation, the olivine melilitite from Laughing Jack Marsh is very fine grained (with a grainsize generally < 0.05 mm) and contains only a few percent of small (0.5 mm) olivine phenocrysts. There is also no evidence for a sudden explosive degassing that might also have causes sudden quenching. The melilitite is a dense aphyric basalt which contains few vesicles.

It is concluded from these observations that, in general, volatile concentrations in natural melilitite and nephelinite magmas are very much lower than those used in the experiments of Brey & Green (1977) [i.e. << 14 wt.%].

2.7.5 The Experimental Phase Relationships of the Laughing Jack Marsh Olivine Melilitite

The preceding arguments are apparently at odds with the conditions of origin for the Laughing Jack Marsh olivine melilitite found by Brey & Green (1977). However, as discussed by Brey & Green (1977), the conditions of garnet lherzolite saturation in the Laughing Jack Marsh olivine melilitite are unlikely to be unique. There probably exist many conditions of P-T-XH_2O-XCO_2 at which garnet lherzolite saturation could occur. Under dry conditions Brey & Green (1974) found that olivine remained the sole liquidus phase up to pressures greater than 35 kb. It may thus have been that Brey & Green were prevented by the limitations of their piston-cylinder apparatus (limited to pressures of 40 kb or less) from studying the

liquidus relationships of phases other than olivine at low volatile concentrations.

2.7.6 Geochemical Continuity and the Continuity of Petrogenetic Processes

The systematic inter-element trends of primitive basalt compositions from individual alkaline basalt provinces (Fig. 21), suggest that a similar continuity of processes and conditions prevailed during the formation of these basalts. If the conditions of origin for part of the compositional range found in a particular alkaline basalt province can be determined, it should be possible to estimate by extrapolation the conditions of origin for all parts of the range. With this objective in mind, a series of liquidus experiments were conducted on two primitive alkaline basalt compositions. One of these was a nepheline-basanite (UT-70489) from Bow Hill (Table 6); the other was a highly silica-undersaturated olivine nephelinite (2854) from Scottsdale in north-eastern Tasmania (see Frey et al., 1978).

2.8 EXPERIMENTAL PHASE RELATIONSHIPS OF THE NEPHELINE BASANITE UT-70489 AND OLIVINE NEPHELINITE 2854

2.8.1 Objectives

There were two primary objectives of the experimental study on nepheline basanite UT-70489; these were (1) to find the pressure and temperature at which its liquidus becomes multiply saturated in garnet, clinopyroxene, orthopyroxene and olivine, and (2) to determine the minimum amounts of H_2O, CO_2 and/or olivine addition necessary to achieve this. Subsequent experiments on the olivine nephelinite 2854 were conducted with similar concentrations of added H_2O and CO_2; this was done to determine whether pressure may have a significant effect on the SiO_2 content of alkali-basaltic liquids in equilibrium with garnet lherzolite. If, as previously suggested, it does, then multiple saturation in 2854 (containing 39.8 wt.% SiO_2) should occur at significantly higher pressure than it does in UT-70489 (containing 44.3 wt.% SiO_2).

2.8.2 Starting Compositions

In terms of its high Mg# (68.6), and high concentrations of Ni (380 ppm) and Cr (529 ppm), UT-70489 is the most primitive of the Oatlands basalts analysed. As previously discussed, its petrography, bulk composition and mineral chemistry are consistent with the analysed composition representing that of an original liquid. The olivine nephelinite 2854 from Scottsdale was chosen for study as a natural alkaline basalt containing approximately 4 wt.% less SiO_2 than UT-70489, but with similar Mg#, and Ni and Cr concentrations. As with UT-70489, it probably also represents an original liquid, being nearly aphyric.

2.8.3 Experimental Apparatus and Methods

Synthetic oxides, carbonates and fayalite were used to make up powders with compositions matching those of UT-70489 and 2854. Compositions were checked by micro probe analysis of polished glass samples prepared by fusing a part of each of the prepared mixtures (see Table 8 for comparison with XRF analyses of the natural samples). Experiments were performed in piston cylinder apparatus of the type described by Boyd & England (1960). Furnace assemblies were of 1/2" diameter with talc/pyrex or salt/pyrex sleeves. A -10% pressure correction was made when talc outer sleeve assemblies were used. Pressures are considered to have been within 1 kb of those stated. Temperatures were measured with a $Pt/Pt_{90}Rh_{10}$ thermocouple placed within 0.5 mm of the sample capsule, and are considered accurate to within $\pm$ 10°C. At temperatures of 1300°C, or more, Pt sample capsules were used for experiments on UT-70489. At lower temperatures $Ag_{50}Pd_{50}$ and $Ag_{75}Pd_{25}$ capsules were used, the latter being employed at temperatures less than 1200°C. Only $Ag_{50}Pd_{50}$ capsules were used for experiments on 2854. A graduated micro-syringe was used to add H_2O to capsules. Carbon dioxide was added as $Ag_2C_2O_4$. While being sealed with an electric-arc welder, capsules were kept frozen to avoid volatile loss. Volatile concentrations within capsules are estimated to have been within $\pm$ 10% of those stated.

After each experiment, a part of the sample was crushed and mounted in oil before being examined with a petrological microscope.

Table 8. Major and minor element analyses of natural basalts and synthetic powders used in experiments

	XRF analyses of natural basalts		micro probe analyses of synthetic powders and natural mineral -phases used in experiments			
	1.	2.	3.	4.	5.	6.
SiO_2	44.30	39.80	44.05	40.26	53.26	56.39
TiO_2	2.36	3.40	2.41	3.35	0.17	0.03
Al_2O_3	11.44	9.58	11.30	9.49	6.59	2.37
Cr_2O_3	0.08	0.06	0.08*	0.06*	0.39	0.41
Fe_2O_3	2.01[1]	2.63[1]	2.04[1]	2.61[1]	0.97	0.57
FeO	10.05	13.05	10.16	13.05	5.54	4.67
MnO	0.20	0.02	0.20*	0.20*	0.12	0.12
NiO	0.05	0.05	0.05*	0.05*		
MgO	12.11	14.08	12.26	14.34	31.29	34.38
CaO	9.46	11.34	9.76	11.20	2.14	0.35
SrO	0.18	0.15	0.18*	0.15*		
Na_2O	4.24	3.02	4.24	3.00	0.07	0.08
K_2O	2.09	1.55	1.95	1.40		
P_2O_5	1.43	1.10	1.54	1.17		
Mg#	68.2	65.8	68.3	66.2	91.0	92.9

1. = nepheline basanite UT-70489, 2. = olivine nephelinite 2854, 3. = synthetic analogue of UT-70489, 4. = synthetic analogue of 2854, 5. = natural orthopyroxene 90683, 6. = natural orthopyroxene 2604 (both 5. and 6. are from Table 3 of Frey & Green (1974))

* components added to mix but below the detection limit of the micro-probe

1 calculated assuming $Fe_2O_3/FeO = 0.2$

Initial phase identifications were made in this way. Larger fragments were then mounted in epoxy resin and polished in preparation for micro probe analysis. Micro probe analyses were made using the same JEOL JXA50A instrument and operating conditions employed for analysing the natural minerals. The results of analyses were used both to confirm the initial phase identifications and to provide information on the compositions of near liquidus phases.

Experiments were mostly of 20 to 40 minutes duration. Longer run times were avoided in order to prevent excessive Fe-loss to the precious metal capsules. When Pt capsules were used, approximately 30% of the original iron was lost from charges after 30 minutes. With $Ag_{50}Pd_{50}$ capsules from 3-8% of original iron was lost during the same period. A minimum of iron loss occurred when salt outer sleeves were used. No apparent Fe-loss occurred from samples contained in $Ag_{75}Pd_{25}$ capsules.

Although experiments were unbuffered, graphite was not observed in the run products of CO_2-bearing experiments; instead finely dispersed carbonate was found as a quench product in all CO_2-bearing runs. This indicates that oxygen activities remained sufficiently high to stabilize CO_3^{2+}.

2.8.4 Results of Experiments on Nepheline Basanite UT-70489

Conditions and results for individual experiments are listed in Table 9. Phase relationships interpreted from these are shown in Fig. 23. Three different combinations of H_2O and CO_2 concentrations were tried. The first of these, with 2 wt.% H_2O and 2 wt.% CO_2 (Fig. 23), represented a minimum estimate of probable H_2O and CO_2 concentrations in the original basanite magma (see previous discussion on H_2O and CO_2 concentrations in basalt magmas). From Fig. 23 it is apparent that at low H_2O concentrations (2 wt.%) the olivine liquidus field does not extend to pressures high enough to meet with the garnet field. With no CO_2 and 4.5 wt.% H_2O (Fig. 23) the olivine and garnet liquidus fields still remain widely separated. However, the addition of 2 wt.% CO_2 lowers the pressure range of the garnet liquidus field sufficiently for it to intersect with the liquidus field of olivine (Fig. 23).

Table 9. Run conditions and results of experiments on UT-70489 and 2854

Run	Capsule	°C	kb	Wt.% H_2O	Wt.% CO_2	time (mins)	Result
				UT-70489			
T-2287	Ag50	1250	28	2.0	2.0	30	Cpx+Gt+Phl?+opaque+Qch xstals+Gl
T-2289	Pt	1320	28	2.0	2.0	20	Cpx+Q-xtals+Gl
T-2291	Pt	1290	28	2.0	2.0	20	Cpx+Q-xtals+Gl
T-2293	Pt	1290	26	2.0	2.0	20	Gl
T-2294	Pt	1270	24	2.0	2.0	20	Cpx+Q-xtals+Gl
T-2295	Ag50	1240	22	2.0	2.0	30	Ol+Q-xtals+Gl
T-2298	Pt	1280	27	4.5		25	Q-xtals+Gl
T-2302	Ag50	1250	27	4.5		30	Ol+Cpx+Q-xtals+Gl
T-2303	Ag50	1250	25	4.5		30	Ol+Cpx close to liquidus
T-2304	Ag50	1230	25	4.5		30	Ol+Cpx+opaque+Phl+Qch xstals+Gl
T-2316	Ag50	1280	27	4.5		25	Q-xtals+Gl
T-2317	Ag50	1265	27	4.5		35	Q-xtals+Gl
T-2320	Ag50	1270	28	4.5		35	Cpx+Q-xtals+Gl
T-2373	Ag50	1300	29.5	4.5		20	Q-xtals+Gl
T-2323	Ag50	1260	26	4.5		30	Cpx+Ol? close to liquidus
T-2378	Ag50	1270	29.5	4.5		30	Cpx+Q-xtals+Gl
T-2385	Ag50	1300	32	4.5		30	Cpx+Q-xtals+Gl
T-2359	Ag50	1235	26	4.5	2.0	30	Q-xtals+Gl
T-2352	Ag50	1220	25	4.5	2.0	40	Q-xtals+Gl
T-2380	Ag50	1190	25	4.5	2.0	29	Q-xtals+Gl
T-2387	Ag75	1150	25	4.5	2.0	40	Amph+Phl+Q-xtals+Gl
T-2393	Ag75	1170	25	4.5	2.0	40	Cpx+Ol+Q-xtals+Gl
T-2395	Ag75	1185	26.5	4.5	2.0	25	Ol+Gt+Cpx+Q-xtals+Gl
T-2398	Ag50	1200	26.5	4.5	2.0	35	Gt+Cpx?+Q-xtals+Gl
			UT-70489 + 5% Orthopyroxene 90863				
T-2442	Ag50	1200	26	4.5	2.0	30	Ol+2604+Cpx?+Q-xtals+Gl
T-2446	Ag50	1200	26	4.5	2.0	30	OL+2604+Cpx?+Q-xtals+Gl
			UT-70489 + 10% orthopyroxene 90863				
T-2455	Ag50	1210	26	4.5	2.0	65	relict 90683+Opx coronas
				2854			
T-2529	Ag50	1280	35	4.5	2.0	37	Ol+Cpx+Gt+Q-xtals+Gl
T-2542	Ag50	1270	33.5	4.5	2.0	35	above liquidus
T-2547	Ag50	1250	33.5	4.5	2.0	30	Ol+Gt+Cpx+Q-xtals+Gl
T-2548	Ag50	1270	33.5	4.5	2.0	39	Ol+Q-xtals+Gl
			2854 + 5% Orthopyroxene 90863				
T-2552	Ag50	1300	34.5	4.5	2.0	40	Ol+Gt+Cpx+Q-xtals+Gl
T-2553	Ag50	1320	34.5	4.5	2.0	35	Gt+Cpx+Q-xtals+Gl
			2854 + 10% Orthopyroxene 90863				
T-2555	Ag50	1320	34.5	2.0	4.5	25	Ol+Gt+Cpx+Q-xtals+Gl
			2854 + 15% Orthopyroxene 2604				
T-2578	Ag50	1315	34	2.0	4.5	30	above liquidus
T-2584	Ag50	1305	35	2.0	4.5	35	residual 2604+Fe-rich Opx rims+Cpx+Q-xtals+Gl
			2854 + 10% Orthopyroxene 2604				
T-2587	Ag50	1300	35	2.0	4.5	30	Ol+Cpx+rare Fe-rich Opx+ xstals+Gl

Ol-olivine, Opx-orthopyroxene, Cpx-clinopyroxene, Gt-garnet, Amph-amphibole, Phl-phlogopite, Q-xtals-quench crystals, Gl-glass.

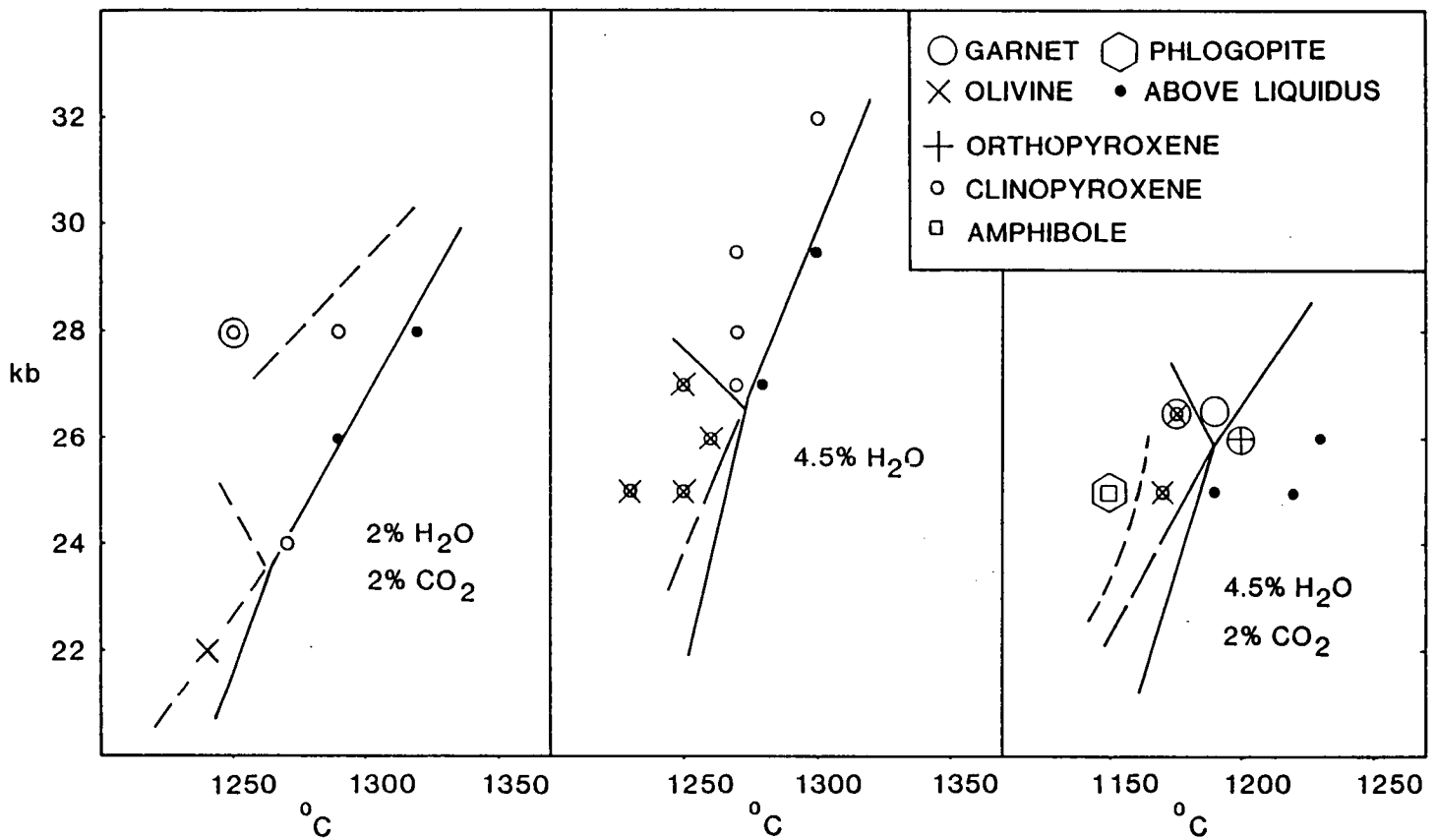

Fig. 23. Liquidus phase relationships for the nepheline basanite UT-70489

Orthopyroxene was not found to crystallize from the basanite under these conditions. The negative slope of the olivine out boundary (Fig. 23) indicates that olivine does not have a reaction relationship with the liquid at the point where the liquid is multiply saturated with garnet, clinopyroxene and olivine. Orthopyroxene may instead have been in a reaction relationship, explaining its non appearance as a liquidus phase. This may have involved the reaction

liquid + orthopyroxene = garnet + clinopyroxene + olivine

proceeding from left to right with decreasing temperature.

To test for this possibility, several experiments were carried out on orthopyroxene enriched compositions. Two different natural orthopyroxenes were used in these experiments (Table 8). One of these was a relatively aluminous, and calcium-rich orthopyroxene (90683) from the Lizard peridotite (see Green, 1964). The other was a more enstatite-rich orthopyroxene (2604) from a Victorian lherzolite nodule (see Frey & Green, 1974). Experiments on compositions containing 5 and 10 wt.% of the orthopyroxene 2604 were run for 30 minutes at 1200^{o}C and 26 kb. These produced mainly olivine and residual enstatite 2604. At slightly higher temperature and pressure (1210^{o}C and 26.5 kb), with orthopyroxene 90683 added in place of 2604, run products contained relict crystals of 90683 surrounded by coronas of a more Fe-rich orthopyroxene (Table 10). A number of small garnet crystals were also found and analysed (Table 10).

Application of the Nickel & Green (1985) orthopyroxene-garnet barometer to the garnet and orthopyroxene-corona compositions gave pressure estimates of 24-26 kb. It seems likely, therefore, that the orthopyroxene coronas were produced in equilibrium with the basanite liquid and that they were not the product of quench growth or local equilibria. Area analyses of the glass and quench crystals between the garnet and orthopyroxene crystals gave a composition similar to that of the basanite starting composition (Table 10). From this and the preceding information, it is concluded that at 26 kb and 1200^{o}C, with 4.5 wt.% H_2O and 2 wt.% CO_2 added to its

Table 10. Near liquidus phases from UT-70489 and 2854, crystallized near to conditions of garnet lherzolite saturation.

	UT-70489						2854			
	gt[1]	cpx[2]	ol[2]	gt[3]	opx[3]	liq.[3]	gt[4]	cpx[4]	ol[5]	opx[6]
SiO_2	41.55	52.96	39.90	41.76	54.24	45.1	41.76	53.07	40.25	55.70
TiO_2	0.55	0.82		0.64	0.22	2.4	0.67		0.35	0.19
Al_2O_3	22.47	4.97		22.39	5.15	12.4	21.84	5.64		3.36
Cr_2O_3	0.54	0.41					0.77	0.46		0.19
FeO	10.59	5.68	16.90	11.41	9.46	11.4	9.51	5.79	13.43	7.67
MgO	18.19	16.13	43.07	17.81	29.49	12.2	18.96	18.06	45.76	31.41
CaO	5.77	17.48	0.13	5.69	1.44	8.8	6.48	15.18	0.17	1.67
Na_2O		1.55				3.8		1.43		
K_2O						2.2				
P_2O_5						1.7				
Mg#	75.4	83.5	82.0	73.6	84.8	65.6	78.0	84.7	85.9	88.0

superscript	1.	2.	3.	4.	5.	6.
run no.	T-2398	T-2393	T-2455	T-2553	T-2548	T-2584
pressure (kb)	26.5	25	26	34.5	33.5	35
temp. (^{o}C)	1200	1170	1210	1320	1270	1305

composition, UT-70489 is saturated or close to saturation with garnet lherzolite.

2.8.5 Results of Experiments on Olivine Nephelinite 2854

The conditions and results of individual experiments are listed in Table 9; phase relationships interpreted from these are shown in Fig. 24. The same volatile concentrations used to achieve garnet lherzolite saturation in UT-70489 (4.5 wt.% H_2O and 2 wt.% CO_2) were also used during experiments on 2854. As shown in Fig. 24, a point of multiple saturation in garnet, clinopyroxene and olivine occurs on the liquidus at approximately 35 kb. This is nearly 10 kb higher in pressure than the equivalent point for UT-70489 (Fig. 23). Orthopyroxene addition experiments were carried out in the same way for 2854 as they were for UT-70489. With 5 and 10 wt.% of orthopyroxene 90683 added to the nephelinite + 4.5 wt.% H_2O + 2 wt.% CO_2 composition, garnet, clinopyroxene and olivine were found to be near liquidus phases at 1300-1320°C and 34.5 kb. No residual 90683 remained. Clinopyroxenes produced during these experiments contained a maximum of about 15.5 wt.% CaO (Table 10). Similar CaO concentrations occur in clinopyroxenes coexisting with orthopyroxene after solidus experiments on pyrolite at similar temperatures and pressures (W. Taylor, unpublished data). Further tests for proximity to orthopyroxene saturation were therefore conducted. In these, the more magnesian and SiO_2-rich orthopyroxene 2604 was used in place of 90683. After an experiment with 15 wt.% added 2604, run at 1305 °C and 35 kb, abundant crystals of residual 2604 were found surrounded by thick rims of a more Fe-rich orthopyroxene (Table 10). Small crystals of primary clinopyroxene were also found, although these were uncommon. At 1320°C the same mixture was completely melted, while at 1310°C and 34.5 kb it crystallized olivine only. An experiment containing 10 wt.% 2604 was run at 1300°C and 35 kb for 40 minutes. This produced mainly olivine and clinopyroxene, with rare lamellae of Fe-rich orthopyroxene occurring in clinopyroxenes.

Although olivine nephelinite 2854 does not seem to be either saturated or close to saturation with orthopyroxene at any point on its liquidus, a liquid composition close to saturation with garnet, clinopyroxene, orthopyroxene and olivine is bracketed between the orthopyroxene enriched compositions and that of 2854. Because

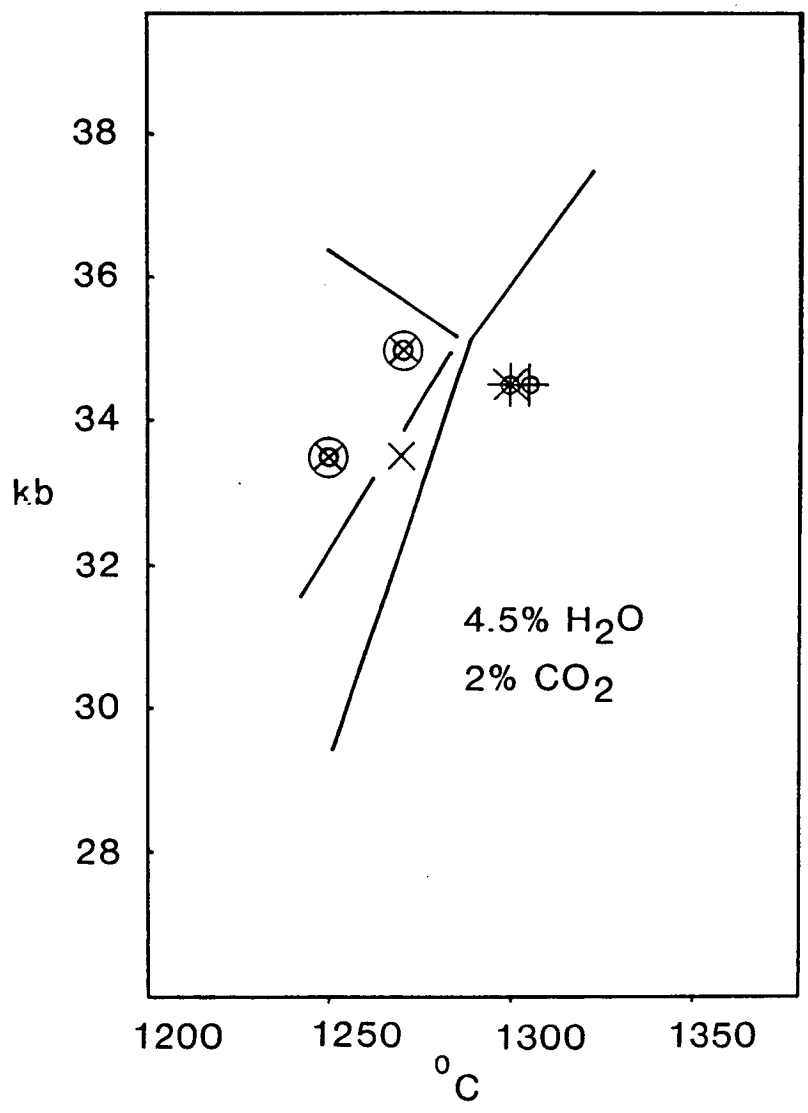

Fig. 24. Liquidus phase relationships for the olivine nephelinite 2854. Symbols as for Fig. 23.

orthopyroxene has a reaction relationship with the liquid, any amount of crystallization will move its composition away from orthopyroxene saturation. The composition containing 15 wt.% added 2604, crystallized at least several percent of orthopyroxene, together with a smaller amount of clinopyroxene. Because the bulk composition used in this experiment contained approximately 42 wt.% SiO_2, the liquid in equilibrium with orthopyroxene must have contained less than this amount. If the Fe-rich orthopyroxene lamellae produced in the run containing 10 wt.% 2604 were in equilibrium with the liquid in the charge, a similar argument could be used to limit the SiO_2 concentration of the liquid in equilibrium with orthopyroxene to less than 41.6 wt.%. Although the amount of crystallization in the two orthopyroxene-bearing runs is difficult to estimate precisely, the SiO_2 concentration of the liquid in equilibrium with orthopyroxene was probably somewhere between 41 and 42 wt.%. This liquid would also have been slightly more magnesian than the original composition of 2854, probably containing close to 15 wt.% MgO.

2.8.6 Primary versus Derivative Origins for UT-70489 and 2854

Primary magmas are magmas which have not been modified by contamination or crystallization between their source or magma segregation depth and surface eruption and quenching. The experimental phase relationships of UT-70489 are consistent with a primary origin. However, because the volatile concentrations originally present in the magma cannot be accurately determined, it is impossible to prove either a primary or derivative origin from the phase relationships alone. Estimates for the Mg# of undepleted upper mantle generally range from 88.0 to 89.0, although lower estimates have also been advocated (e.g. Carter, 1970; Wilkinson, 1985). Depending on the value of K_d chosen for the Fe^{+2}-Mg olivine-liquid partition coefficient, UT-70489 may have been in equilibrium with upper mantle near to the Fe-rich end of this range (Mg# 88.0). Because NiO and Cr_2O_3 concentrations in olivine and clinopyroxene phenocryst cores from UT-70489 (Table 5) are similar to those in the olivines and clinopyroxenes of Cr-diopside lherzolites, it seems unlikely that large amounts of olivine or clinopyroxene fractionation (> 5 %) occurred. Larger amounts of fractionation would imply a source considerably richer in NiO and Cr_2O_3 than

typical Cr-diopside lherzolites. In the absence of any strong evidence for the source of UT-70489 having had Mg# much higher than 88.0, it will be assumed that, at most, only small amounts of olivine fractionation occurred (probably less than 5 %), and that the phase relationships shown in Fig. 23 are similar to those of the primary basanite magma.

In the case of olivine nephelinite 2854, a similar primary or near primary origin is less easily supported. This is because orthopyroxene saturation was definitely achieved only after 15 wt.% of orthopyroxene was added to the nephelinites original composition. Both Mg# and Cr are slightly lower in 2854 than in UT-70489. These differences may be the result of 2854 having lost small amounts of clinopyroxene and olivine (probably less than 10 %) prior to eruption and quenching. Total volatile concentrations and/or CO_2/H_2O may also have been higher in the original nephelinite magma than they were in the experimental composition. Alternatively, alkali loss may have occurred during or after eruption. All of these effects would move the original magma composition away from orthopyroxene saturation.

It must also be remembered, that although 15 wt.% of orthopyroxene was used to achieve saturation, this amount was in excess of that actually required. Because of the reaction relationship between orthopyroxene and liquid, the bulk composition must contain an excess of orthopyroxene before orthopyroxene can crystallize as a visible phase. Secondly, as found during experiments on the nepheline basanite UT-70489, the physical conditions of orthopyroxene saturation must be closely matched before orthopyroxene will crystallize. If the most favourable conditions for orthopyroxene saturation were missed, it would have been necessary to add more orthopyroxene to the original composition than was actually needed.

2.8.7 Depths of Magma Segregation

Shown in Fig. 25 is a plot of pressures of equilibration versus SiO_2 concentrations in basaltic liquids that have been experimentally equilibrated with lherzolite, $\pm$ plagioclase, spinel and garnet. Volatile-free compositions produced during peridotite

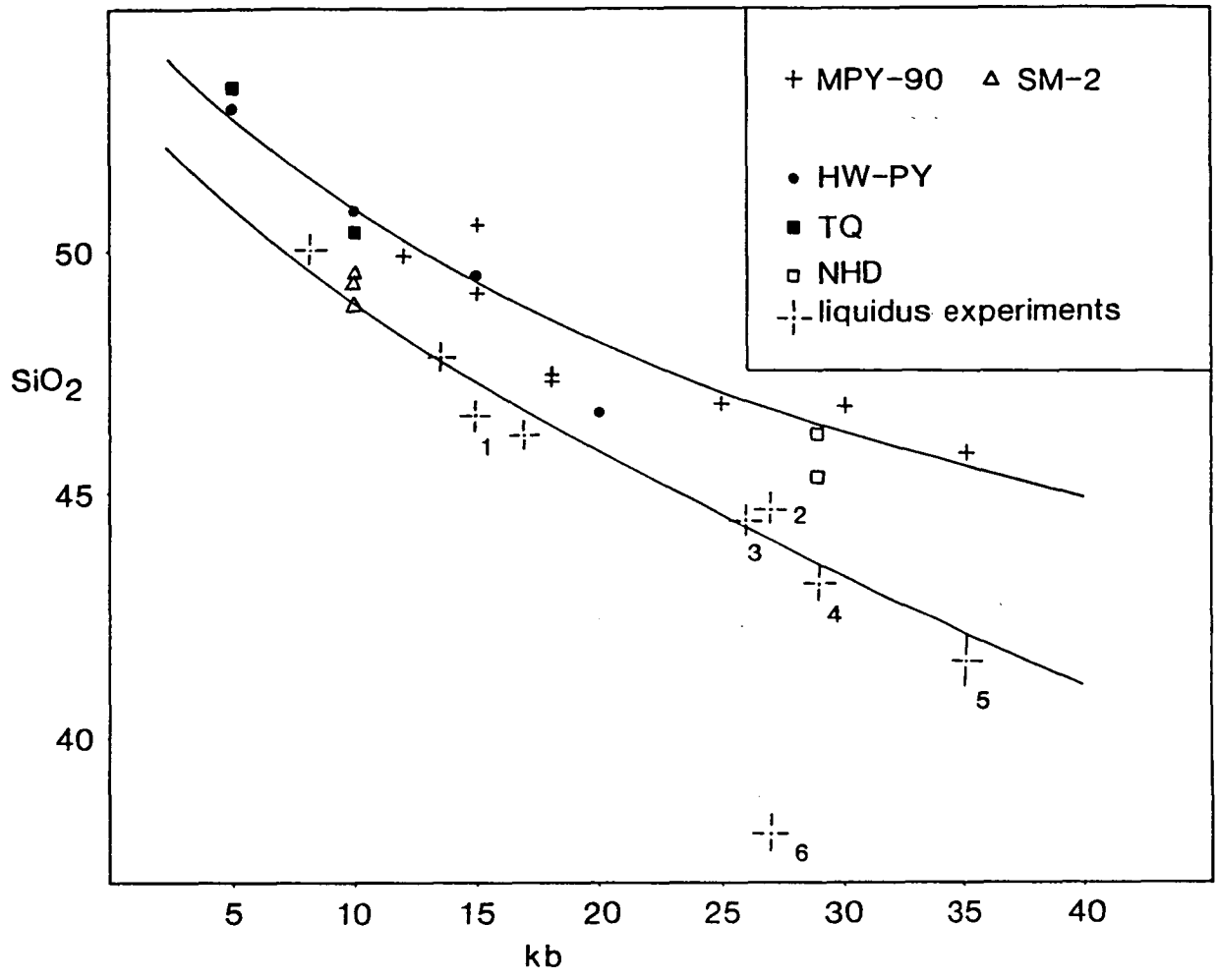

Fig. 25. Variation of SiO_2 concentrations in basaltic liquids experimentally equilibrated with lherzolite ± plagioclase ± spinel ± garnet with pressure of equilibration. Excepting those which indicate liquidus experiments, symbols represent peridotite starting compositions used in sandwich experiments. These include: MPY-90 (MORB pyrolite Mg# 90), MPY-87 (MORB pyrolite Mg# 87), HW-PY (Hawaiian pyrolite), TQ (Tinaquillo lherzolite), NHD (average peridotite xenolith from the north Hessian depression), and SM-2 (an arbitrary combination of spinel lherzolite phases). The two curved lines highlight separate trends formed by peridotite melting experiments, and liquidus experiments on natural compositions. Numbers beside symbols for liquidus experiments correspond to volatile concentrations as follows: 1. = 2% H_2O; 2. = 4.5% H_2O; 3. = 4.5% H_2O + 2% CO_2; 4. = an unknown H_2O concentration less than 6%; 5. = 4.5% H_2O + 2% CO_2; 6. = 7% H_2O + 7% CO_2. Data sources are Green & Hibberson (1970), Green (1973), Thompson (1974), Brey & Green (1977), Fujii & Kushiro (1977), Takahashi & Kushiro (1983), Fujii & Scarfe (1985), Falloon & Green (1988), Falloon et al. (1988), Mengel & Green (1988), and this study.

melting experiments show a general trend of decreasing SiO_2 concentrations with increasing pressure. There appears to be a tailing off in this effect at higher pressures. Natural compositions equilibrated with olivine, orthopyroxene and clinopyroxene ± plagioclase and garnet during liquidus experiments show a similar trend, although the tailing off in the effect of pressure is less apparent. In the natural compositions, concentrations of TiO_2, P_2O_5, alkalis, H_2O and CO_2 generally increase with decreasing SiO_2. This trend appears to compensate for the normal decrease in the effect of pressure on SiO_2 concentrations that is observed in the volatile-free peridotite melting systems. If the relationships shown in Fig. 25 are applicable to natural magmas, it can be deduced that primary olivine basalt and alkali olivine basalt magmas may form at pressures between 10 and 20 kb, those of basanites and nepheline basanites at 20 to 30 kb, and those of olivine nephelinites at 30 to 40 kb.

For olivine melilitites (with < 40 wt.% SiO_2), there are two possible conditions of origin that can be inferred from Fig. 25. These include a relatively high pressure origin (40-50 kb) in the presence of low or moderate volatile concentrations (4-8 wt.% H_2O + CO_2), and a relatively low pressure origin (25-30 kb) in the presence of higher volatile concentrations (approximately 14 wt.% H_2O + CO_2). For a number of reasons, the former possibility seems to be more likely, at least in the case of Tasmanian melilitites.

As previously mentioned, there is little independent evidence for volatile concentrations in highly alkaline basalt magmas of more than 4-8 wt.% (see previous discussion on volatile concentrations in basalt magmas). It is also difficult to reconcile a low pressure volatile-rich origin for the Laughing Jack Marsh olivine melilitite with experimental and geochemical data for other Tasmanian and southeastern Australian alkaline basalts. Shown in Table 11 are concentrations of alkalis, P_2O_5 and LREE in five Tasmanian and southeast Australian basalts, and a basalt from Auckland Island, that have been used in experimental studies. For four of these compositions (1-4, Table 11) conditions of garnet lherzolite saturation have been determined. Basalts represented by the other two compositions (5 & 6, Table 11) were used to duplicate the conditions of formation of natural megacrysts (olivine,

Table 11. Concentrations of incompatible elements and volatiles used in experiments on natural alkaline basalts from Tasmania, southeastern Australia and Auckland Island

	1. UT-70489	2. 2854	3. 2927	4. 2650	5. 2900	6. MU-6896
K_2O	2.08	1.55	1.43	2.22	0.95	2.16
P_2O_5	1.43	1.10	1.35	1.14	0.6	1.16
La	103	62	75	52		
Ce	194	140	160	108		
Nd	82	57	64	56		
H_2O	4.5	4.5	7	4.5	2	2-5
CO_2	2	2	7			

Concentrations of oxides are in wt.%, whereas those of La, Ce and Nd are in ppm

1. = nepheline basanite from Oatlands (this work)
2. = olivine nephelinite from Scottsdale (this work)
3. = olivine melilitite from Laughing Jack Marsh (Brey & Green, 1977)
4. = nepheline basanite from Mt. Leura, Victoria (Green, 1973a)
5. = olivine basalt from Auckland Island (Green & Hibberson, 1970)
6. = hawaiite from Comboyne, New South Wales (Knutson & Green, 1975)

orthopyroxene, clinopyroxene, Fe-Ti-oxides and plagioclase) found in the same basalts. For comparison with analysed incompatible element concentrations in the basalts, the concentrations of H_2O and CO_2 used either to achieve garnet lherzolite saturation, or to duplicate natural megacryst assemblages, are also shown.

It can be seen that concentrations of volatiles, relative to those of other incompatible components, were very much higher (by over a factor of 2) for the Laughing Jack Marsh olivine melilitite than they were for the other five compositions. All of the basalts represented in Table 11 are of similar geochemical affinity with compositions typical of sodic alkaline basalts found on ocean islands and in continental intraplate settings (see Coombs & Wilkinson, 1969). In this context, it would be surprising if concentrations of volatiles (H_2O and CO_2), relative to those of other incompatible components (LREE, Sr and P) were greatly different in the original magmas of the different basalts. Indeed, when the regular correlations between the concentrations of volatiles and other highly incompatible components in quenched submarine glasses are considered (e.g. Schilling et al., 1980; Michael, 1987; Dixon et al., 1988), it seems highly unlikely that this would have occurred.

At present, a relatively high pressure origin (at 40-50 kb) for the Laughing Jack Marsh olivine melilitite appears to provide the most consistent interpretation of the available data. Although similar conditions of origin are also probable for other Tasmanian melilitites, it is possible that at least some melilitites and nephelinites form in the presence of comparatively high CO_2 concentrations. Le Bas (1978) has pointed out that there are petrographic and compositional differences between the clinopyroxene-rich nephelinites associated with carbonatite volcanism, and the more olivine-rich nephelinites characteristic of provinces such as Hawaii and eastern Australia (where carbonatite volcanism is absent). It is possible that at least some of these differences are due to different volatile concentrations in different source regions.

2.9 SOURCE MINERALOGY AND RESIDUAL PHASES

A major premise of this study has been the commonly held belief that most primary basalt magmas are derived by partial melting of peridotite sources, and that they leave behind them residual olivine and orthopyroxene, with or without residual clinopyroxene, spinel, garnet or other phases. This assumption is based upon mineralogical models of the earth's upper mantle that have developed from studies of peridotite xenoliths in alkaline basalts and kimberlites, and peridotites in ultramafic masses (e.g. Kuno & Aoki, 1970; Ringwood, 1975; Jagoutz et al., 1979; Carter, 1970). It is interesting, therefore, to compare the compositions of near liquidus phases experimentally crystallized from the nepheline basanite UT-70489, and the olivine nephelinite 2854, with natural peridotite phases.

2.9.1 Pyroxenes

Plotted in Figs. 26 and 27 are the compositions of pyroxenes experimentally crystallized from the nepheline basanite UT-70489 and the olivine nephelinite 2854. For comparison, the compositions of pyroxenes found in xenoliths and as megacrysts in Cainozoic alkaline basalts from Tasmania and Victoria are also shown. The experimental pyroxenes are Na- and Ti-bearing aluminian augites according to the classification scheme of Morimoto (1988). They share compositional characteristics with pyroxenes from garnet and spinel lherzolite xenoliths [group I xenoliths of Frey & Prinz (1978)], and pyroxenes found as megacrysts and in igneous textured pyroxenite and wherlite xenoliths [included in group II of Frey & Prinz (1978)]. The experimental clinopyroxenes differ from those found in group I xenoliths mainly by having relatively low Cr concentrations and low Mg#. These differences reflect both the subliquidus nature of the experimental pyroxenes and the relatively Fe-rich character of the experimental basanite composition.

2.9.2 Amphiboles

The experimental amphiboles crystallized from UT-70489 are similar to some of the more titanian and alkali-rich amphiboles in spinel lherzolite xenoliths from the Lake Gnotuk and Bullenmerri

Fig. 26 The compositions of pyroxenes experimentally crystallized from UT-70489 and 2854 plotted in the pyroxene quadrilateral. Plotted for comparison are the compositional fields of pyroxene megacrysts, and of pyroxenes in type I and type II xenoliths from Tasmanian and Victorian Cainozoic basalts. Symbols for reversal experiments refer to coexisting clinopyroxene and orthopyroxene crystallized during an attempted reversal experiment on UT-70489 at 1210^{o}C and 26 kb (see appendix 3.2). Tie lines connect coexisting pyroxenes from xenoliths and experimental runs. Data on natural xenoliths are from Ellis (1976), Varne (1977), Nickel & Green (1984), and Stolz & Davies (1988). Wo = wollastonite, Di = diopside, En = enstatite, Hd = hedenbergite, Fs = ferrosilite.

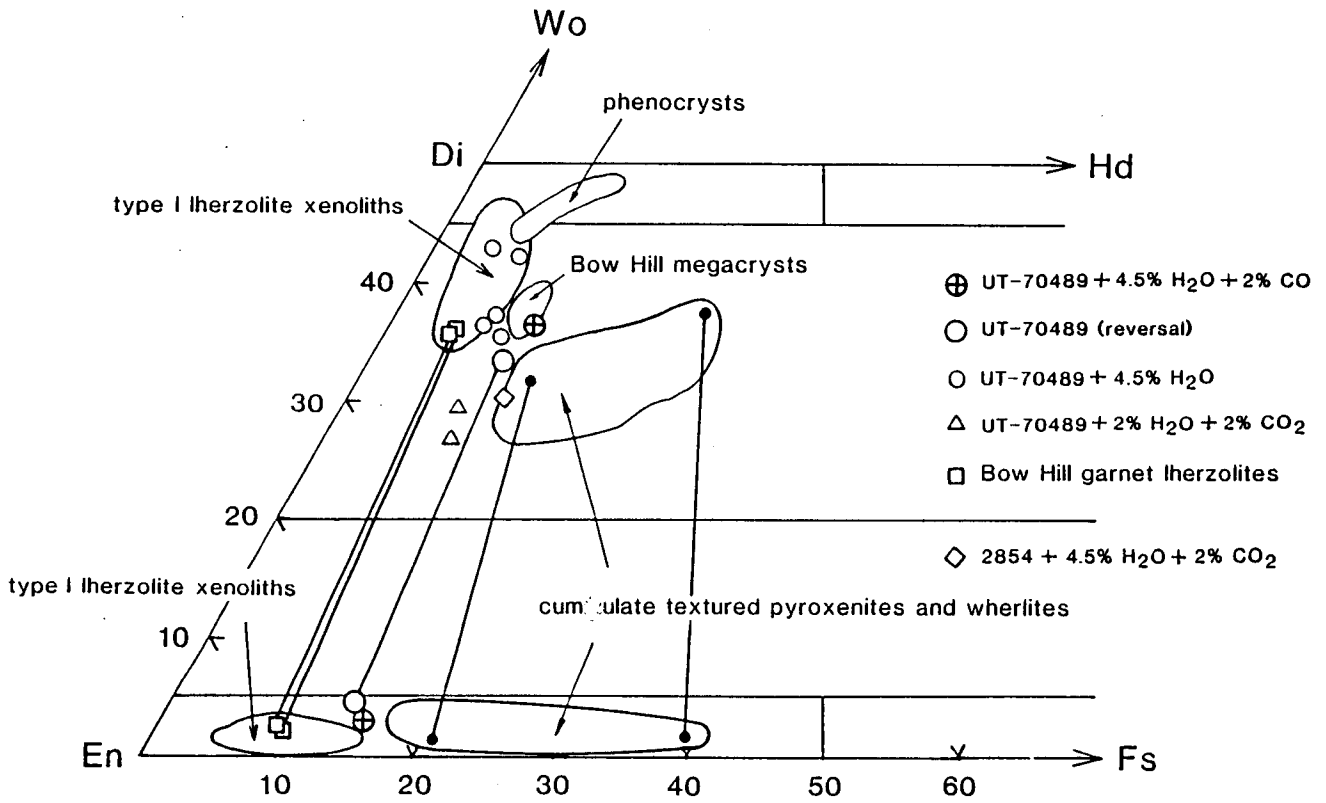
Wo
phenocrysts
Di
Hd
type I lherzolite xenoliths
Bow Hill megacrysts
40
30
20
type I lherzolite xenoliths
10
cumulate textured pyroxenites and wherlites
En
Fs
10
20
30
40
50
60
UT-70489 + 4.5% H2O + 2% CO
UT-70489 (reversal)
UT-70489 + 4.5% H2O
UT-70489 + 2% H2O + 2% CO2
Bow Hill garnet lherzolites
2854 + 4.5% H2O + 2% CO2

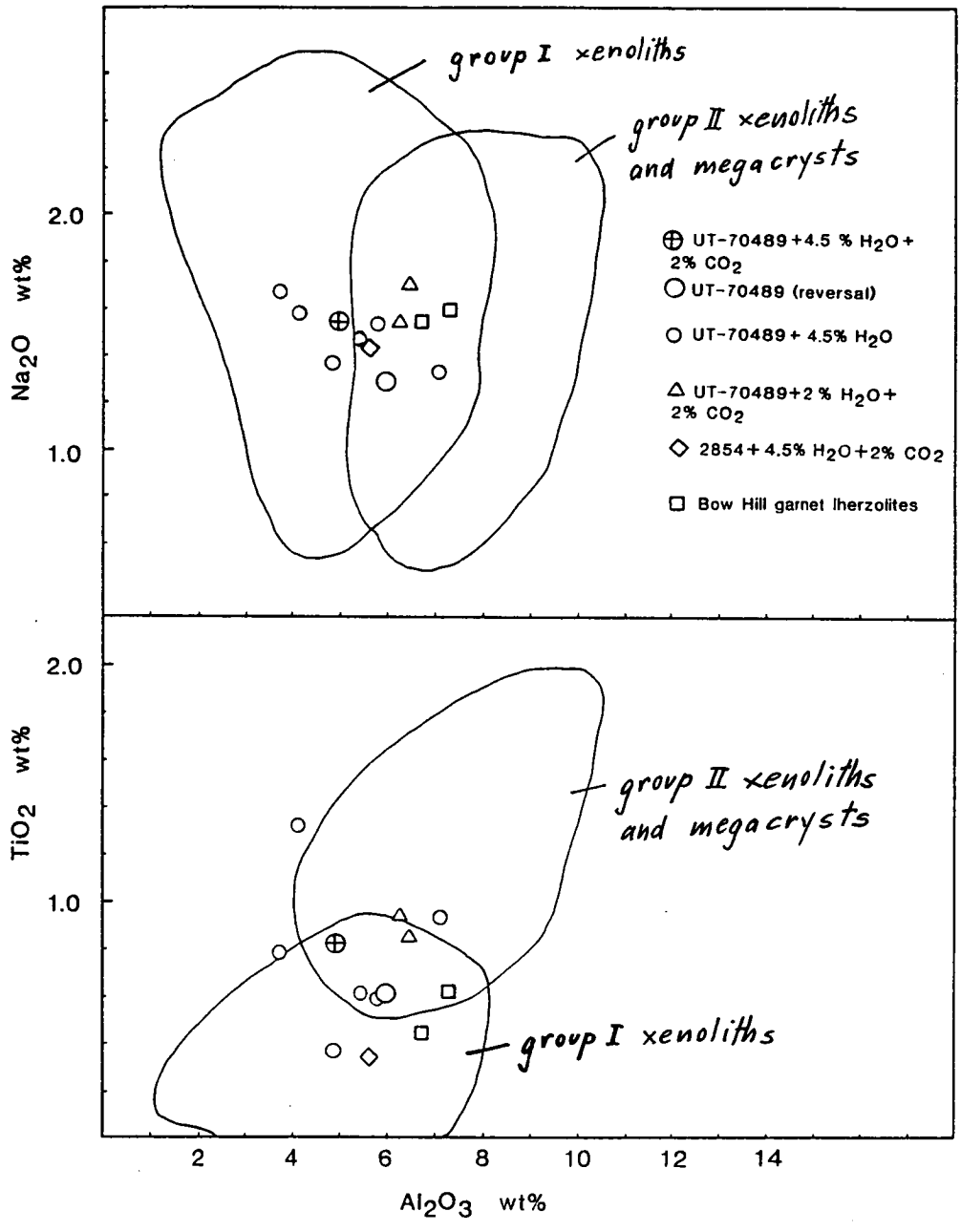

Fig. 27 Concentrations of Na_2O and TiO_2 in experimentally crystallized pyroxenes from UT-70489 and 2854. Plotted for comparison are the compositional fields of natural pyroxene megacrysts, and of pyroxenes in type I and type II xenoliths from Tasmanian and Victorian Cainozoic basalts. Symbols and references are as for Fig. 26.

maars of western Victoria (Fig. 28, Table 12). They are mainly edenite-K-richterite solid solutions and are both Si-rich and Ti-poor when compared to amphibole megacrysts from alkaline basalts (Table 12). Although they contain more TiO_2 than commonly found in amphiboles from spinel lherzolite xenoliths, the exerimental amphiboles differ from this group mainly by having lower Mg# values.

2.9.3 Micas

The phlogopite micas crystallized from UT-70489 (Table 12) are similar to natural phlogopites from garnet and spinel lherzolites found in alkaline basalts (Table 12). They differ by being relatively Fe-rich.

2.9.4 Garnets

Experimentally produced garnet compositions are plotted in Fig. 29. They show a wide range of relative CaO, MgO and FeO concentrations when compared to natural garnets from garnet lherzolites in alkaline basalts. Garnets crystallized from UT-70489 under conditions close to those of multiple saturation with clinopyroxene, orthopyroxene and olivine have compositions quite similar to those of some megacrysts from alkaline basalts. They differ from garnets in garnet lherzolites (from alkaline basalts) by having slightly lower TiO_2 and lower Mg# (see Table 12).

In summary, the experimental phases crystallized from UT-70489 and 2854 have compositions intermediate between those of Cr-diopside lherzolite (group I) xenoliths, and those found as megacrysts, and in cum ulate (group II) pyroxenite and wherlite xenoliths from alkaline basalts. They differ from phases in group I xenoliths mainly by having relatively low Mg# values; they are, however, quite similar to the phases found in some natural Fe-rich lherzolites, and to some megacrysts. These observations are consistent with a peridotite mantle source with similarities to the Cr-diopside lherzolite (group I) xenoliths, and with the commonly proposed derivitive origin for group II phases as high pressure precipitates of their alkaline host or related magmas (see Irving, 1974 and references therein).

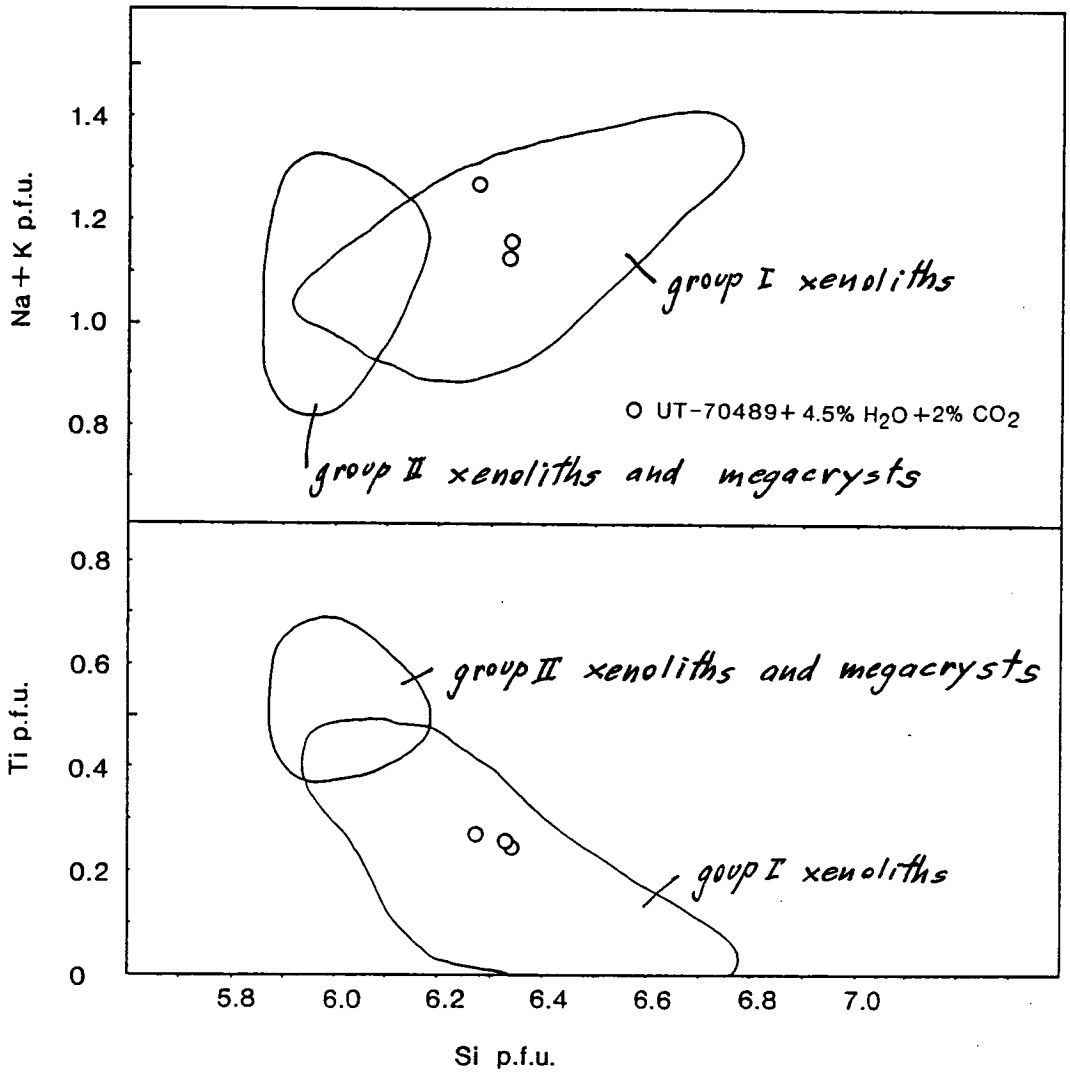

Fig. 28 Na + K, and Ti versus Si atoms [per formula unit of 23 oxygens (p.f.u.)] in experimentally crystallized amphiboles from UT-70489. Plotted for comparison are the compositional fields of amphibole megacrysts, and amphiboles occurring as disseminated grains in spinel lherzolite (type I) xenoliths from Tasmania and Victoria. Data on amphiboles in lherzolite zenoliths are from Nickel & Green (1984), and Stolz & Davies (1988). Data for amphibole megacrysts are from Irving (1974), Ellis (1976), and unpublished data.

Table 12. Experimentally crystallized amphibole, mica and garnet from nepheline basanite UT-70489, and natural phases found in xenoliths and as megacrysts in alkaline basalts

	experimental phases			natural phases from peridotite xenoliths in alkaline basalts					megacrysts	
No.	1.	2.	3.	4.	5.	6.	7.	8.	9.	10.
	amph	mica	garnet	amph.	amph.	mica	mica	garnet	amph.	garnet
Run	T-2387	T-2387	T-2398							
SiO_2	43.7	39.0	41.6	42.91	44.34	37.43	38.84	42.38	41.04	41.35
TiO_2	2.5	2.9	0.6	3.83	0.46	5.73	5.52	0.35	4.69	0.51
Al_2O_3	13.0	15.9	22.7	12.55	13.25	15.58	15.96	23.17	14.76	23.44
Cr_2O_3			0.6	0.30	1.77	0.26	1.26	0.99		
FeO	9.5	8.6	10.7	6.57	4.25	7.04	4.68	7.28	8.98	10.76
MnO			0.2					0.22		0.29
MgO	15.6	19.1	18.1	16.11	17.88	18.98	19.61	21.05	13.34	18.50
CaO	8.7	0.2	5.8	10.12	10.63			10.80	5.08	4.73
Na_2O	3.1	0.8		3.08	3.65				2.29	0.07
K_2O	1.9	8.5		1.47	0.84	8.84	9.50		2.20	
Σ	98.0	95.0	100·3	96·94	97·07	93·86	95·37	106·24	92·38	99·65
Mg#	74.4	79.9	75.2	81.4	88.2	82.8	88.3	83.7	72.6	75.4

4., 5. & 6. = amphiboles and micas in spinel lherzolite xenoliths from the Lake Gnotuk maar of western Victoria (Stolz & Davies, 1988)

7. = phogopite in a garnet lherzolite xenolith found in an alkaline basalt from Mingxi, eastern China (Cao & Zhu, 1987)

8. = garnet in garnet lherzolite xenolith from Bow Hill, Tasmania (Adam, unpublished data)

9. = amphibole megacryst from Risdon Dam, Tasmania (Adam, unpublished data)

10. = garnet megacryst from the Kakanui breccia pipe, New Zealand (Mason & Allen, 1973)

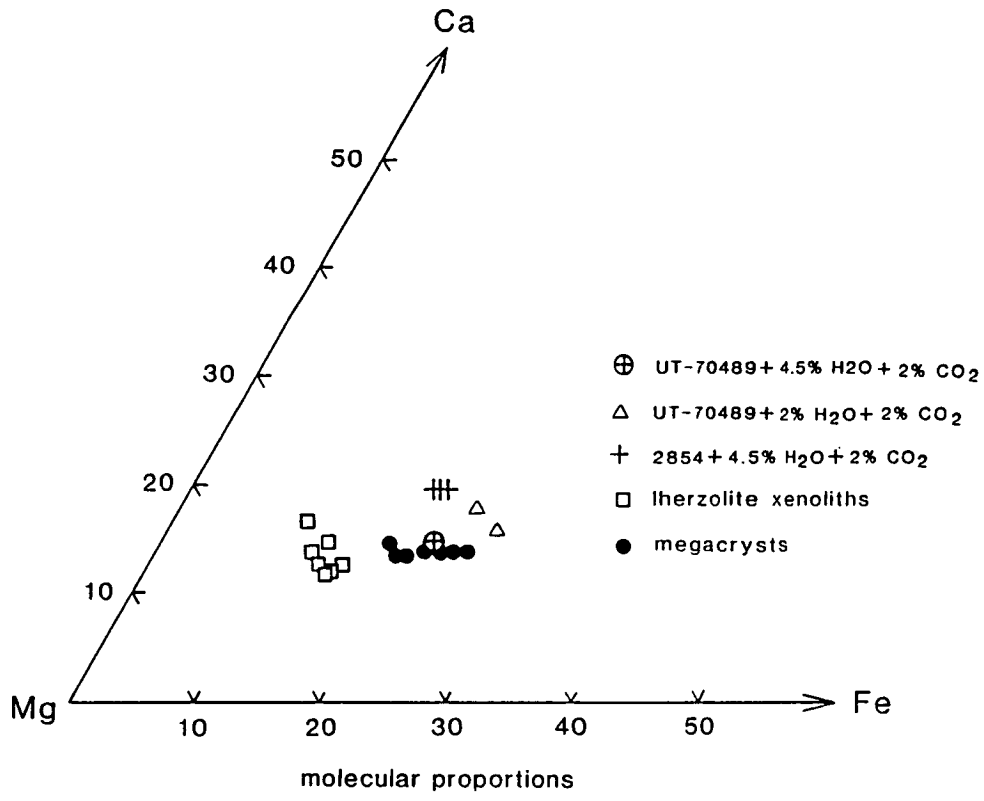

Fig. 29 Ca, Mg and Fe in garnets experimentally crystallized from UT-70489 and 2854. Plotted for comparison are the compositions of garnet megacrysts, and garnets in lherzolite (type I) xenoliths from Cainozoic alkaline basalts. Data on natural garnets are from Frisch & Wright (1971), Mason & Allen (1973), Chapman (1976), Skewes & Stern (1979), Ruoxin et al. (1985), and this work (Table 12).

2.9.5 Garnet as a Residual Phase

It has already been accepted (as a prior assumption to the liquidus experiments) that garnet, clinopyroxne, orthopyroxene and olivine are residual phases from nepheline basanite and olivine nephelinite formation. This assumption is supported by experimental evidence and by the occurrence of garnet lherzolite xenoliths in basanite lavas (as at Bow Hill). At pressures much less than 20 kb (at approximately 1200°C) garnet lherzolite is not stable (Green & Ringwood, 1970; Jenkins & Newton, 1979; Mengel & Green, 1988) and therefore cannot be a residual product. As previously discussed, most olivine basalts and olivine tholeiites probably form at pressures less than 20 kb. The primary magmas of such basalts are therefore unlikely to equilibrate with residual garnet. This conclusion is consistent with experimentally determined liquidus phase relationships for alkali olivine basalts, olivine basalts and olivine tholeiites (Green & Ringwood, 1967; Green & Hibberson, 1970; Thompson, 1974; Fujii & Kushiro, 1977; Takahashi & Kushiro, 1983); it is at odds, however, with inferences that have been made based on REE concentrations (e.g. Feigenson et al., 1983; Hofmann et al., 1984).

2.9.6 Amphibole and Mica as Residual Phases

Amphibole and/or phlogopite have been suggested as possible residual phases from the formation of basanite and more highly silica-undersaturated magmas (Sun & Hanson, 1975; Clague & Frey, 1982). This was done to explain negative correlations between concentrations of Rb, Ba and K_2O (components retained by phlogopite and/or amphibole), and those of Th and P_2O_5 (components not retained by phlogopite or amphibole). Although such correlations are not apparent in the data for Oatlands (Fig. 30), phlogopite and amphibole occur within approximately 30°C of the liquidus of UT-70489 (Fig. 23). Furthermore, although amphibole megacrysts have not been found in alkaline basalts from the Oatlands district, they occur in basanite lava and basaltic tuff in the neighbouring Hobart area (Sutherland, 1976, 1977; see also Table 12). Holloway & Ford (1975) showed that a 43 % substitution of F for OH in amphibole can increase its thermal stability by 80°C or more. Foley et al. (1986) showed a similar effect for F in phlogopite. However, F

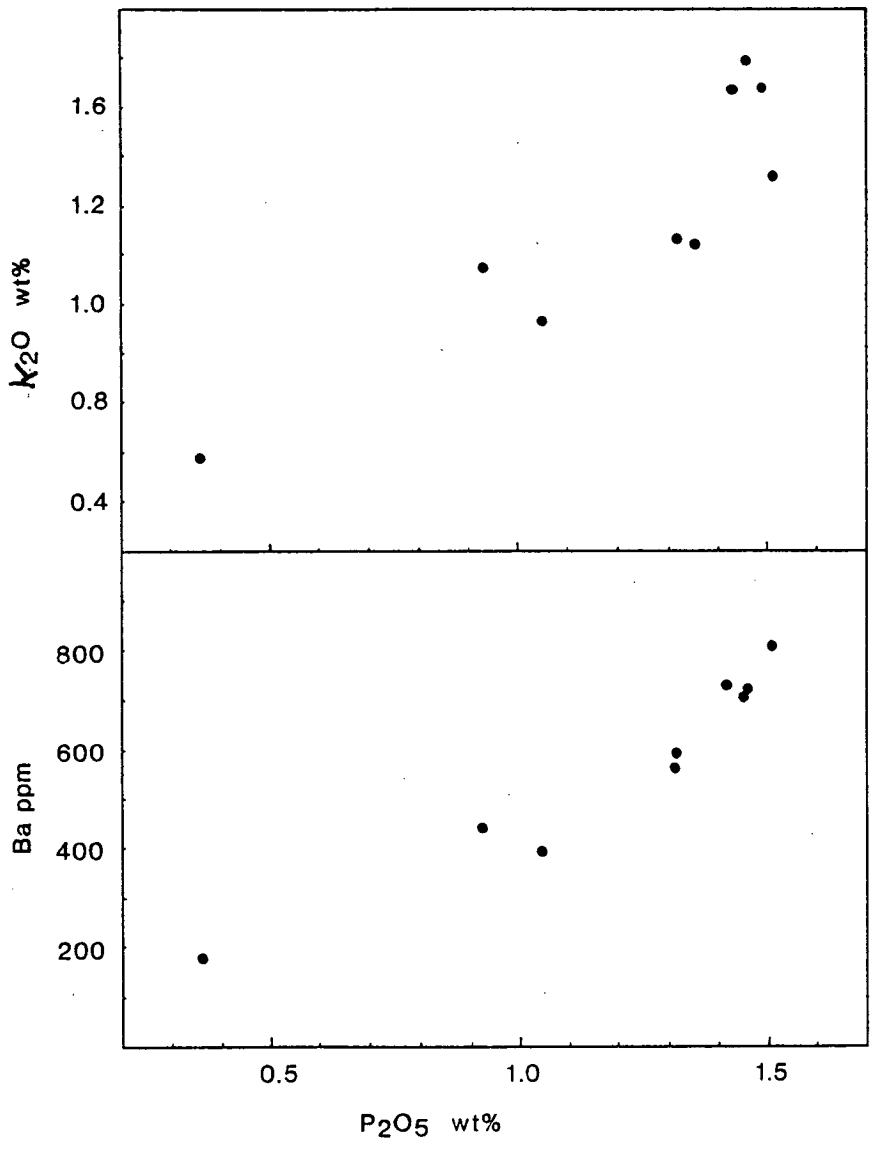

Fig. 30. K_2O and Ba versus P_2O_5 in basalts from the Oatlands district

concentrations in amphibole and phlogopite megacrysts from alkaline basalts are usually less than 0.3 wt.% (Boettcher & O'Neil, 1980; Matson et al. 1984), and it is difficult to decide from the experimental data alone whether amphibole or phlogopite were residual phases.

Least squares mixing calculations were used to model the reaction

75 amphibole + 2 mica + 23 orthopyroxene = 52 basanite + 25 garnet + 16 clinopyroxene + 7 olivine (1)

The amphibole and mica compositions were those of amphibole and mica in spinel lherzolite xenoliths from the Lake Gnotuk maar of western Victoria (Stolz & Davies, 1988). Other compositions used were those of near liquidus phases from UT-70489. Amphiboles in spinel lherzolites from Lake Gnotuk and Bullenmerri are H_2O-rich (with close to 2 wt.% H_2O) [Stolz & Bailey, unpublished gas-extraction mass spectrometry data] and contain, on average, approximately 0.8 wt.% K_2O (Nickel & Green, 1984; Stolz & Davies, 1988); a consequence of these values is that reaction (1) balances with approximately 4.5 wt.% H_2O and 2.0 wt.% K_2O in the basanite melt - the same concentrations as those used in the experimental composition. These observations are consistent with nepheline basanite magmas in the Oatlands district having formed largely by incongruent melting of amphibole, together with relatively minor amounts of mica. However, the relationships shown in Fig. 30 for K_2O and Ba, and the rarity of amphibole megacrysts (particularly Mg-rich examples), suggest that amphibole and mica were not residual phases, although they may have been present in the source prior to melting.

2.10 POSSIBLE SOURCE REGION COMPOSITIONS FOR THE OATLANDS BASALTS

The compositions of residual phases in a basalt source region can be estimated from the compositions of near-liquidus phases (those formed after only a few percent of crystallization) crystallized from the basalt near to the point at which it is multiply saturated in the residual phases. Experiments do not, however, provide information on either the relative proportions of residual phases or on the degree of partial melting which produced

them. Independent chemical and geological evidence must therefore be used to constrain the compositions of source regions.

Studies of peridotite xenoliths in alkaline basalts and kimberlites, and of peridotites in ultramafic masses, have provided the basis for most chemical and mineralogical models of the earth's upper mantle. These peridotites are generally considered to represent refractory lithospheric mantle from which basaltic components (TiO_2, Al_2O_3, CaO, alkalis and P_2O_5) have been removed by one or more partial melting events. They vary greatly, however, in their degree of depletion, and include highly refractory dunites and harzburgites, as well as lherzolites variously enriched in basaltic components. The least depleted samples have been assumed to be similar in composition to the undepleted upper mantle (e.g. Jagoutz et al., 1979; Nickel & Green, 1984; Hart & Zindler, 1986; Arai, 1987).

An alternative approach has been to use assumed complementary relationships between primitive basalts or komatiites and their peridotitic or dunitic residues (e.g. Ringwood, 1975; Sun & Nesbitt, 1977; Green et al., 1979). In general, there is relatively good agreement between many of the estimates obtained by both techniques. This is particularly so for the relative concentrations of SiO_2, FeO and MgO, and somewhat less so for Al_2O_3, CaO and Na_2O. More significant differences occur for the minor oxides TiO_2, K_2O and P_2O_5. Volatile components such as H_2O, CO_2, S, Cl and F have rarely been considered (although see Schilling et al., 1980; Michael, 1987).

Differences between the various estimates may partially be due to differences in approach. They probably also reflect real variations within a mantle that is relatively homogeneous in major components, and more heterogeneous in minor and trace components. Geochemical and isotopic studies have already shown, not only that such heterogeneities exist, but that they have existed for long periods of geological time (Zindler & Hart, 1986).

2.10.1 Enriched Source Regions

Various processes have been suggested, by which chemical heterogeneities within the mantle may be formed. One of these, which enriches the mantle in LREE, highly incompatible trace elements, and basaltic components generally, is mantle metasomatism (Bailey, 1970, 1972). Mantle metasomatism has particular relevance to discussions of alkaline basalt genesis. In this context it has often been used to reconcile the apparent need for a source enriched in incompatible components, but which has isotopic characteristics implying a time integrated depletion in LREE and large ion lithophile elements (Lloyd & Bailey, 1975; Menzies & Murthy, 1980; Wass & Rogers, 1980; Chauvel & Jahn, 1984; Wedepohl, 1985).

A number of examples have been described of material that may represent the metasomatized source regions of alkaline basalts. These include peridotite xenoliths from Nunivak Island, southeastern Australia and Germany, and material from the massive peridotites on the Islands of St. Paul and Zabargad (Roden et al., 1983, 1984; Wedepohl, 1985; Bonatti et al., 1986; O'Reilly & Griffin, 1988; Stolz & Davies, 1988). Many of these examples contain amphibole and apatite: more rarely phlogopite or other volatile-bearing phases are also present.

To test for the possibility of the Oatlands basalts having derived from a source similar to these examples, a number of calculations were made. In the first of these, least squares mixing calculations were used to match various proportions of UT-70489 and its near liquidus phases (garnet, clinopyroxene, orthopyroxene and olivine: see Table 10) to natural metasomatized peridotite compositions. Similar calculations were also performed for 2854 and its near liquidus phases. Analyses of subliquidus pyroxenes and olivines used in these calculations had their Fe/Mg ratios recalculated to have Mg# equal to 87.0 (assuming a crystal/liquid K_d for Fe^{+2}-Mg exchange of approximately 0.3). None of the compositions used, except those of the basanite and nephelinite, are strictly those of liquidus phases. Nevertheless, they are probably sufficiently good approximations for the calculations still to be meaningful.

The most successful calculations were those that modelled the source of UT-70489 and 2854 on natural relatively Fe-rich spinel lherzolite compositions. This seemed largely (although not completely) to be a function of their iron content. Shown in Table 13 are the results of calculations used to model possible source compositions for UT-70489 and 2854 on two relatively fertile and Fe-rich spinel lherzolite compositions. Calculations for both of the model compositions gave solutions for residual garnet, clinopyroxene, orthopyroxene and olivine. They also suggest that UT-70489 would form by 4-5%, and 2854 by 5-6% partial melting of the model compositions. These melting intervals are well within the ranges commonly estimated for basanite and nephelinite formation (e.g. Sun & Hanson, 1975; Frey et al., 1978; Clague & Frey, 1982).

Several published estimates for the composition of the upper mantle are shown in Table 14. By comparison with these, the calculated source compositions are enriched in FeO, K_2O and P_2O_5, and depleted in Al_2O_3 and CaO. These differences are also shared by metasomatized group I spinel lherzolite xenoliths from the Lake Bullenmerri and Gnotuk maars of western Victoria. The average composition of 51 of these xenoliths (Table 14) is similar to the calculated source compositions, although it has less iron and is depleted in TiO_2.

Although chromium is low in the calculated compositions, this is probably due to the pyroxene and garnet compositions used in the calculations being those of subliquidus, rather than actual liquidus phases (i.e. those formed after at least several percent crystallization rather than an infinitely small degree of crystallization). Because Cr is strongly concentrated into pyroxenes and garnet relative to the liquid, crystallization of even a few percent of these phases will cause a significant decrease in Cr concentrations, both within the liquid, and in any crystal phases in equilibrium with it.

Clinopyroxene phenocryst cores in UT-70489 contain up to 1.2 wt.% Cr_2O_3 (in contrast to a maximum of 0.6 wt.% Cr_2O_3 in the experimentally crystallized clinopyroxenes). This value is within the range of Cr concentrations found in clinopyroxenes from natural spinel lherzolite xenoliths. Unless Cr partition coefficients are

Table 13. Results of least squares mixing calculations used to model possible source compositions for UT-70489 and 2854

Reactants	% amounts			
UT-70489	4.83	4.44		
2854			5.48	4.95
Garnet	4.16	1.57	3.51	3.06
Clinopyroxene	14.22	6.97	15.51	5.75
Orthopyroxene	6.21	24.35	10.59	30.39
Olivine	70.58	62.67	64.91	55.85
Products				
GN-24	100.00		100.00	
D		100.00		100.00
Σr^2	0.196	0.113	0.096	0.127

Σr^2 = sum of residues squared

The calculations model the reactions

UT-70489 + garnet + clinopyroxene + orthopyroxene + olivine = peridotite (GN-24 or D)

and

2854 + garnet + clinopyroxene + orthopyroxene + olivine = peridotite (GN-24 or D)

for further explanation see text.

Table 14. Major and trace element concentrations in natural spinel lherzolite xenoliths and in various estimates of upper mantle composition

	natural xenoliths		calculated source models			published estimates for the upper mantle		
	GN24	D	(GN24)	(D)	G/B	1.	2.	3.
SiO_2	43.10	44.63	43.08	44.65	44.16	45.13	44.5	45.0
TiO_2	0.26	0.24	0.26	0.22	0.10	0.22	0.22	0.17
Al_2O_3	2.49	2.39	2.48	2.43	2.04	3.96	4.31	4.4
Cr_2O_3	0.38	0.30	0.10	0.09		0.46		
FeO	10.91	10.84	10.66	10.78	8.79	7.82	8.37	7.6
MgO	38.71	38.59	38.73	38.63	40.95	38.30	38.0	38.8
CaO	3.45	2.14	3.37	2.17	2.29	3.50	3.50	3.4
Na_2O	0.21	0.39	0.41	0.29	0.35	0.33	0.40	0.40
K_2O	0.06	0.12	0.10	0.09	0.05	0.03	0.02	0.03
P_2O_5	0.05	0.04	0.07	0.06	0.12	0.01		
H_2O			0.22	0.20	0.32			
CO_2			0.10	0.09	0.08			
Mg#	86.3	86.4	86.6	86.5	89.5	89.7	89.0	90.1
Σr^2			0.196	0.113				

GN24 = amphibole-bearing spinel lherzolite xenolith analysed by Stolz & Davies (1988)

D = average of 10 Fe-rich lherzolite xenoliths compiled by Kuno & Aoki (1970)

G/B = average of 51 spinel lherzolite xenoliths from the Lake Gnotuk and Bullenmerri maars (data from O'Reilly & Griffin 1988, and Stolz & Davies 1988)

1. = undepleted upper mantle composition of Jagoutz et al. (1979)

2. = primitive mantle of Sun (1982)

3. = MORB pyrolite of Green et al. (1979)

Σr = sum of residuals squared from least squares mixing calculations

* FeO = total iron

significantly affected by pressure or small temperature differences, it seems likely that Cr concentrations in the source of UT-70489 would have been similar to those in natural spinel lherzolite xenoliths. For a similar reason, Ni concentrations in the source would probably also have been similar to Ni concentrations in Fe-rich spinel lherzolite zenoliths.

To test whether the concentrations of other trace elements in the source may have been similar to those in the metasomatized xenoliths, trace element concentrations in the two model sources were calculated. This was done using essentially the same techniques and assumptions as were followed by Frey et al. (1978). Trace element compositions used in these calculations included those of UT-70489, UT-70492, UT-70493, UT-70496 and UT-70497. These samples include the compositional range from olivine tholeiite to olivine melilitite that occurs in the Oatlands district. For comparison, source concentrations were also calculated for the Scottsdale olivine nephelinite 2854.

A prior assumption of the calculations was that all of the basalts derived from a source with an Mg# of 86.5. Most of the basalts have Mg# ratios too low for them to have derived directly from such a source (assuming an olivine/liquid Fe-Mg exchange K_d of 0.3). The example of Frey et al. (1978) was therefore followed. Olivine of appropriate composition was added in 1% increments until the basalts obtained compositions appropriate for them to have been in equilibrium with residual olivine of Mg# 87.0. Trace element concentrations in the basalts were correspondingly adjusted for these added olivine contents.

The degrees of melting and relative proportions of residual phases needed to form UT-70489 and 2854, were given by the results of the least squares mixing calculations. Degrees of melting for the other samples were calculated by assuming P_2O_5 to be completely incompatible in the residues. Appropriate fractions of major and minor elements were then subtracted from the source compositions to give bulk residue compositions. The compositions of experimentally produced near-liquidus phases were then used in least squares mixing calculations to estimate the relative proportions of residual phases. For the nepheline basanite UT-70493, the liquidus phases of

the nepheline basanite UT-70489 were used. For the olivine melilitite 70496, the liquidus phases of the olivine nephelinite 2854 were used, whereas for the alkali olivine basalt UT-70492 and the olivine tholeiite UT-70497, the liquidus phases used were those of the Auckland Island olivine basalt (see Green & Hibberson, 1972). Partition coefficients for the calculations (Table 15) were taken from two sources. One set came from the preferred values of Frey et al. (1978); a second group of higher REE partition coefficients was derived from REE concentrations in megacryst/host basalt pairs, as determined by Irving & Frey (1978; 1984). Where partition coefficients had not been determined for a particular REE, they were obtained by interpolation. Following the suggestion of Frey et al. (1978), P was assumed to have a similar compatibility in the residue to Nd.

The results of some of the calculations are listed in Table 16. Nearly all of the trace elements in the source can be modelled to vary by less than a factor of 2. Exceptions to this are Rb, Sc and Yb. The large variations in Rb and Yb concentrations are largely a function of their exceptionally high concentrations in the olivine melilitite UT-70496. The range of Sc concentrations is more difficult to explain. Calculated source concentrations, when chondrite-normalized (Figs. 31 and 32), have straight REE patterns with high La/Yb (13-6) and show a general enrichment in incompatible components. The later trend (Fig. 32) is broken by large relative depletions in Rb and K. Slight negative anomalies also occur for Sr when the higher partition coefficients for REE are used. The calculated source patterns generally reflect those of the basalts themselves, although variations are less pronounced.

Shown in Figs. 31 and 32, for comparison with the range of calculated trace element concentrations in the Oatlands source, are average REE and trace element patterns for between 14 and 50 Cr-diopside lherzolite xenoliths from the Bullenmerri and Gnotuk maars of western Victoria. (see also Table 14). Trace element concentrations in the calculated and natural compositions show a number of similarities. Both show general increases in chondrite-normalized values from Yb to Nb, followed by a fall to lower values with K, Rb and Ba. Depending upon the K_d values used for REE, both patterns may also have negative Sr anomalies. The average pattern of

Table 15. Partition coefficients used in trace element calculations

	set A				set B		
	Cpx	Opx	Ol	Gt	Cpx	Opx	Gt
La	0.2	0.0005	0.0005	0.001	0.058	0.007	0.005
Ce	0.04	0.0009	0.0008	0.003	0.10	0.008	0.007
Pr	0.06*	0.0014*	0.001*	0.01*	0.19*	0.009*	0.016*
Nd	0.09	0.002	0.0013	0.018	0.22	0.011	0.026
Sm	0.14	0.003	0.002	0.0013	0.45	0.019	0.105
Eu	0.16	0.004	0.002	0.133	0.48	0.022	0.225
Gd	0.17*	0.004*	0.002*	0.19*	0.50	0.033	0.50
Dy	0.19*	0.007*	0.002*	0.6*	0.60	0.061	1.4
Er	0.2*	0.012*	0.003*	1.7*	0.61	0.094	3.1
Yb	0.2	0.0286	0.004	4.0	0.58	0.14	5.7
Rb	0.0	0.0	0.0	0.0	0.03	0.00	0.0
Sr	0.165	0.016	0.016	0.014	0.1	0.0	0.014
Ba	0.0	0.0	0.0	0.0	0.005	0.0	0.0
Y	0.20	0.009	0.002	1.4	0.58	0.009	2.0
Sc	3.1	1.1	0.25	6.5	2.0	1.1	7.1
V	1.5	0.3	0.09	0.27	1.5	0.3	0.27

set A is from Table A-1 (set 1) and Table A-2 of Frey et al. (1978)
set B was calculated from average megacryst/host pairs given by Irving & Frey (1978; 1984)
partition coefficients for Nb, Zr, Zn and Cu were assumed to be close to 0.0
* values obtained by interpolation

Table 16. Calculated trace element concentrations in the Oatlands source region, and measured trace element concentrations in metasomatized xenoliths from western Victoria.

	calculated D model*		L. Gnotuk/Bullenmerri xenoliths	
	average	range	average	σn
Rb	1.9	(1.1-3.8)	0.89	± 0.99
Sr	82	(67-106)	77.5	± 71.5
Ba	31	(26-35)	26	± 28
Zr	20	(12-22)	69	± 18
Nb	5.5	(4.1-7.1)	5.2	± 6.3
Cu	2.6	(2.3-3.0)	4.8	± 4.5
Zn	7.3	(5.9-8.6)	69	± 18
Sc	15	(10-19)	11.5	± 4.7
V	49	(40-58)	51	± 23
Y	3.2	(2.8-4.2)	3.7	± 2.8
La	4.1	(3.1-4.7)	8.6	± 9.0
Ce	8.2	(7.8-9.3)	17.3	± 16.3
Nd	4.0	(3.8-4.2)	7.7	± 7.0
Sm	0.76	(0.77-0.82)	1.4	± 1.3
Eu	0.23	(0.22-0.29)	0.44	± 0.38
Gd	0.73	(0.65-0.95)	0.16	± 0.11
Dy	0.64	(0.56-0.84)		
Er	0.32	(0.25-0.39)	0.40	±
Yb	0.26	(0.18-0.36)	0.31	± 0.16

* partition coefficients used for calculating model source region concentrations were from set A in Table 15.
Residual modes were calculated on the basis of a major element composition similar to D (Table 14)
n = 14 for Gd, Dy and Er, and 32 for other REE.
For other trace elements n = 51

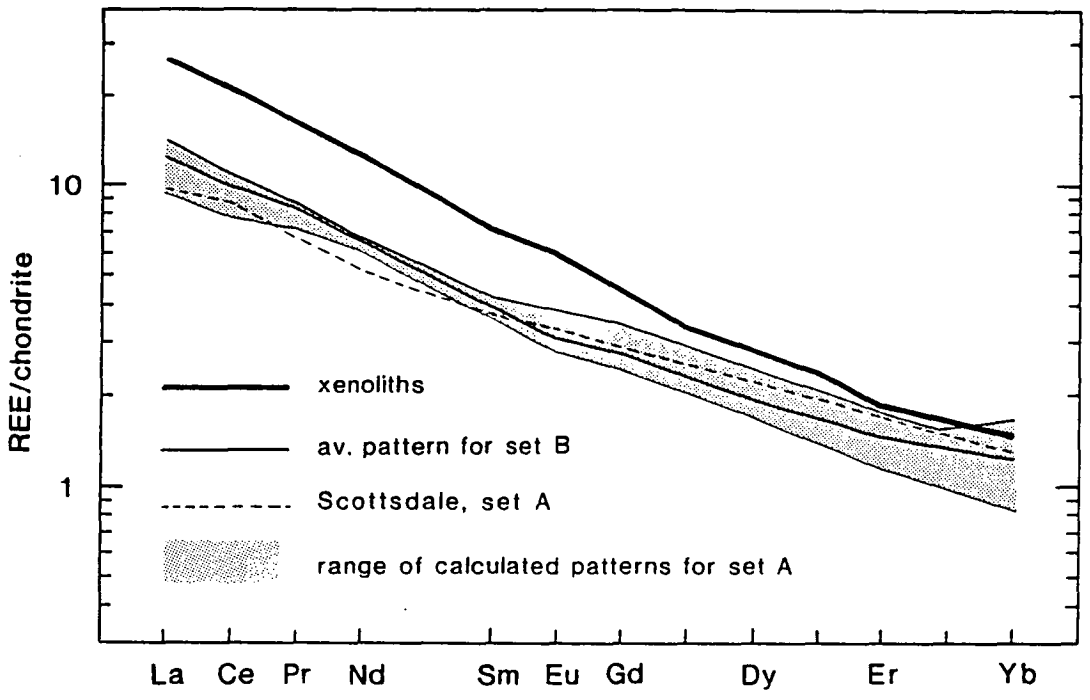

Fig. 31. Chondrite-normalized patterns for calculated REE concentrations in the source region of the Oatlands basalts (calculated assuming a major element concentration in the source region similar to composition D: Table 14), and using the preferred partition coefficients of Frey et al. 1978: set A, Table 15). The heavy line represents average concentrations in spinel lherzolite xenoliths from the Lake Gnotuk and Lake Bullenmerri Maars of western Victoria (data from O'Reilly & Griffin 1987, and Stolz & Davies 1988). The lighter continuous line represents an average source pattern calculated using the higher K_d values from set B (Table 15). The dashed line represents source concentrations for the Scottsdale nephelinite 2854 calculated using K_d values from set A

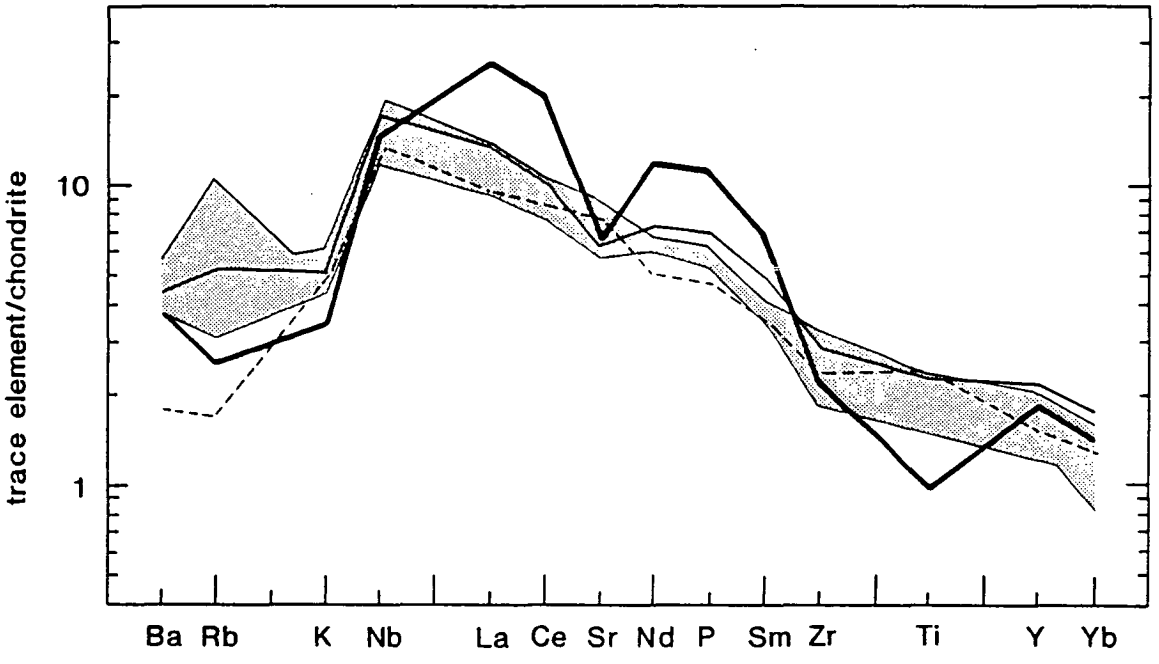

Fig. 32. Chondrite-normalized patterns for calculated trace element concentrations in the source region of the Oatlands basalts. Symbols are as for Fig. 31

the natural xenoliths is far more accentuated than are those of the calculated compositions, with higher LREE values and lower values of alkalis, Ba and Ti. The limited isotopic data available for Tasmanian Cainozoic basalts (McDonough et al., 1985; Ewart et al., 1988) also suggests that the Oatlands source contained lower $^{87}Sr/^{86}Sr$ and higher $^{143}Nd/^{144}Nd$ than present in the average xenolith composition (Griffin et al., 1988; Stolz & Davies, 1988). More detailed comparisons are probably not meaningful, particularly when the heterogeneity of the xenoliths is considered. The main result of the calculations is to show that the Oatlands basalts could have derived from a relatively homogeneous source similar in composition to regions of metasomatized upper mantle beneath southeastern Australia.

2.10.2 Non Enriched Source Regions

It has been suggested that highly alkaline basalts, such as nepheline basanites and olivine melilitites, can be produced by very small degrees of melting (< 2 %) of chondritic or more depleted (MORB type) sources (Gast, 1968; Kay & Gast, 1973). An advantage of this solution is that the isotopic similarities sometimes observed between highly alkaline basalts and MORB's (e.g. O'Nions et al., 1977; Chen & Frey, 1985; McDonough et al., 1985) can be simply explained. Although solutions to the mixing calculations previously described suggest higher degrees of melting (4-6% for basanite and nephelinite compositions), these results do not indicate unique solutions and other possibilities remain.

To examine the possibility of the Oatlands basalts having formed by very small degrees of melting of conventional (lherzolite) sources, trace element concentrations were calculated for the source of the nepheline basanite UT-70489. These are shown as chondrite-normalized patterns in Fig. 33. The patterns were calculated on the basis of UT-70489 having formed as a 1%, 0.1%, and an infinitely small degree of melting of a source containing major element concentrations similar to those in the upper mantle composition of Jagoutz et al. (1979). It can be seen that if UT-70489 were to have derived from such a source, either the source would need to have been relatively enriched in LREE, or UT-70489 would need to have formed by very small degrees of melting (<< 1%).

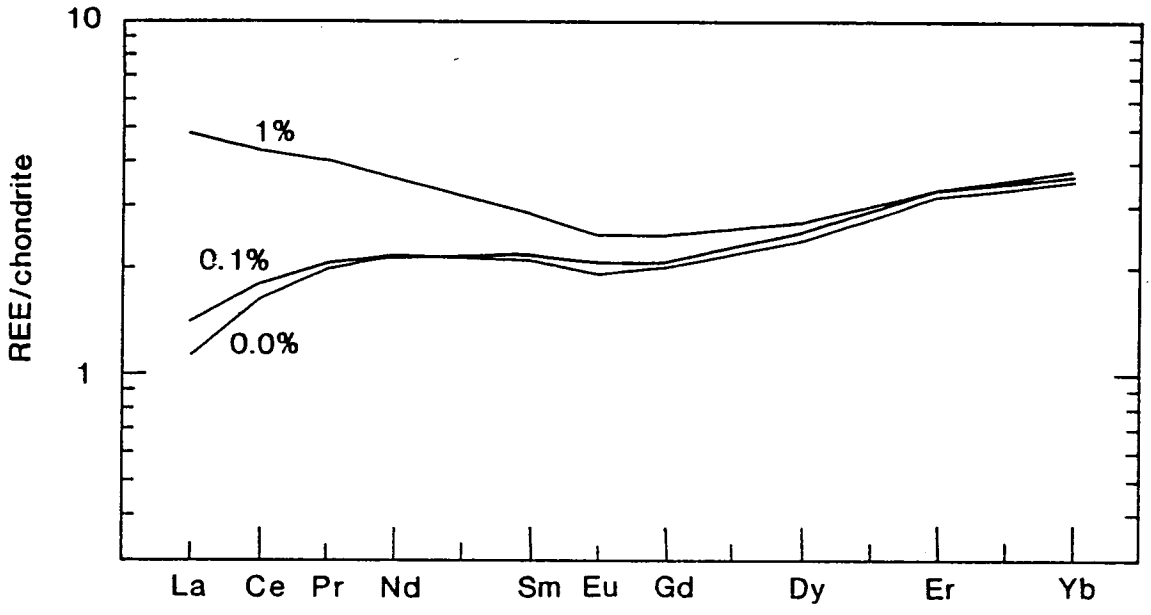

Fig. 33. Chondrite-normalized source patterns for the nepheline basanite UT-70489 based on 1%, 0.1% and an infinitely small degree of melting of a peridotite source similar to that of Jagoutz et al. (1979). The partition coefficients used were from set A in Table 15

Theoretical modelling by von Bargen & Waff (1986) has shown that it is possible to extract melt fractions much less than 1% from a residual matrix, provided that appropriate wetting relationships occur between the melt and matrix. There have, however, been relatively few experimental studies on wetting relationships between basaltic melts and natural peridotite phases (see Fujii et al., 1986, and references therein). Further work will be needed before it is known whether SiO_2-poor volatile-rich basaltic melts (such as nepheline basanite magmas) can be extracted from the mantle at very low degrees of melting.

Leaving such problems aside, there are other difficulties that occur with very low degree melting models if it is assumed that basalts such as nepheline basanites, alkali olivine basalts, and olivine tholeiites are derived from similar lherzolite sources. At low degrees of melting (< 1%) concentrations of highly incompatible elements in the melt phase are strongly affected by large relative changes in the degree of melting (e.g. 0.1% to 0.5%). The opposite is true, however, for compatible trace elements and elements which occur as structural components in mineral phases (e.g. TiO_2 and Na_2O in pyroxenes). Because of these effects, very small degrees of melting can produce large changes in the concentrations of highly incompatible elements (such as P and LREE), but should result in comparatively minor variations in elements such as TiO_2 and Na_2O.

Shown in Fig. 34 is a plot of P_2O_5 concentrations versus Na_2O in primitive alkaline basalts from Oatlands, the Newer Basalts of Victoria, Honolulu, the north Hessian Depression of Germany, the Canary Islands, and the Balcones province of Texas. It can be seen that there is a large range in both P_2O_5 and Na_2O concentrations, and that the two are positively correlated. These features are contrary to those expected from very small degrees of melting of an approximately homogeneous lherzolite source; instead, they more closely resemble the trends produced by about 5-20% melting of pyrolite (Falloon & Green, 1988). If very small degrees of melting are still favoured, then either the source would need to have been heterogeneous with respect to at least Na_2O, or a normal lherzolite source would need to be abandoned in favour of some other alternative. The regular correlation between Na_2O, SiO_2, CaO/Al_2O_3 and P_2O_5 in primitive alkaline basalts (see Figs. 21 and 30), makes

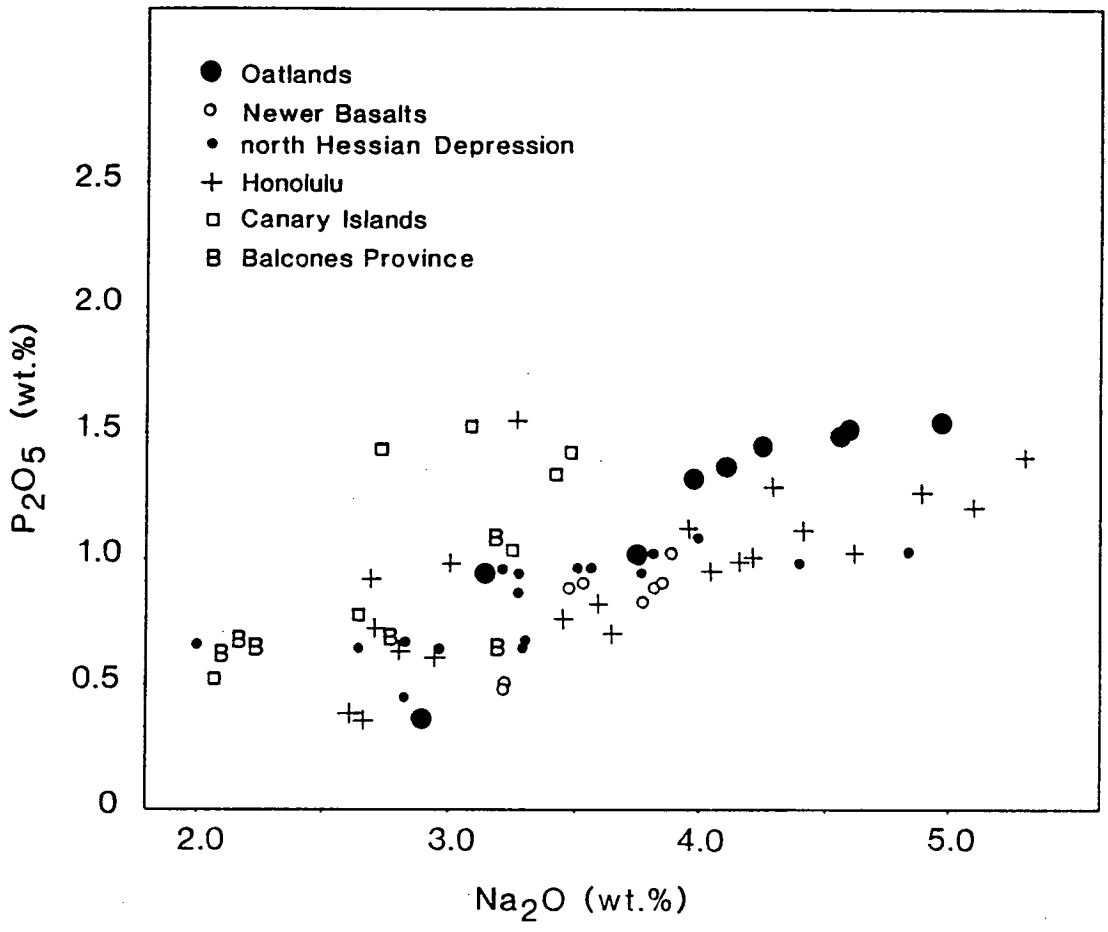

Fig. 34. Concentrations of P_2O_5 and Na_2O in primitive alkaline basalts. Data are from the the same set used for Fig. 21.

a fortuitous relationship between these variables unlikely. Because of this, simple source heterogeneity also appears to be an unlikely explanation for the variation in Na_2O concentrations. As at present there seems to be no good reason for abandoning a conventional lherzolite source, very small degree melting models are not favoured.

Dynamic melting models (e.g. McKenzie, 1984; Ribe, 1988) have also been advocated as a means of deriving enriched basaltic compositions from comparatively depleted sources. Although these models may be more realistic approximations of upper mantle melting processes than simple batch melting models, they do not by themselves produce exceptional incompatible element enrichments unless very small degrees of melting are also involved (Richter, 1986; Ribe, 1988).

2.11 MANTLE SOURCE REGIONS

Intraplate basalts (IB) generally contain higher concentrations of TiO_2, FeO, alkalis, light rare earth elements, and other incompatible trace elements than mid-ocean ridge basalts (MORB). They also tend to have higher ratios of $^{87}Sr/^{86}Sr$ and lower $^{143}Nd/^{144}Nd$. The source regions of IB and MORB are therefore also expected to differ. Because of the great volume, widespread distribution and relative homogeneity of MORB, the composition of the MORB source region has often been thought to generally represent that of the upper mantle. Within this context, various hypotheses have assigned the source of IB to different regions of the mantle. These hypotheses can be grouped into three alternative models, which include:

(1) a lithospheric and/or upper asthenospheric source model in which the IB source occurs above the MORB source (e.g. Lloyd & Bailey, 1975; Green & Liebermann, 1976; Wass & Rodgers, 1980; Wright, 1984; Wedepohl, 1985);

(2) a deep asthenosphere source model in which the IB source is located beneath the MORB source (e.g. Morgan, 1971; Anderson, 1981; Hofmann & White, 1982);

(3) a heterogeneous mantle ('plum pudding') model in which regions of IB source material are randomly distributed within an upper mantle with dominantly MORB source characteristics (e.g. Zindler et al., 1984; Sleep, 1984).

The intraplate basalts in the Oatlands district are similar to those which occur in many other parts of the world. They must fit, therefore, within a general earth model for the origin of intraplate and mid-ocean ridge basalts. In the following section, geochemical and experimental evidence will be used to evaluate each of the previously mentioned models as appropriate or otherwise to the Oatlands district.

2.11.1 Lithospheric Source Models

There have been very few studies published on lithospheric xenoliths from alkaline basalts in Tasmania (although see Varne, 1976; and Sutherland et al., 1984). None of them provide geochemical data with which to make comparisons. In spite of this, it may be assumed that prior to volcanism during the Oligocene, the lithosphere beneath Oatlands was affected by the production of large volumes of tholeiitic magmas during the Jurassic. There is, however, little evidence for the Oligocene basalts having been influenced by this. Cainozoic basalts from Oatlands and other parts of Tasmania have very unradiogenic Sr and radiogenic Nd (close to depleted MORB values), and low ratios of Rb, K and Pb to LREE when compared to primitive mantle values (McDonough et al., 1985; Ewart et al., 1988; this work). These features are similar to those of alkaline basalts from a variety of other geological and tectonic environments (e.g. Allegre et al., 1981; Chen & Frey, 1985; Fitton & Dunlop, 1985; Halliday et al., 1988). They show no tendency toward the highly radiogenic Sr and unradiogenic Nd (near crustal values), and high Rb, K and Pb, relative to LREE, that characterize the Tasmanian dolerites (Herg t, 1987).

The anhydrous spinel and garnet lherzolite xenoliths found within the Oatlands district also seem unlikely source material from which to have formed H_2O-rich alkaline basalt magmas. Nevertheless, it is still possible that the alkaline basalts of the Oatlands district derived from unsampled and more volatile-rich parts of the

lower lithosphere or uppermost asthenosphere. If this was the case, then these regions must have been enriched in volatiles and other incompatible components during some period between the Jurassic and Oligocene.

There are at least two ways in which an enriched lithosperic source region could have evolved: one is that the lower lithosphere was enriched (metasomatized) by fluids or melts infiltrating upwards from deeper within the mantle (Frey & Green, 1974; Lloyd & Bailey, 1975; Green & Liebermann, 1976; Wass & Rogers, 1980; Wright, 1984; Chauvel & Jahn, 1984; Wedepohl, 1985): the other is for previously enriched asthenosphere to have been added to the base of the lithosphere (Ringwood, 1986). Possible similarities between the Oatlands source and metasomatized xenoliths from beneath southeastern Australia do not necessarily help to distinguish the more likely of these alternatives. This is because the metasomatized xenoliths may either reflect the processes by which enriched alkaline basalt source regions are formed, or simply indicate the presence of such a source immediately beneath the source region of the xenoliths. Some support for the latter alternative can be found in the xenoliths themselves. Many of these have relatively high Sr^{87}/Sr^{86} but very low Rb/Sr (Griffin et al., 1988; Stolz & Davies, 1988). Most probably the Sr in these xenoliths derived from a deeper source which was already enriched in Rb/Sr.

2.11.2 Asthenospheric Source Models

It was noticed by Wellman & McDougall (1974), that in eastern Australia, Cainozoic basalts not related to hot spot volcanism have a scattered distribution. There is no systematic relationship between the age of individual basalts, or their provinces, and the latitude in which they occur. There is, however, a tendency for the age of volcanism to increase towards the east at any latitude. Such a distribution is difficult to reconcile with a deep mantle plume hypothesis as originally envisaged by Morgan (1971). A heterogeneous mantle source would be more consistent. In this later case, it would also have to be argued that the melting process was extremely selective; this is because Cainozoic basalts similar in composition to MORB have yet to be found in eastern Australia.

Sleep (1984), has shown that within a heterogeneous mantle, small anomalies (< 20 km across) enriched in low melting point components will be melted preferentially. This occurs both because they begin to melt at lower temperatures and because, being small, they are able to derive latent heat consumed during melting from their surroundings. Although this process may satisfactorily explain heterogeneity about mid-ocean ridges (e.g. Zindler et al., 1984), it seems less likely that it would be able to produce the range of Cainozoic basalt compositions found in eastern Australia, from a mantle with predominantly MORB source characteristics. This is because the compositional contrasts between Cainozoic basalts in eastern Australia, and typical MORB, are far greater than those discussed by Zindler et al. (1984) for mid-ocean ridges and their associated seamounts.

Both deep mantle plume and heterogeneous mantle ('plum pudding') models for the Oatlands source appear to be inconsistent with the overall distribution and compositional characteristics of Cainozoic basalts in eastern Australia. These conclusions are consistent with experimental and petrological data which suggest a relatively shallow (upper asthenospheric or lower lithospheric) derivation for the source region. Plotted in Fig. 35 are the experimentally determined conditions of origin for UT-70489 and 2854. Shown for comparison are the estimated conditions of final equilibration for three garnet lherzolite xenoliths from Bow Hill. For all of these, conditions of origin plot close to the xenolith-derived geotherm of O'Reilly & Griffin (1985). This geotherm (Fig. 35) was interpreted by O'Reilly & Griffin as a perturbed geotherm that resulted from upward movement of mantle material during events related to Cainozoic volcanism.

Because the inferred conditions of origin for UT-70489 and 2854 lie close to the xenolith geotherm, it is unlikely that their source regions were produced by rapid upwelling of material from deep within the mantle. If this had occurred, then considerably higher temperatures for their origin (approximately 1400^{o}C) would be expected (Anderson, 1987). This would be particularly so for UT-70489. It is also unlikely that the source was located at depths much less than about 70 km. At pressures corresponding to depths less than 70 km (approximately 20 kb) the xenolith geotherm crosses

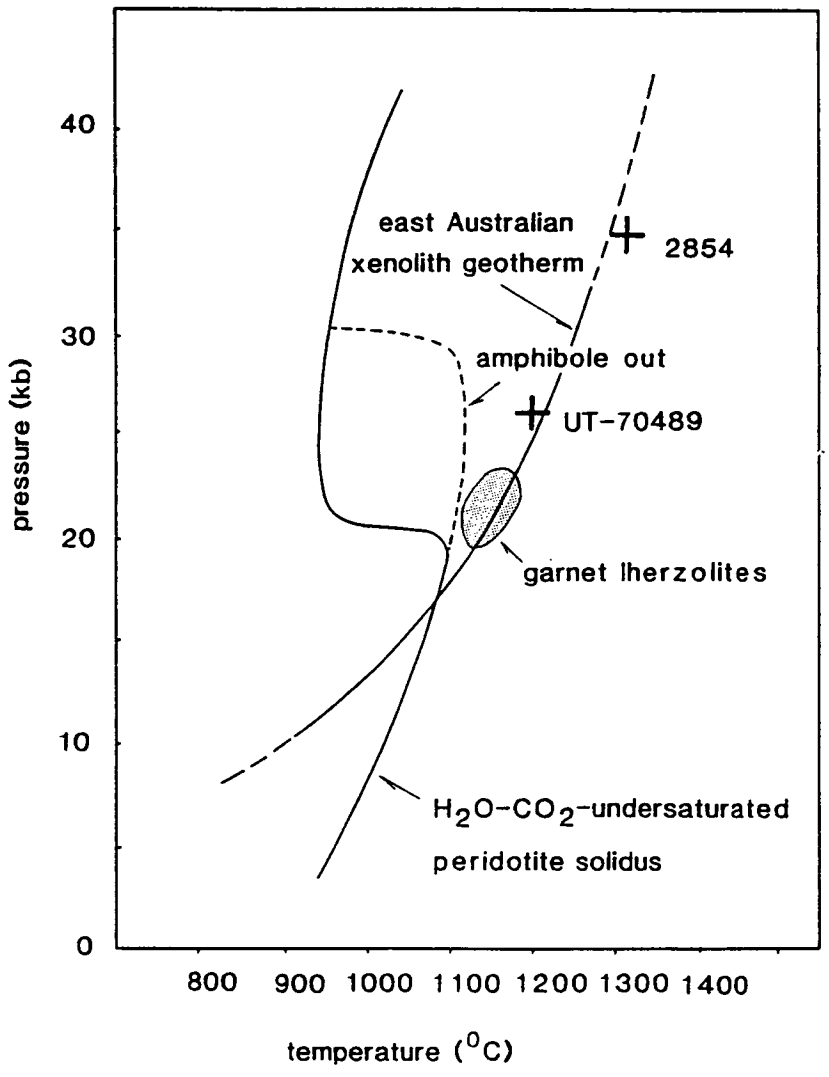

Fig. 35. Conditions of origin for UT-70489 and 2854 inferred from liquidus experiments, & estimated conditions of final equilibration for garnet lherzolite xenoliths from Bow Hill. The later were calculated using the formulations of Wells (1977) and Nickel & Green (1985). Mineralogical data for the garnet lherzolites came from Sutherland et al. (1984) and unpublished data. The H_2O-CO_2-undersaturated peridotite solidus is from Wallace & Green (1988).

the H_2O-CO_2-undersaturated peridotite solidus (Fig. 35). As previously mentioned, it also seems unlikely that the anhydrous garnet and spinel lherzolite xenoliths found in lavas of the Oatlands district could represent source material for volatile-rich alkaline magmas.

If the previously discussed relationship between SiO_2 concentrations in primary basalts and their depths of origin is real, the source region may have been located at depths to 150-170 km. This is the approximate depth of origin estimated (by extrapolation) for the olivine melilitite UT-70496 from Shannon Tier. Unless the original lithosphere beneath Oatlands was exceptionally thick (> 150 km), it is likely that the source included regions of the upper asthenosphere.

Similarities between the calculated source compositions and those of metasomatized spinel lherzolite xenoliths from southeastern Australia, indicate that the source of the Oatlands basalts may have been enriched in incompatible components by processes similar to those which affected the lherzolite xenoliths. However, differences between the calculated source compositions and those of the metasomatized xenoliths (particularly in TiO_2) indicate that the source of the basalts is unlikely to have been depleted lithosphere that was subsequently re-enriched.

2.12 THE CAUSES OF HIGH INCOMPATIBLE ELEMENT CONCENTRATIONS IN THE OATLANDS BASALT SOURCE REGION

Two possible agents for enriching basalt source regions in incompatible elements are:

1. an incompatible-element-enriched C-O-H fluid phase;

2. an incompatible-element-enriched silicate or carbonate melt phase.

Because of the possibility of open system fractionation, only very general constraints can be placed on the nature of the enriching agent. Relatively pure H_2O-CO_2-fluids can be excluded on the basis of H_2O-CO_2-peridotite phase relationships (Fig. 36). At pressures

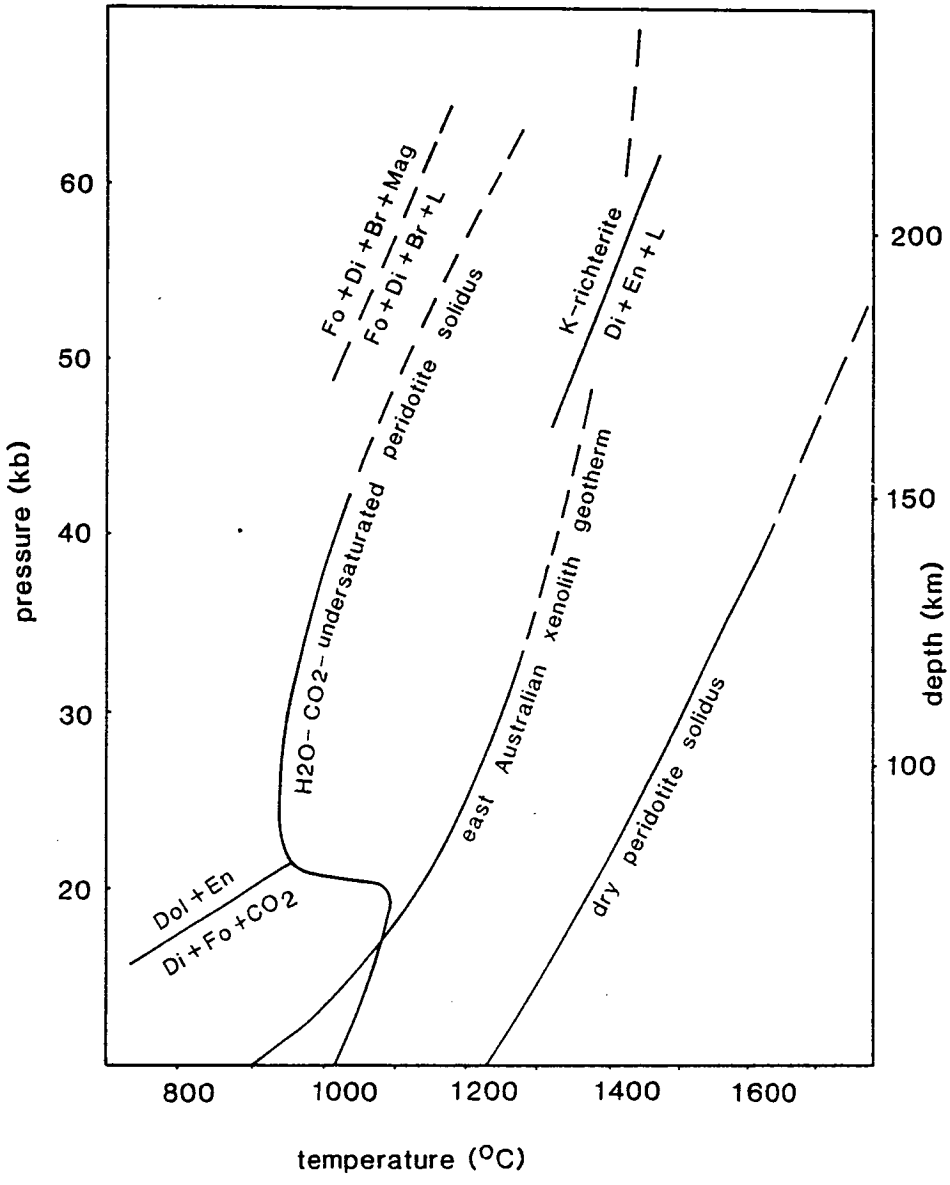

Fig. 36 High pressure peridotite melting relationships in the presence of H_2O and CO_2. The K-richterite and magnesite melting reactions are from Tronnes et al. (1988) and Canil et al. (1988). The dry peridotite solidus is from Green & Ringwood (1967). Other references are as for Fig. 35. Fo = forsterite, Di = diopside, En = enstatite, Br = brucite, Mag = magnesite, L = liquid.

much above 20 kb, CO_2 reacts with olivine and clinopyroxene to form dolomite and orthopyroxene; together with H_2O, it also has a significant effect on the melting temperature of peridotite. As can be seen from Fig. 36, the volatile-free peridotite solidus is lowered as much as 500°C by the presence of H_2O and CO_2. Under a prevailing geotherm similar to the xenolith geotherm (Figs. 35 & 36) of O'Reilly & Griffin (1985) a free H_2O-CO_2-fluid phase would not be possible above about 20 kb. Although a free H_2O-fluid phase might be possible at pressures between 50 and 100 kb [at pressures much greater than 100 kb H_2O will be incorporated into either brucite or a melt phase (Ellis & Wyllie, 1979)], the presence of CO_2 as well as H_2O in erupted basalts requires a source for both of these components. This later observation excludes H_2O-poor carbonatite melts, although such melts have been advocated as a source of metasomatic effects in some upper mantle xenoliths (Menzies & Wass, 1983; Meen, 1987; Green & Wallace, 1988).

CH_4-rich fluids may co-exist with peridotite at relatively high temperatures and pressures, and have been advocated as metasomatic agents within kimberlitic and alkaline basalt source regions (Taylor & Green, 1986; 1988; Foley, 1988). Because of the relatively oxidized character of most kimberlites and alkaline basalts (which often contain carbonate), it has been necessary to argue that oxidation of CH_4-fluids occurs during metasomatism; this leads to the production of H_2O and CO_2, and melting of the source region (redox melting). One factor against this model is the relatively high K_2O/H_2O and P_2O_5/H_2O that are required in the Oatlands source ($\geq$ 0.5 and $\geq$ 0.3 respectively). It is known that the solubility of CH_4 in silicate melts is extremely low. Taylor & Green (1988) found that at 30 kb, less than 0.2 wt.% C was dissolved by CH_4-saturated jadeite and Na-melilite melts. It is unlikely, therefore, that CH_4 fluids would be capable of transporting the high concentrations of alkalis, LREE and P that the metasomatic fluid would have to contain. Although this problem would be overcome by open system enrichment, such an alternative is not possible if redox melting and metasomatism are coupled processes.

A potential metasomatic agent with relative concentrations of volatiles and other highly incompatible components similar to

those inferred for the Oatlands source is that described from micro-inclusions in diamonds (Navon et al., 1988). The inclusions contain volatile-rich melts with high concentrations of H_2O, CO_3^{2-}, K_2O and REE, but low concentrations of MgO. Navon et al. (1988) considered that these melts might represent supercritical fluids formed under conditions of complete miscibility between H_2O-CO_2-fluid and silicate-melt. Eggler (1987) had earlier suggested that such fluids were possible on the basis of experimentally determined solubilities between H_2O-CO_2-fluids and alkali-rich silicate melts.

If melilitite source regions occur to depths of 150-170 km (as previously suggested), the metasomatic fluids or melts responsible for their incompatible-element enrichments are also likely to originate at depths greater than 150-170 km. Relatively few studies have been made of H_2O-CO_2-peridotite melting relations at pressures above 40 kb. There is also no precise knowledge about the distribution of temperature within the asthenospheric mantle (see Jeanloz & Morris, 1986). However, some indication of the depths to which melting may occur is given by the relationships shown in Fig. 36. In a natural peridotite containing sufficient H_2O to be incorporated into K-richterite or phlogopite only, melting will occur at relatively high temperatures (1350-1450°C at 50-60 kb) and will therefore probably be restricted to depths < 200 km [the melting temperature of phlogopite at 55-60 kb is similar that of K-richterite (Tronnes et al., 1988)]. Simple system (MgO-CaO-SiO_2) reactions involving both H_2O and CO_2 indicate that melting may occur at considerably lower temperatures than those of K-richterite or phlogopite breakdown. In the presence of brucite, forsterite and diopside, magnesite melts at temperatures < 1100°C between 50 and 60 kb (Canil et al., 1988). In regions of the mantle containing both H_2O and CO_2 it is possible that melting occurs to depths of several hundred kilometres.

An important feature to note is that the amounts of melting involved may be extremely small. To produce H_2O-CO_2-kimberlitic melts (with 20-30 wt.% H_2O) similar to those described from diamond inclusions (Navon et al., 1988), little more than than 0.01% partial melting of a MORB source containing 0.003 wt.% H_2O (Michael, 1988) is required. Higher degrees of melting may occur at low pressures (< 50 kb) and in source regions more H_2O-rich than those of MORB.

At depths of 650 km and more, silicate perovskites become stable within the mantle (Ringwood, 1982; 1986). Experimental studies have shown that silicate perovskites strongly retain U, Th, Sr, Nb, Zr and LREE during partial melting of peridotite and basaltic compositions (Kato et al., 1988). 650 km is therefore the maximum depth at which melts or fluids enriched in U, Th, Sr, Nb, Zr, and LREE are likely to occur in the mantle. Because intraplate basalts are characteristically enriched in these components it is likely that their source regions also originate at depths < 650 km.

2.13 SUMMARY OF CONCLUSIONS

1. Although H_2O and CO_2 may significantly affect the liquidus phase relationships of basalts (if present in sufficiently high concentrations), they are probably contributing rather than prime factors for determining the major element compositions of nephelinitic and melilitite magmas; such magmas probably originate at pressures of 30-50 kb in the presence of low to moderate H_2O and CO_2 concentrations (< 8 wt.%).

2. Experimental and geochemical data for basalts from Oatlands and Scottsdale in Tasmania are consistent with the derivation of these basalts from Rb, K, Sr, Ba, Zr, Nb, P, LREE, Fe, H_2O and CO_2-enriched lherzolite and garnet lherzolite sources.

3. Intraplate alkaline basalt sources probably derive their high incompatible element concentrations from H_2O-CO_2-rich melts at depths between 150 and 650 km.

APPENDIX 1

ANALYSES OF MINERAL PHASES FROM LIQUIDUS EXPERIMENTS

A list of mineral compositions from liquidus experiments on the CMAS system is given in Table 17. The analyses were made primarily to confirm the identity of mineral phases noted during optical examinations. They do not enable a systematic analysis of compositional relationships between co-existing mineral phases or minerals and liquids. Nevertheless, a number of general observations can be made.

Calcium concentrations in garnets increased with the CaO content of the melt phase (assumed to be approximately equal to that of the starting composition) and were highest in garnets equilibrated with clinopyroxenes. The lowest CaO concentrations were found in garnets crystallized from CO_2-bearing mixes. These garnets were not in equilibrium with clinopyroxene, but were produced from starting compositions (e.g. mix 30) containing CaO concentrations similar to those used in volatile-free and hydrous experiments (e.g. mixes 14, 16 and 26) from which garnets with relatively high CaO contents were crystallized. The effect of CO_2 may therefore have been to preferentially incorporate CaO into the liquid phase rather than the garnet structure.

Al_2O_3 concentrations in orthopyroxenes increased with temperature and with the Al_2O_3 content of the starting mixes from which they crystallized. The maximum Al_2O_3 concentrations were produced in orthopyroxenes equilibrated with garnet, whereas the lowest concentrations were found in orthopyroxenes synthesized during low temperature (1180 °C) experiments on hydrous Al_2O_3-poor compositions.

The compositions of mineral phases produced during liquidus experiments on the nepheline basanite UT-70489 and the olivine nephelinite 2854 are presented in Table 18. Although the analyses were not made for the specific purpose of examining compositional relationships between crystals and liquids, they also showed a number of features worth noting.

TABLE 17

LIQUIDUS PHASES FROM CMAS EXPERIMENTS

	Opx	Opx	Opx	Gt	Gt	Opx	Opx	Opx	Opx	Gt	Opx	Gt	Di	Di
Run	T-1561	T-1561	T-1919	T-1733	T-1776	T-1790	T-1790	T-1844	T-1844	T-1844	T-1837	T-1813	T-1813	T-1813
T(°C)	1600	1600	1570	1500	1520	1180	1180	1050	1050	1050	1150	1100	1100	1100
Mix	4	4	29	14	16	17	17	26	26	26	25	27	27	27
H_2O Wt.%						20	20	20	20	20	20	19.5	19.5	19.5
CO_2 Wt.%														
SiO_2	58.65	58.62	54.97	44.72	43.23	59.84	60.22	56.97	57.96	44.43	60.00	44.42	59.76	54.05
Al_2O_3	4.74	4.52	7.57	24.55	24.58	0.54	0.73	5.62	4.80	25.03	2.73	24.39	3.04	4.34
MgO	38.57	38.49	34.07	25.28	25.05	40.00	39.82	36.57	37.15	23.27	39.14	22.33	19.56	18.71
CaO	0.97	0.93	1.74	6.48	5.45	0.35	0.39	0.91	0.80	8.84	0.46	10.68	23.47	24.19
Σ	102.92	102.56	98.36	101.03	98.31	100.74	101.16	100.08	100.70	101.57	102.34	101.82	100.84	101.29
Oxygens	6	6	6	12	12	6	6	6	6	12	6	12	6	6
Si	1.910	1.916	1.874	3.024	2.997	1.987	1.991	1.906	1.925	3.008	1.960	3.017	1.942	1.912
Al	0.182	0.174	0.304	1.957	2.008	0.021	0.028	0.222	0.188	1.996	0.105	1.952	0.127	0.181
Mg	1.873	1.875	1.732	2.548	2.588	1.981	1.962	1.823	1.839	2.348	1.906	2.261	1.034	0.986
Ca	0.034	0.033	0.064	0.497	0.405	0.013	0.014	0.033	0.028	0.642	0.016	0.777	0.892	0.917
Σ	3.999	3.997	3.974	8.026	7.999	4.002	3.995	3.984	3.981	7.994	3.987	8.007	3.994	3.997

TABLE 17 (cont.)

LIQUIDUS PHASES FROM CMAS EXPERIMENTS

	Opx	Opx	Gt	Opx	Opx	Cpx	Gt	Cpx	Gt	Cpx	Opx	Gt	Opx	Cpx	Gt
Run	T-1875	T-1875	T-1900	T-1900	T-2000	T-2004	T-2002	T-2002	T-2013	T-2013	T-2013	T-2013	T-2237	T-2237	T-2237
T	1450	1450	1450	1450	1350	1330	1330	1310	1310	1320	1320	1320	1100	1100	1100
Mix	5	5	30	30	36	36	36	36	36	38	38	38	40	40	40
H_2O															
CO_2	8	8	10	10	10.3	10.3	10.3	10.3	10.3	10.9	10.9	10.9	11	11	11
SiO_2	55.88	55.25	42.58	43.37	56.31	54.09	46.78	53.59	44.63	51.79	57.63	44.16	55.40	53.73	44.20
Al_2O_3	7.02	7.79	24.19	9.47	6.95	6.82	25.99	5.47	24.61	5.55	5.20	24.89	6.36	3.07	23.93
MgO	36.17	36.04	26.27	34.62	35.28	20.62	25.95	21.71	23.77	21.91	35.83	24.84	35.85	19.43	24.61
CaO	1.09	0.95	2.98	1.12	2.56	21.33	7.18	20.10	8.10	18.54	2.14	6.26	1.24	23.77	7.19
Σ	100.16	100.02	96.03	99.59	101.10	102.86	105.91	100.86	101.10	97.78	100.81	100.15	98.86	100.00	99.92
Oxygens	6	6	12	6	6	6	2	6	12	6	6	12	6	6	6
Si	1.870	1.852	3.001	1.830	1.875	1.867	3.020	1.883	3.028	1.873	1.919	3.009	1.880	1.927	3.029
Al	0.277	0.308	2.009	0.376	0.273	0.278	1.978	0.226	1.968	0.237	0.204	2.000	0.254	0.130	1.933
Mg	1.805	1.800	2.759	1.736	1.750	1.061	2.497	0.137	2.404	1.181	1.778	2.524	1.813	1.038	2.514
Ca	0.040	0.034	0.225	0.040	0.091	0.789	0.497	0.757	0.589	0.718	0.076	0.457	0.045	0.913	0.528
Σ	3.991	3.994	7.994	3.982	3.989	3.995	7.992	4.003	7.989	4.009	3.978	7.990	3.993	4.008	8.004

TABLE 18

NEAR-LIQUIDUS PHASES FROM EXPERIMENTS ON NEPHELINE BASANITE UT-70489

	Garnet	Cpx	ol	Cpx	Cpx	Cpx	Cpx	ol	Cpx	ol	Cpx	Cpx	Cpx	ol	ol	Gt	Gt
Run	T-2287	T2294	T-2295	T-2291	T-2291	T-2303	T-2303	T-2303	T-2317	T-2302	T-2316	T2320	T2393	T-2393	T-2395	T-2395	T-2398
P(kb)	28	24	22	28	28	25	25	25	27	27	27	28	25	25	26.5	26.5	26.5
T(°C)	1250	1270	1240	1290	1290	1250	1250	1250	1265	1250	1280	1270	1170	1170	1185	1185	1200
H_2O	2.0	2.0	2.0	2.0	2.0	4.5	4.5	4.5	4.5	4.5	4.5	4.5	4.5	4.5	4.5	4.5	4.5
SiO_2	41.15	50.30	40.33	53.97	53.95	52.37	52.71	40.54	55.19	42.79	53.02	52.68	52.89	41.39	40.10	44.21	43.08
TiO_2	1.10	0.93	-	0.93	0.84	1.32	0.78	-	0.36	-	0.49	0.61	0.82	-	-	1.27	0.58
Al_2O_3	21.85	7.16	-	6.24	6.46	4.10	3.74	-	4.82	-	5.79	5.48	4.97	-	-	22.49	23.56
Cr_2O_3	-	0.28	-	0.26	0.27	0.36	0.38	-	0.61	-	0.62	0.44	0.41	-	-	0.58	0.59
FeO	12.94	4.92	18.29	5.44	4.61	4.47	4.24	13.18	4.89	14.29	4.94	5.58	5.68	17.52	16.24	13.08	11.07
NiO	-	-	0.39	-	-	-	-	0.33	-	0.35	-	-	-	-	0.34	-	-
MgO	16.12	16.38	44.03	19.64	18.56	15.54	16.00	46.71	18.10	48.51	16.56	16.77	16.11	44.68	44.40	18.02	18.82
CaO	6.01	14.88	0.14	13.92	14.87	19.51	19.77	0.18	18.47	0.19	18.14	17.38	17.45	0.13	-	7.56	6.02
Na_2O	-	1.33	-	1.54	1.72	1.59	1.64	-	1.37	-	1.54	1.47	1.55	-	-	-	-
Σ	99.16	96.18	103.18	101.95	101.28	99.27	99.27	100.94	103.82	106.13	101.11	100.42	99.86	103.7	101.09	107.20	103.67
Mg#	69.0	85.6	81.1	86.5	87.8	86.1	87.1	86.3	86.8	85.8	85.7	84.3	83.5	82.0	83.0	71.1	75.2
Oxygens	12	6	4	6	6	6	6	4	6	4	4	6	6	6 4	4	12	12
Si	3.011	1.877	0.995	1.894	1.904	1.919	1.930	1.000	1.921	1.005	1.899	1.902	1.921	1.008	1.001	2.9977	2.987
Ti	0.060	0.0261	-	0.025	0.022	0.036	0.022	-	0.009	-	0.013	0.017	0.022	-	-	0.0649	0.030
Al	1.884	0.3149	-	0.258	0.268	0.177	0.162	-	0.198	-	0.244	0.233	0.212	-	-	1.797	1.925
Cr	-	0.008	-	0.007	0.007	0.010	0.011	-	0.017	-	0.018	0.013	0.012	-	-	0.031	0.029
Fe	0.792	0.154	0.378	0.560	0.136	0.137	0.130	0.272	0.143	0.281	0.148	0.169	0.172	0.357	0.339	0.742	0.642
Ni	-	-	0.008	-	-	-	-	0.006	-	0.007	-	-	-	-	0.0069	-	-
Mg	1.758	0.911	1.620	1.028	0.976	0.849	0.874	1.717	0.939	1.698	0.884	0.903	0.872	1.623	1.652	1.821	1.945
Ca	0.472	0.595	0.004	0.524	0.562	0.766	0.776	0.005	0.689	0.005	0.696	0.672	0.679	0.003	-	7.56	0.447
Na	-	0.096	-	0.105	0.118	0.113	0.116	-	0.092	-	0.107	0.103	0.109	-	-	-	-
Σ	7.996	3.983	3.004	4.000	3.995	4.007	4.020	3.000	4.008	2.995	4.010	4.010	3.999	2.991	2.999	8.003	8.005

TABLE 18 (CONT.)

NEAR-LIQUIDUS PHASES FROM EXPERIMENTS ON NEPHELINE BASANITE UT-70489 AND OLIVINE NEPHELINITE 2854

	Mica	Mica	Amph	Amph	Opx	Opx	Gt	Cpx	ol	Gt	ol	Opx	Opx	Cpx	Cpx	Opx	ol
Run	T-2387	T-2387	T-2387	T-2387	T-2455	T-2455	T-2455	T-2529	T-2529	T-2529	T-2548	T-2548	T-2548	T-2548	T-2587	T-2587	T-2587
P	25	25	25	25	26	26	26	35	35	35	33.5	35	35	35	35	35	35
T	1150	1150	1150	1150	1210	1210	1210	1280	1280	1280	1270	1305	1305	1305	1300	1300	1300
H_2O	4.5	4.5	4.5	4.5	4.5	4.5	4.5	4.5	4.5	4.5	4.5	4.5	4.5	4.5	4.5	4.5	4.5
CO_2	2.0	2.0	2.0	2.0	2.0	2.0	2.0	2.0	2.0	2.0	2.0	2.0	2.0	2.0	2.0	2.0	2.0
SiO_2	38.36	37.99	42.26	42.69	54.23	53.96	41.76	52.74	41.86	42.87	41.61	57.86	58.53	56.08	56.88	57.63	42.49
TiO_2	2.84	3.20	2.41	2.29	0.22	0.36	0.64	0.76	-	0.86	-	-	-	0.51	0.19	0.17	-
Al_2O_3	15.81	16.02	13.36	12.91	5.21	5.05	22.39	6.83	-	22.91	-	3.36	3.57	4.82	3.66	4.52	-
Cr_2O_3	-	-	0.19	-	-	-	-	-	-	0.30	-	0.19	-	0.28	0.35	0.42	-
FeO	8.37	8.39	9.22	8.84	9.53	9.03	11.41	6.29	16.13	10.28	13.88	7.67	8.89	6.75	6.77	8.00	12.86
MgO	18.88	18.72	15.29	15.21	29.35	28.07	17.81	-	-	-	0.41	-	-	-	23.33	31.45	49.31
CaO	-	0.20	7.59	8.95	1.46	3.17	5.69	15.81	46.85	18.02	47.31	31.41	33.63	18.61	11.87	2.78	-
Na_2O	0.62	0.78	2.79	2.88	-	-	-	18.11	0.15	7.98	0.18	1.67	0.88	15.72	0.98	0.26	-
K_2O	8.58	8.67	2.55	1.58	-	-	-	1.27	-	-	-	-	-	1.93			
Σ	93.46	93.97	95.67	95.37	100.00	99.64	99.70	101.80	105.00	103.20	103.40	103.88	105.5	104.71	104.03	105.23	104.67
Mg#	80.1	79.9	74.7	75.4	84.6	84.7	73.6	81.7	83.8	75.7	85.9	88.0	87.1	83.1	86.0	87.5	87.2
Oxygens	22	22	23	23	6	6	12	6	4	12	4	6	6	6	6	6	4
Si	5.620	5.552	6.272	6.330	1.899	1.903	3.014	1.882	1.001	2.989	1.003	1.936	1.931	1.935	1.950	1.912	1.004
Ti	0.312	0.351	0.269	0.255	0.006	0.009	0.035	0.020	-	0.045	-	-	-	0.0134	0.005	0.004	-
Al	2.730	2.759	2.337	2.256	0.215	0.210	1.906	0.287	-	1.883	-	4.138	0.139	0.196	0.148	0.177	-
Cr	-	-	0.023	-	-	-	-	-	-	0.016	-	0.005	-	0.008	0.010	0.011	-
Fe	1.026	1.026	1.144	1.096	0.279	0.266	0.689	0.188	0.323	0.600	0.280	0.223	0.245	0.195	0.194	0.222	0.254
Mg	4.124	4.078	3.383	3.362	1.534	1.475	1.916	-	-	-	0/008	-	-	-	1.192	1.555	1.737
Ca	-	0.031	1.207	1.422	0.055	0.120	0.440	0.841	1.670	1.873	1.700	1.628	1.654	0.957	0.436	0.099	-
Na	0.178	0.222	0.804	0.828	-	-	-	0.693	0.004	0.596	0.005	0.062	0.031	0.581	0.065	0.016	-
K	1.603	1.617	0.484	0.299	-	-	-	0.088	-	-	-	-	-	0.129			
Σ	15.592	15.636	15.923	15.850	3.988	3.983	8.000	3.998	2.998	8.002	2.996	3.992	4.000	4.014	3.999	3.997	2.996

Concentrations of TiO_2, CaO and Na_2O in clinopyroxenes increased with increasing degree of crystallization and with decreasing Mg/(Mg + Fe), whereas Al_2O_3 increased with increasing pressure. CaO concentrations appeared to decrease with decreasing volatile content (and therefore also with increasing temperature) and increasing CO_2/H_2O. Garnets increased in TiO_2 and CaO, and decreased in Mg/(Mg + Fe) with increasing degree of crystallization.

The compositions of the experimentally produced near liquidus phases do not closely resemble those of similar phases found in Cr-diopside lherzolite xenoliths or as megacrysts; instead, they have characteristics which are intermediate between these two associations. The closest match was found with natural pyroxenes, amphiboles and micas in Fe-Ti-rich Cr-diopside lherzolite xenoliths from the Lake Gnotuk and Bullenmerri Maars of western Victoria (see Stolz & Davies, 1988).

APPENDIX 2

REVERSAL EXPERIMENTS

An original intention of the liquidus experiments on nepheline basanite UT-70489 was the establishment of initial conditions for later peridotite melting experiments (i.e. attempts to directly determine the liquid compositions formed by small degrees of melting of garnet lherzolite). By using a sandwich technique to overcome the difficulties involved in quenching volatile-rich melts produced by low degrees of melting (see Takahashi & Kushiro, 1983), it was hoped to examine the effects of pressure and variable H_2O/CO_2 on basanite and nephelinitic liquids in equilibrium with garnet lherzolite.

During peridotite melting experiments in which a sandwich technique is used, a layer of basaltic composition is held between two peridotite layers. Under experimental conditions the basaltic layer melts and partial melting of the two peridotite layers occurs. Equilibrium between liquid in the basalt and peridotite layers occurs during the run so that the composition of the basaltic layer becomes representative of the melt phase in equilibrium with the peridotite residue. Because of the volume of the basaltic layer, modifications to its composition caused by crystallization during

quenching are minimized. Ideally, therefore, even if the basaltic layer does not quench to a glass or fine-grained charge, its average composition can still be used to determine the original composition of the melt phase.

Using the sandwich technique, attempts were made to equilibrate UT-70489 with two different peridotite compositions. These included the Hawaiian pyrolite-40% olivine composition used by Jaques & Green (1980) and a second composition that represented an arbitrary combination of near liquidus ('residual') phases from UT-70489 (see Table 10). The conditions of the experiments were set to match those at which UT-70489 was multiply saturated with garnet, clinopyroxene, orthopyroxene and olivine (26 kb and 1200-1210°C with 4.5% H_2O and 2% CO_2 in the melt phase).

Care was taken to avoid large relative errors (in concentrations of H_2O, CO_2 and other oxides, due to the small amounts involved) during the addition of H_2O and CO_2. This was initially done by trapping H_2O in glass (for the basanite layer) and amphibole (in the peridotite layers) and by including CO_2 in the basanite composition as $MgCO_3$. In later experiments that involved relatively high melt:peridotite ratios (55:45), H_2O and CO_2 were added directly to each experiment as water and silver oxalate ($Ag_2C_2O_4$). Run times varied between 40 minutes and two hours.

The first experiment was made using the Hawaiian pyrolite-40% olivine composition and a basanite to peridotite ratio of 1:9. Both this and later experiments (in which higher basanite:peridotite ratios were used) failed due to the basanite layer merging with surrounding peridotite layers. The failure of the melt layer to maintain its integrity was a surprise considering the success of experiments on anhydrous compositions that involved much higher degrees of melting and longer run times (up to 45 hours, see Takahashi & Kushiro, 1983, and Falloon & Green, 1988). Presumably, the viscosity of the volatile-rich basanite liquid was so low, and its tendency to wet peridotite phases sufficiently high, that the two peridotite layers were able to absorb the basanite liquid and merge together.

In an attempt to overcome the problems encountered in the first set of experiments, a modified experimental procedure was adopted. This involved only a single peridotite layer and an increased basanite to peridotite ratio (of 35:65). The basanite layer was placed above the peridotite layer in the hope that a melt layer would 'float' above an underlying layer of melt and residual crystals. The peridotite layer was composed of a 3:7 mixture of basanite and residual peridotite composition. This mixture was adopted in the hope of minimizing any problems that may have been caused by reactions involving melts from the peridotite and basanite layers that were not initially in equilibrium.

The second group of experiments produced a set of stratified charges. These contained a lower predominantly peridotite layer (with some quench crystals and glass) and an upper layer containing poikolitic garnets and smaller clinopyroxenes set within a porous matrix of feathery pyroxene crystals and glass. Although the peridotite phases produced in these experiments were generally uniform in composition throughout the charge (excepting some trapped as inclusion in garnets), the basalt layer was so heterogeneous that only a very approximate estimate of its original composition could be obtained. For this reason, melting experiments were abandoned in favour of further liquidus experiments on a natural olivine nephelinite composition.

One positive result of the reversal experiments was the reproduction of the compositions of near liquidus phases crystallized from the basanite near conditions at which it was multiply saturated with garnet, clinopyroxene, orthopyroxene and olivine. For comparison, the compositions of near liquidus phases and those produced in an experiment at 1210°C and 26 kb on a 55:44 mixture of basanite and residue compositions are shown in Table 19. Although the near liquidus clinopyroxene composition is slightly more CaO-rich and has lower Mg/(Mg + Fe) than that equilibrated with orthopyroxene in the reversal experiment, this is probably due to it having crystallized at slightly lower temperature and pressure under subliquidus rather than liquidus conditions.

TABLE 19

Peridotite Phases Crystallized During Reversal Experiments and Liquidus Experiments

	Liquidus Experiments			Reversal Experiments			Peridotite Starting Compositions	
	Gt	Cpx	Opx	Gt	Cpx	Opx	1.	2.
T(°C)	1200	1170	1210	1210	1210	1210		
P(kb)	26.5	25	26	26	26	26		
Run	T-2398	T-2398	T-2455					
SiO_2	41.5	52.9	54.2	41.9	52.8	54.4	47.7	49.75
TiO_2	0.6	0.8	0.2	0.6	0.6	0.3	1.2	0.51
Al_2O_3	22.5	5.0	5.1	22.8	6.0	5.6	6.3	5.78
Cr_2O_3	0.5	0.4		0.4	0.4	0.3	0.65	0.26
FeO	10.6	5.7	9.5	11.3	5.3	8.6	7.8	7.61
MgO	18.2	16.1	29.5	17.9	17.1	29.2	29.8	25.62
CaO	5.8	17.5	1.5	5.3	16.5	2.0	5.2	9.68
Na_2O	-	1.5	-	-	1.3	-	0.86	0.78
Mg#	75.4	83.5	84.8	73.8	85.2	85.9	87.2	85.7

1. Hawaiian pyrolite-40% olivine
2. Residue composition calculated as a mixture of near liquidus garnet (10%), clinopyroxene (50%), orthopyroxene (20%) and olivine (20%) from liquidus experiments in UT-70489.

APPENDIX 3

FLUID INCLUSIONS IN MEGACRYSTS FROM BOW HILL

Fluid inclusions were found to be common in clinopyroxene and olivine megacrysts from Bow Hill; they were examined as part of a wider study of fluid inclusions in mantle materials that was subsequently discontinued. The inclusions occurred along healed fractures and veins of magmatic alteration that extended inward from crystal margins. Three types of inclusions were recognized for purposes of description. They included:

1. approximately spherical inclusions 10-30μ in diameter with faceted sides. These contained both liquid and vapour and were commonly surrounded by smaller inclusions which decorated small fractures caused by partial decrepetation of the larger inclusions;

2. irregularly shaped inclusions containing both liquid and vapour together with smaller amounts of glass. These were sometimes interconnected to form dendritic or web shaped patterns;

3. equant to irregularly shaped inclusions 5-50μ in average diameter containing daughter crystals of amphibole, opaque oxide and other phases, together with glass and a relatively small fluid bubble.

Drawings of some of these inclusions are shown in Figure 37.

In all of the inclusions examined, the fluid phase homogenized at temperatures of 35°C, or less, indicating that the fluid was probably CO_2-rich. To test for the presence of other components, several clinopyroxene megacrysts were crushed under vacuum so that the released gases could be analysed in a mass spectrometer. Only CO_2 was detected by this method. Possible CO was masked by a high N_2 background. H_2O may also have been present but remained undetected due to adsorption of the small amounts involved onto metal surfaces and newly exposed surfaces on the crushed samples.

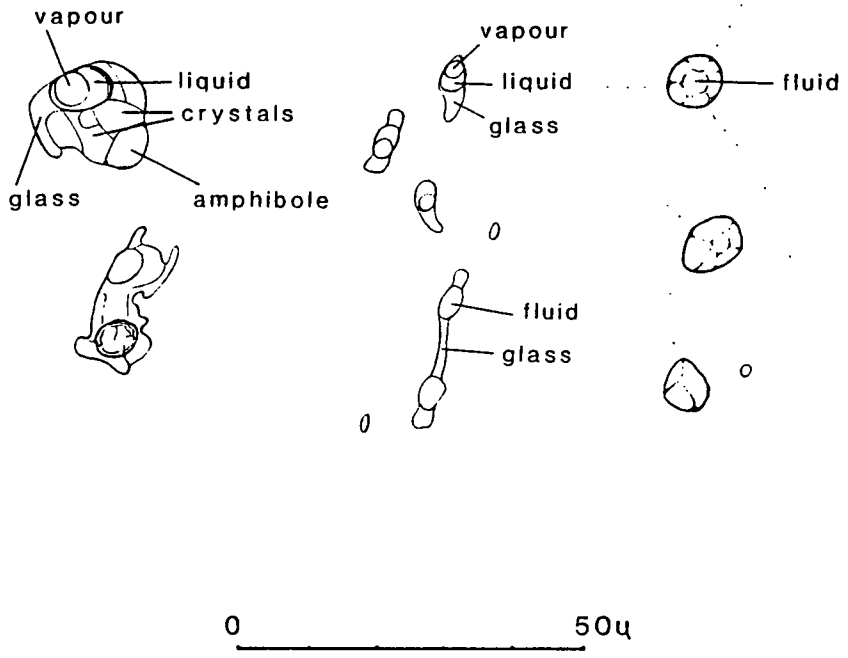

Fig. 37 Fluid inclusions in pyroxene megacrysts from Bow Hill

All of the CO_2 inclusions homogenized at temperatures between 24 and 35°C. Assuming the fluid in the inclusions to have been pure CO_2 and that they were trapped at 1100-1200°C, a maximum pressure in the inclusions of about 3.5 kb can be estimated using the isochores calculated by Anderson et al. (1987). As many of the inclusions showed signs of partial decrepitation, this estimate may represent a minimum value relative to the original trapping pressures.

3.3.1 Discussion

Similar fluid inclusions to those found at Bow Hill were also found by Anderson et al. (1987) in pyroxene megacrysts and pyroxenite xenoliths from alkaline basalts in other parts of eastern Australia, the southwestern United States, and western Europe. These inclusions were often associated with sulphide inclusions and were interpreted by Anderson et al. (1987) as primary magmatic features. In the case of the fluid inclusions found at Bow Hill, it seems unlikely that they were related to the original formation of the megacrysts; rather, they seem to be secondary features more closely related to the host basalts in which the megacrysts were found. It is probable that the megacrysts acted as 'bottles' in which exsolved fluids from the host magmas were trapped during their ascent to the surface.

The trapped fluids provide potential material for studies of carbon and noble gas isotopes in continental alkaline basalts. Combined with studies of CO_2-rich fluid inclusions in metasomatized Cr-diopside lherzolite xenoliths (from the same host basalts), such studies might enable constraints to be placed on relationships between fluids in alkaline basalt source regions and lithospheric fluids associated with metasomatic effects in Cr-diopside lherzolite xenoliths.

REFERENCES CITED

Aggrey, K. E., Muenow, D. W., & Sinton, J. M., 1988. Volatile abundances in submarine glasses from the North Fijii and Lau back-arc basins. Geochim. Cosmochim. Acta **52**, 2501-2506.

Alibert, C., Michard, A., & Alberade, F., 1983. The transition from alkali basalts to kimberlites : isotope and trace element evidence from melilitites. Contrib. Mineral. Petrol. **82**, 176-186.

Allegre, C. J., Dupre, B., Lambert, B., & Richard, P., 1981. The subcontinental versus the suboceanic debate - I. lead-neodynium-strontium isotopes in primary alkali basalts from a shield area: the Ahaggar volcanic suite. Earth Planet. Sci. Lett. **52**, 85-92.

Anderson, D. L., 1981. Hotspots, basalts, and the evolution of the mantle. Science **213**, 82-89.

--------, 1987. The depths of mantle reservoirs: in Magmatic Processes: Physiochemical Principles. The Geochemical Society, Spec. Pub. **1**, 3-12.

Anderson, T., Griffin, W. L., & O'Reilly, S, 1987, Primary sulphide melt inclusions in mantle derived megacrysts and pyroxenites. Lithos **20**, 279-294.

Arai, S., 1987. An estimate of the least depleted spinel peridotite on the basis of olivine-spinel mantle array. N. Jb. Miner. Mh. **8**, 347-354.

Arculus, A. J., 1975. Melting behavior of two basanites in the range 10-35 kbar and the effect of TiO_2 on the olivine-diopside reactions at high pressures. Carnegie Inst. Yearb. **74**, 512-515.

Bailey, D. K., 1970. Volatile flux, heat focusing and generation of magma. Geol. J. Spec. Issue **2**, 177-186.

------, 1972. Uplift, rifting and magmatism in continental plates. J. Earth Sci. (Leeds) **8**, 225-239.

Banks, M. R., & Clarke, M. J., 1987. Changes in the geography of the Tasmania Basin in the Late Proterozoic: in McKenzie, G. D. (Ed), Gondwana Six: Stratigraphy, Sedimentology and Paleontology. American Geophysical Union Monograph **41**, 1-14.

Barker, D. S., Mitchel, R. H., & McKay, D., 1987. Late Cretaceous nephelinite to phonolite magmatism in the Balcones province, Texas. Geol. Soc. Am. special paper **215**, 293-304.

Barreiro, B. A., & Cooper, A. F., 1987. A Sr, Nd, and Pb isotope study of alkaline lamprophyres and related rocks from Westland and Otago, South Island, New Zealand. Geol. Soc. Am. Bull. Spec. Paper **215**, 115-125.

Berry, R. F., & Banks, M. R., 1985. Striations on minor faults and the structure of the Parmeener Super-group near Hobart, Tasmania. Papers Proc. Royal Soc. Tasmania **119**, 23-29.

Boettcher, A. L., & O'Neil, J. R. ,1980. Stable isotopes, chemical and petrographic studies of high-pressure amphiboles and micas: evidence for metasomatism in the mantle source regions of alkali basalts and kimberlites. Am. J. Sci. **280-A**, 594-621.

Bonatti, E., Ottonello, G., & Hamlyn, P. R., 1986. Peridotites from the island of Zabargad (St. John), Red Sea: petrology and geochemistry. J. Geophys. Res. **91**, 599-631.

Bowen, N. L., & Schairer, J. F., 1935. The system MgO-FeO-SiO_2. Am. J. Sci. **29**, 151-217.

Boyd, F. R., & England, J. L., 1960. Apparatus for phase-equilibrium measurements at pressures up to 50 kilobars and temperatures up to 1750°C. J. Geophys. Res., **65**, 741-748.

Brey, G., & Green D. H., 1974. The role of CO_2 in the genesis of olivine melilitite. Contrib. Mineral. Petrol. **49**, 93-103.

Brey, G., & Green, D. H., 1977. Systematic study of liquidus phase relationships in olivine melilitite + H_2O + CO_2 at high pressures and petrogenesis of an olivine melilitite magma. Contrib. Mineral. Petrol. **61**, 141-162.

Bultitude, R. J., & Green, D. H., 1968. Experimental study at high pressures on the origin of olivine nephelinite and olivine melilite nephelinite magmas. Earth Planet. Sci. Lett. **3**. 325-327.

Bultitude, R. J., & Green, D. H., 1971. Experimental studies of crystal-liquid relationships at high pressures in olivine nephelinite and basanite compositions. J. Petrol. **12**, 121-147.

Burnham, C. W., & Jahns, R. H., 1962. A method for determining the solubility of water in silicate melts. Am. J. Sci. **260**, 721-745.

Byers, C. D., Garcia, M. O., & Muenow, D. W., 1985. Volatiles in pillow rim glasses from Loihi and Kilauea volcanoes, Hawaii. Geochim. Cosmochim. Acta **49**, 1887-1896.

Canil, D., Scarfe, C. M., & Tronnes, 1988. Magnesite stability and melting relations of carbonated peridotite in the system CaO-MgO-SiO_2-CO_2 at high pressure. EOS **69**, 1466.

Cao, R., & Zhu, S., 1987. Mantle xenoliths and alkali-rich host rocks in eastern China. In: Nixon, P. H. (ed.), Mantle Xenoliths. ps. 167-180, John Wiley & Sons Ltd.

Carter, J. L., 1970. Mineralogy and chemistry of the earth's upper mantle based on the partial fusion-partial crystallization model. Geol. Soc. Am. Bull., **81**, 2021.

Chapman, N. A., 1976. Inclusions and megacrysts from undersaturated tuffs and basanites, East Fife, Scotland. J. Petrology **17**, 472-498.

Chauvel, C., & Jahn, B., 1984. Nd-Sr isotope and REE geochemistry of alkali basalts from the Massif Central, France. Geochim. Cosmochim. Acta **49**, 93-110.

Chen , C. H., & Presnall, D. C., 1975. The system Mg_2SiO_4-SiO_2 at pressures up to 20 kilobars. Am. Mineral. **60**, 398-406.

Chen, C. Y., & Frey, F. A., 1985. Trace element and isotopic geochemistry of lavas from Haleakala volcano, East Maui, Hawaii: implications for the origin of Hawaiian basalts. J. Geophys. Res. **90**, 8743-8768.

Clague, D. A., & Frey, F. A., 1982. Petrology and trace element geochemistry of the Honolulu Volcanics, Oahu : Implications for the oceanic mantle below Hawaii. J. Petrol. **64**, 123-126.

Coombs, D. S., & Wilkinson, J. F. G., 1969. Lineages and fractionation trends in undersaturated volcanic rocks from the East Otago volcanic province (New Zealand) and related rocks. J. Petrol. **10**, 440-501.

Davis, B. T. C., 1964. The system diopside-forsterite-pyrope at 40 kilobars. Carnegie Inst. Yearb. **63**, 165-171.

-----, & Schairer, J. F., 1965. Melting relations in the join diopside-forsterite-pyrope at 40 kilobars and at one atmosphere. Carnegie Inst. Yearb. **64**, 123-126.

Delaney, J. R., Muenow, D. W., & Graham, D. G., 1978. Abundance and distribution of water, carbon and sulfur in the glassy rims of submarine pillow basalts. Geochim. Cosmochim. Acta **42**, 581-594.

Dixon, J. E., Stolper, E., & Delaney, 1988. Infrared spectroscopic measurements of CO_2 and H_2O in Jaun de Fuca Ridge basaltic glasses. Earth Planet. Sci. Lett. **90**, 87-104.

Duncumb, P., & Reed, S. J. B., 1968. The calculation of stopping power and backscatter effects in electron probe microanalysis. In Heinrich, K. F. J. (ed), Quantitive Electron Probe Microanalysis. Nat. Bur. Stands. Spec. Publ. **298**, Washington: U. S. Department of Commerce.

Edwards, A. B., 1950. The petrology of the Cainozoic basaltic rocks of Tasmania. Proc. roy. Soc. Vict., **62**, 97-120.

Eggler, D. H., 1978. The effect of CO_2 upon partial melting of peridotite in the system Na_2O-CaO-Al_2O_3-MgO-SiO_2-CO_2 to 35 kb, with an analysis of melting in a peridotite-H_2O-CO_2 system. Am. J. Sci. **278**, 305-343.

------, 1987. Solubility of major and trace elements in mantle metasomatic fluids: experimental constraints. In: Menzies, M. A., & Hawkesworth, C. J. (eds), Mantle Metasomatism., Academic Press, ps. 21-39.

------, & Rosenhauer, M., 1978. Carbon dioxide in silicate melts: II. solubilities of CO_2 and H_2O in $CaMgSiO_6$ (diopside) liquids and vapours at pressures to 40 kb. Am. J. Sci. **278**, 64-94.

Ellis, E. E., & Wyllie, P. J., 1979. Hydration and melting relations in the system MgO-SiO_2-H_2O at pressures up to 100 kb. Am. Mineral. **64**, 41-48.

Ellis, D. J., 1976. High pressure inclusions in the Newer Volcanics of Victoria. Contrib. Mineral. Petrol., **58**, 149-180.

Ewart, A., Chappell, B. W., & Menzies, M. A., 1988. An overview of the geochemical and isotopic characteristics of the eastern Australian Cainozoic volcanic provinces. In Menzies, M. A., & Cox, K. G. (eds), Oceanic and Continental Lithosphere: Similarities and Differences. J. Petrol., special issue, 225-273.

Falloon, T. J., & Green, D. H., 1988. Anhydrous partial melting of peridotite from 8 to 35 kbar and the petrogenesis of MORB. In Menzies, M. A. & Cox, K. G. (eds), Oceanic and Continental Lithosphere: Similarities and Differences. J. Petrol., special issue, 379-414.

-------,-----, Hatton, C. J., & Harris, K. L., 1988. The anhydrous partial melting of a fertile and depleted peridotite from 2 to 30 kbar and application to basalt petrogenesis. J. Petrol. (in press).

Feigenson, M. D., Hofmann, A. W., & Spera, F. J., 1983. Case studies on the origin of basalt II. The transition from tholeiitic to alkalic volcanism on Kohala volcano, Hawaii. Contrib. Mineral. Petrol. **84**, 390-405.

Fitton, J. G., & Dunlop, H. M., 1985. The Cameroon line, West Africa and its bearing on the origin of oceanic and continental alkali basalt. Earth Planet. Sci. Lett. **72**, 23-38.

Foley, S. F., 1988. The genesis of continental alkaline basalts: an interpretation in terms of redox melting. In Menzies, M. A. & Cox,

K. G. (eds), Oceanic and Continental Lithosphere : Similarities and Differences, J. Petrol., special issue, 139-162.

-----, Taylor, W. R., & Green, D. H., 1986. The effect of fluorine on phase relationships in the system $KAlSiO_4$-Mg_2SiO_4-SiO_2 at 28 kb and the solution mechanism of fluorine in silicate melts. Contrib. Mineral. Petrol. **93**, 46-55.

Frey, F. A., & Green, D. H., 1974. The mineralogy, geochemistry and origin of lherzolite inclusions in Victorian basanites. Geochim. Cosmochim. Acta **37**, 137-155.

----,-----, & Roy, S. D., 1978. Integrated models of basalt petrogenesis : a study of quartz tholeiites to olivine melilitites from South Eastern Australia utilizing geochemical and experimental data. J. Petrol. **19**, 463-513.

----, & Prinz, M. A., 1978. Ultramafic inclusions from San Carlos, Arizona: petrologic and geochemical data bearing on their petrogenesis. Earth Planet Sci. Lett. **38**, 129-76.

Frisch, T., & Wright, J. B., 1971. Chemical composition of high-pressure megacrysts from Nigerian lavas. N. Jahrbuch f. Min. Mon. 289-304.

Fujii, T., & Kushiro, I., 1977. Melting relations and viscosity of an abyssal tholeiite. Carnegie Inst. Washington Yearb. **76**, 461-465.

Fujii, T., Osamura, K, & Takahashi, E., 1986. Effect of water saturation on the distribution of partial melts in the olivine-pyroxene-plagioclase system. J. Geophys. Res. **91-B9**, 9254-9259.

Fujii, T., & Scarfe, C. M., 1985. Compositions of liquids coexisting with spinel-lherzolite at 10 kb and the genesis of MORBs. Contrib. Mineral. Petrol. **90**, 18-28.

Garcia, M. O., Liu, N. W., & Muenow, D. W., 1978. Volatiles in submarine volcanic rocks from the Mariana Island arc and trough. Geochim. Cosmochim. Acta, **43**, 305-312.

Gast, P. W., 1968. Trace element fractionation and the origin of tholeiitic and alkaline magma types. Geochim. Cosmochim. Acta **32**, 1057-1086.

Goto, K., & Arai, S., 1987. Petrology of peridotite xenoliths in lamprophyre from Shingu, southwestern Japan: implications for origin of Fe-rich mantle peridotite. Mineral. Petrol. **37**, 137-155.

Green, D. H., 1964. The petrogenesis of the high temperature peridotite intrusion in the Lizard area, Cornwall. J. Petrol. **5**, 134-188.

-----, 1973a. Conditions of melting of basanite magma from garnet peridotite: Earth Planet. Sci. Lett. **17**, 456-465.

-----, 1973b. Experimental melting studies on a model upper mantle composition at high pressure under water-saturated and water-undersaturated conditions. Earth Planet. Sci. Lett. **17**, 456-465.

-----, & Hibberson, W. O., 1970. Experimental duplication of conditions of precipitation of high pressure phenocrysts in a basaltic magma: Phys. Earth Planet. Inter. **3**, 247-254.

-----, ---------, & Jaques, A. L., 1979. Petrogenesis of mid-ocean ridge basalts., In : Mc Elhinny,M.W. ed., The Earth : Its origin, structure and evolution. London Academic Press, p. 265-299.

-----, & Liebermann, R. C., 1976. Phase equilibria and elastic properties of a pyrolite model for the oceanic upper mantle. Tectonophysics **32**, 61-92.

-----, & Ringwood, A. E., 1967. The stability fields of aluminous pyroxene peridotite and garnet peridotite and their relevance in upper mantle structure. Earth Planet. Sci. Lett. **3**, 151-160.

-----, --------, 1967b. The genesis of basaltic magmas. Contrib. Mineral. Petrol. **15**, 103-190.

-----, --------, 1970. Mineralogy of peridotitic compositions under upper mantle conditions. Phys. Earth Planet. Int. **3**, 359-371.

-----, & Wallace, M. E., 1988. Mantle metasomatism by ephemeral carbonatite melts. Nature **336**, 459-461.

Greenland, L. P., Rose, W. I., & Stokes, J. B., 1985. An estimate of gas emissions and magmatic gas content from Kilauea volcano. Geochim. Cosmochim. Acta **49**, 125-129.

Griffin, W. L., O'Reilly, S. Y., & Stabel, A., 1988. Mantle metasomatism beneath western Victoria, Australia: II. isotopic geochemistry of Cr-diopside lherzolites and Al-augite pyroxenites. Geochim. et Cosmochim. Acta **52**, 449-460.

Gulline, A. B., & Forsyth, S. M., 1976. Tasmanian Geological Atlas Series, Sheet **SK 55-6**: Geological Survey of Tasmania - Department of Mines - Hobart.

Gunn, P. J., 1975. Mesozoic-Cainozoic tectonics and igneous activity : southeastern Australia. J. Geol. Soc. Aust. **22**, 215-221.

Gupta, A. K., Green, D. H., & Taylor, W., 1987. The liquidus surface of the system forsterite-nepheline-silica at 28kb. Am. J. Sci. **287**, 560-565.

Halliday, A. N., Dicken, A. P., Fallick, A. E., & Fitton, J. G., 1988. Mantle dynamics: a Nd, Sr, Pb and O isotopic study of the Cameroon line volcanic chain. J. Petrology. **29**, 181-211.

Harris, D. H., & Anderson, A. T., 1983. Concentrations, sources and losses of H_2O, CO_2 and S in Kilauean basalt. Geochim. Cosmochim. Acta **47**, 1139-1150.

Hart, S. R., & Zindler, A., 1986. In search of a bulk Earth composition. Chem. Geol. **57**, 247-267.

Hergt, J. M., 1987. The origin and evolution of the Tasmanian dolerites (unpublished Ph. D.)

Hill, R., & Roeder, P., 1974. The crystallization of spinel from basaltic liquid as a function of oxygen fugacity. J. Geology **82**, 709-729.

Hodges, F. N., 1974. The solubility of H_2O in silicate melts. Carnegie Inst. Washington Yearb. **73**, 251-258.

Hofmann, A. W., & White, W. M., 1982. Mantle plumes from ancient oceanic crust. Earth Planet. Sci. Lett. **57**, 421-436.

-------, Feigenson, M. D., & Raczek, I., 1984. Case studies on the origin of basalt: III. petrogenesis of the Mauna Ulu eruption, Kilauea, 1969-1971. Contrib. Mineral. Petrol. **88**, 24-35.

Holloway, J. R., & Ford, C. E., 1975. Fluid absent melting of the flurohydroxy-amphibole pargasite. Earth Planet. Sci. Lett. **25**, 44-48.

Irving, A. J., 1974. Megacrysts from the Newer Basalts and other basaltic rocks of southeastern Australia. Geol. Soc. Am. Bull. **85**, 1503-1514.

------, & Green, D. H., 1976. Geochemistry and petrogenesis of the Newer Basalts of Victoria and South Australia. J. Geol. Soc. Aust. **23**, 45-66.

------, & Frey, F. A., 1978. Distributions of trace elements between garnet megacrysts and host volcanic liquids of kimberlitic to rhyolitic composition. Geochim. Cosmochim. Acta **42**, 771-787.

------,----, 1984. Trace element abundances in megacrysts and their host lavas: constraints on partition coefficients and megacryst genesis. Gechim. Cosmochim. Acta **48**, 1201-1221.

Jagoutz, E., Palme, H., Baddenhausen, H., Blum, K., Cendales, M., Dreibus, G., Spettel, B., Lorenz, V., & Wanke, H., 1979. The abundances of major and trace elements in the earth's mantle as derived from primitive ultramafic nodules. Proc. 10th Lunar Planet. Sci. Conf. **2**, 2031-2050.

Jaques, A. L., & Green, D. H., 1980. Anhydrous melting of peridotite at 0-15 kb pressure and the genesis of tholeiitic basalts. Contrib. Mineral. Petrol. **73**, 287-310.

Jeanloz, R., & Morris, S., 1986. Temperature distribution in the crust and mantle. Ann. Rev. Earth Planet. Sci., **14**, 377-415.

Jenkins, D. M., & Newton, R. C., 1979. Experimental determinations of the spinel peridotite to garnet peridotite inversion at 900°C and 1100°C in the system $CaO-MgO-Al_2O_3-SiO_2$, and at 900°C with natural garnet and olivine. Contrib. Mineral. Petrol. **68**, 407-419.

Kato, I., Ringwood, A. E., & Irifune, T., 1988. Experimental determination of element partitioning between silicate perovskites, garnets and liquids : constraints on early differentiation in the mantle. Earth Planet. Sci. Lett. **89**, 123-145.

Kay, R. P., & Gast, P. W., 1973. The rare earth content and origin of alkali basalts. J. Geol. **81**, 653-682.

Killingley, J. S., & Muenow, D. M., 1975. Volatiles from Hawaiian submarine basalts determined by dynamic high temperature mass spectrometry. Geochim. Cosmochim. Acta **39**, 1467-1473.

Knutson, J., & Green, T. H., 1975. Experimental duplication of a high-pressure megacryst/cumulate assemblage in a near-saturated hawaiite. Contrib. Mineral. Petrol. **52**, 121-132.

Kuno, H., & Aoki, K., 1970. Chemistry of ultramafic nodules and their bearing on the origin of basaltic magmas. Phys. Earth Planet. Interiors **3**, 273-301.

Kushiro, I., 1968. Compositions of magmas formed by partial melting of the earths upper mantle. J. Geophys. Res. **73**, 619-634.

-------, 1969. The system forsterite-diopside-silica with and without water at high pressures. Am. J. Sci., Schairer Vol. **267A**, 269-294.

--------, 1972. Effect of water on the composition of magmas formed at high pressures. J. Petrol. **13**, 311-334.

--------, 1980. Changes with pressure of degree of partial melting and K_2O content of liquids in the system $Mg_2SiO_4-KAlSiO_4-SiO_2$. Carnegie Inst. Washington Yearb. **79**, 267-271.

-------, Yoder, H. S., & Nishikawa, M., 1968. Effect of water on the melting of enstatite. Geol. Soc. Am. Bull. **79**, 1685-1692.

La Bas, M. J., 1978. Nephelinite volcanism at plate interiors: Bull. Volcanol. **41-44**, 454-462.

Liotard, J. M., Briot, D., & Boivin, P., 1988. Petrological and geochemical relationships between pyroxene megacrysts and associated alkali-basalts from Massif Central (France). Contrib. Mineral. Petrol. **98**, 81-90.

Llyod, F. E., & Bailey, D. K., 1975. Light element metasomatism of the continental mantle, the evidence and the consequences. Phys. Chem. Earth **9**, 309-416.

Macdonald, G. A., & Katsura, T., 1964. chemical composition of Hawaiian lavas. J. Petrol. **5**, 82-133.

MacGregor, I. D., 1965. The effect of pressure on the minimum melting composition in the system MgO-SiO_2-TiO_2. Carnegie Inst. Yearb. **64**, 135-139.

Mason, B. & Allen, R. O., 1973. Minor and major elements in augite, hornblende, and pyrope megacrysts from Kakanui, New Zealand. N.Z. Journal Geol. Geophys. **16**, 935-947.

Matson, W. M., Muenow, D. W., & Garcia, M. O., 1984. Volatiles in amphiboles from xenoliths, Vulcans's Throne, Grand Canyon, Arizona, USA. Geochim. Cosmochim. Acta **48**, 1629-1636.

Maurel, C., & Maurel, P., 1982. Etude experimentale de la solubilite du chrome dans les bains silicates basiques et de sa distribution entre liquide et mineraux coexistants: conditions d'existence du spinelle chromifere. Bull. Minerall. **105**, 640-647.

McDonough, W. F., McCulloch, M. T., & Sun, S. S., 1985. Isotopic and geochemical systematics in Tertiary-Recent basalts from southeastern Australia and implications for the evolution of the sub-continental lithosphere. Geochim. Cosmochim. Acta **49**, 2051-2067.

McKenzie, D., 1984. The generation and compaction of molten rock. J. Petrol. **25**, 713-765.

Meen, J. K., 1987. Mantle metasomatism and carbonatites; an experimental study of a complex relationship. Geol. Soc. Am. Spec. Paper **215**, 91-100.

Mengel, K., & Green, D. H., 1988. Stability of amphibole and phlogopite in metasomatized peridotite under water-saturated and water-undersaturated conditions. In Kimberlites and Related Rocks **1**, Geological Society of Australia (in press).

Menzies, M. A., & Murthy, V. C., 1980. Nd and Sr isotope geochemistry of hydrous mantle nodules and their host alkali basalts: implications for local heterogeneities in metasomatically veined mantle. Earth Planet. Sci. Lett. **46**, 323-334.

Morimoto, N., 1988. Nomenclature of pyroxenes. Mineralogical Magazine 52, 535-50.

-------, & Wass, S. Y., 1983. CO_3- and LREE-rich mantle below eastern Australia; a REE and isotopic study of alkaline magmas and apatite-rich mantle xenoliths from the Southern Highlands Province, Australia. Earth Planet. Sci. Lett., **65**, 287-302.

Merril, R. B., & Wyllie, P. J., 1975. Kaersutite and kaersutite eclogite from Kakanui, New Zealand - water-excess and water deficient melting to 30 kilobars. Geol. Soc. Am. Bull. **86**, 555-570.

Michael, P. J., 1988. The concentration, behavior and storage of H_2O in the suboceanic upper mantle: implications for mantle metasomatism. Geochim. Cosmochim. Acta **52**, 555-566.

Moore, G. J., 1965. Petrology of deep sea basalt near Hawaii. Am. J. Sci. **263**, 40-52.

-----, 1970. Water content of basalt erupted on the ocean floor. Contrib. Mineral. Petrol. **28**, 272-279.

-----, & Schilling, J., 1973. Vesicles, water, and sulfur in Reykjanes ridge basalts. Contrib. Mineral. Petrol. **41**, 105-118.

Morgan, J. W., 1971. Convection plumes in the lower mantle. Nature **230**, 32-43.

Muenow, D. W., Graham, D. G., & Liu, N. W. K., 1979. The abundance of volatiles in Hawaiian tholeiitic submarine glasses. Earth Planet. Sci. Lett. **42**, 71-76.

Muenow, D. W., Liu, W. K., Garcia, M. O., & Saunders, A. D., 1980. Volatiles in submarine volcanic rocks from the spreading axis of the East Scotia Sea back-arc basin. Earth Planet. Sci. Lett. **43**, 305-312.

Mysen, B. O. R., Arculus, R. J., & Eggler, D. H., 1975. Solubility of carbon dioxide in natural nephelinite, tholeiite and andesite melts to 30 kbar pressure. Contrib. Mineral. Petrol. **53**, 227-239.

Mysen, B. O., & Boettcher, A. L., 1975. Melting of a hydrous mantle, II, Geochemistry of crystals and liquids formed by anatexis of mantle peridotite at high pressures and pressures and temperatures as a function of controlled activities of water, carbon dioxide and hydrogen. J. Petrol. **16**, 549-590.

Navon, O., Hutcheon, I. D., Rossman, G. R., & Wasserburg, G. J., *1988*. Mantle-derived fluids in diamond micro-inclusions. Nature **335**, 784-789.

Nicholls, I. A., 1974. Liquids in equilibrium with peridotitic mineral assemblages at high water pressures. Contrib. Mineral. Petrol. **45**, 289-316.

--------, & Ringwood, A. E., 1973. Effect of water on olivine stability in tholeiites and the production of silica-saturated magmas in the island-arc environment. J. Geology **81**, 285-300.

Nickel, K. G., & Green, D. H., 1984. The nature of the upper-most mantle beneath Victoria, as deduced from ultramafic xenoliths. In Kornprost,J. (ed), Kimberlites II: The Mantle and Crust-Mantle Relationships 161-178.

------,------, 1985. Empirical geothermobarometry for garnet peridotites and implications for the nature fo the lithosphere, kimberlites and diamonds. Earth Planet. Sci. Lett., **73**, 158-170.

Norrish, K., & Chappell, B. W., 1977. X-ray fluorescence spectrometry. In Zussmann, J. (ed.) Physical Methods in Determinitive Mineralogy, p. 201-272. Academic Press, London.

O'Hara, M. J., 1968. The bearing of phase equilibria studies in synthetic and natural systems on the origin and evolution of basic and ultrabasic rocks. Earth Sci. Rev. **4**, 69-113.

------, & Yoder, H. S., 1967. Formation and fractionation of basaltic magmas at high pressures. Scott. J. Geol. **3**, 67-117.

O'Neill, H. St. C, & Wall, V. J., 1987. The olivine-orthopyroxene-spinel oxygen geobarometer, the nickel precipitation curve, and the oxygen fugacity of the earth's upper mantle. J. Petrol., **28**, 1169-1191.

O'Nions, R. K., Hamilton, P. J., & Evenson, N. M., 1977. Variations in $^{143}Nd/^{144}Nd$ and $^{87}Sr/^{86}Sr$ ratios in oceanic basalts. Earth Planet. Sci. Lett., **34**, 13-22.

O'Reilly, S. Y., & Griffin, W. L., 1985. A xenolith derived geotherm for southeastern Australia and its geophysical implications. Tectonophysics, **111**, p. 41-63.

-------,-------, 1988. Mantle metasomatism beneath western Victoria, Australia: I. metasomatic processes in Cr-diopside lherzolites. Geochim. et Cosmochim. Acta, **52**, 433-448.

Poreda, R., Schilling, J. G., & Craig, H., 1986. Helium and hydrogen isotopes in ocean-ridge basalts north and south of Iceland. Earth Planet. Sci. Lett., **78**, 1-17.

Presnall, D. C., Dixon, S. A., O'Donnell, T. H., & Dixon, S. A., 1979. Generation of mid-ocean ridge tholeiites. J. Petrol., **20**, 3-35.

Price, R. C., Gray, C. M., & Frey, F. A., 1988. Geochemistry of plains basalts of the Western Districts volcanics province of Victoria. 9th Australian Geol. Conv. Abst. Volume, p. 330.

Ribe, N. W., 1988. Dynamical geochemistry of the Hawaiian plume. Earth Planet. Sci. Lett., **88**, 37-46.

Richter, F. M., 1986. Simple models for trace element fractionation during melt segregation. Earth Planet. Sci. Lett., **77**, 333-344.

Ringwood, A. E., 1975. Composition and petrology of the Earth's Mantle. 618pp Mc Graw-Hill, New York.

--------, 1982. Phase transformations and differentiation in subducted lithosphere : implications for mantle dynamics, basalt petrogenesis and crustal evolution. J. Geol. **90**, 611-643.

---------, 1986. Dynamics of subducted lithosphere and implications for basalt petrogenesis. Terra Cognita **6**, 67-77.

Robinson, P., Higgins, N. C., & Jenner, G. A., 1986. Determinations of rare-earth elements, yttrium and scandium in rocks by an ion exchange-X-ray fluoresence technique. Chem. Geol., **55**, 121-137.

Rock, N. M. S., 1977. The nature and origin of lamprophyres: some definitions, distinctions, and derivations. Earth Sci. Reviews **13**, 123-169.

Roden, M. F., Frey, F. A., & Francis, D. M., 1984. An example of consequent metasomatism in peridotite inclusions from Nunivak Island, Alaska. J. Petrol., **25**, 546-577.

Roden, M. F., Hart, S.R., Frey, F. A., & Melson, W. L., 1984. Sr, Nd and Pb isotopic and REE geochemistry of St. Paul's Rocks: the metamorphic and metasomatic development of an alkali basalt mantle source. Contrib. Mineral. Petrol., **85**, 376-390.

Roeder, P. L., & Emslie, R. F., 1970. Olivine-liquid equilibria. Contrib. Mineral. Petrol., **29**, 275-289.

Ruoxin, L., Qichen, F., & Jianzhong, S., 1985. Study of garnet lherzolite xenoliths from eastern China. Acta Petrologica Sinica **1**, 24-33.

Ryabchikov, I. D., & Green, D. H., 1978. The role of carbon dioxide in the petrogenesis of highly potassic magmas., In : Problems of petrology of earths crust and upper mantle: Trudy Instituta Geologii Geofizik So An SSR 403 Novosibirsk Nauka Publishers.

Sakai, H., Des Marais, D. J., Ueda, A., & Moore, J. G., 1984. Concentrations and isotope ratios of carbon, nitrogen and sulfur in ocean-floor basalts. Geochim. Cosmochim. Acta **48**, 2433-2441.

Schilling, J-B., Bergeron, M. B., & Evans, R., 1980. Halogens in the mantle beneath the north Atlantic: Phil. Trans. R. Soc. Lond., **A297**, 147-178.

Sen, G., & Presnall, D. C., 1984. Liquidus phase relationships on the join anorthite-forsterite-quartz at 10 kb with applications to basalt petrogenesis. Contrib. Mineral. Petrol. **85**, 404-408.

Skewes, M. A., & Stern, C. R., 1979. Petrology and geochemistry of alkali basalts and ultramafic inclusions from the Palei-aike volcanic field in southern Chile and the origin of the Patagonian plateau lavas. J. Volcanol. Geotherm. Res. **6**, 3-25.

Sleep, N. H., 1984. Tapping of magmas from ubiquitous mantle heterogeneities: an alternative to mantle plumes?. J. Geophys. Res., **89**, 10029-10041.

Stern, C. R., Haung, W., & Wyllie, P. J., 1975. Basalt-andersite-rhyolite-H_2O : crystallization intervals with excess H_2O and H_2O-undersaturated liquidus surfaces to 35 kilobars, with implications for magma genesis. Earth Planet. Sci. Lett. **28**, 189-196.

Stolper, E., 1980. A phase diagram for mid-ocean-ridge basalts : preliminary results and implications for petrogenesis. Contrib. Mineral. Petrol. **74**, 13-27.

-------, & Holloway, J. R., 1988. Experimental determination of the solubility of carbon dioxide in molten basalt at low pressure. Earth & Planet. Sci. Lett. **87**, 397-408.

Stolz, A. J., & Davies, G. R., 1988. Chemical and isotopic evidence from spinel lherzolite xenoliths for episodic metasomatism of the upper mantle beneath SE Australia. In Menzies, M. A., and Cox, K. G. (eds), Oceanic and Continental Lithosphere: Similarities and Differences. J. Petrol., special volume, p. 303-330.

Stuckless, J. S., & Irving, A. J., 1976. Strontium isotope geochemistry of megacrysts and host basalts from southeastern Australia. Geochim. Cosmochim. Acta **40**, 209-213.

Sun, S., 1982. Chemical composition and origin of the earth's primitive mantle. Geochim. Cosmochim. Acta **46**, 179-192.

Sun, S. S., & Hanson, G. N., 1975. Origin of Ross Island basanitoids and limitations upon the heterogeneity of mantle sources for alkali basalts and nephelinites. Contrib. Mineral. Petrol. **52**, 77-106.

Sun, S. S., & Nesbitt, R. W., 1977. Chemical heterogeneity of the Archaean mantle, composition of the Earth and mantle evolution. Earth Planet. Sci. Lett. **35**, 429-448.

Sutherland, F L., 1976. Cainozoic Volcanic Rocks. In: Leaman, D. E., Geological Survey Explanatory Report, Geological Atlas 1:50,000 Series. Sheet 82 (8312S) Hobart.

----------, 1977. Cainozoic Volcanic Rocks. In: Leaman, D. E., Geological Survey Explanatory Report, Geological Atlas 1:50,000 Series. Sheet 75 (8312N) Brighton.

----------, 1984. Cainozoic basalts. In: Fortsyth,S.M. ed., Oatlands, Geol. Surv. Tasm. Explan. Rep.

----------, 1974. High pressure inclusions in tholeiitic basalt and the range of lherzolite-bearing magmas in the Tasmanian volcanic province. Earth Planet. Sci. Lett., **24**, 317-324.

----------, & Wellman, P., 1986. Potassium-argon ages of Tertiary volcanic rocks, Tasmania. Pap. Proc. R. Soc. Tasmania, **120**, 77-86.

----------, Green,D.C. and Wyatt,B.W. ,1973. Age of the Great Lake basalts, Tasmania, in relation to Australian Cainozoic volcanism. J. Geol. Soc. Aust., **20**, 85-93.

----------, Hollis, J. D., & Barron, L. M., 1984. Garnet lherzolite and other inclusions from a basalt flow, Bow Hill, Tasmania. Proc. 3rd Int. Kimberlite Conf. **2**, 145-160.

Takahashi, E., 1980. Melting relations of an alkali-olivine-basalt to 30 kbar and their bearing on the origin of alkali basaltic magmas. Carnegie Inst. Washington Yearb. **79**, 271-276.

Takahashi, E., & Kushiro, I., 1983. Melting of a dry peridotite at high pressures and basalt magma genesis. Contrib. Mineral. Petrol. **73**, 287-310.

Taylor, W. R., & Green, D. H., 1986. Mantle methane and the role of reduced volatiles in 'redox melting' of the mantle. Fourth Int. Kim. Conf. Extended Abstracts: Geol. Soc. Australia Abs. **16**, 211-213.

-----, -----, 1988. Measurement of reduced peridotite-C-O-H solidus and implications for redox melting of the mantle. Nature **332**, 349-352.

------, Stolz, A. J., & Adam, J. D., 1988. Mineralogy and geochemistry of melilite nephelinite and ijolite from Shannon Tier, central Tasmania. 9th Aust. Geol. Conv. Abst. Volume, p. 398.

Thompson, R. N., 1974. Primary basalts and magma genesis. Am. Mineral. **60**, 859-879.

--------, 1982. Magmatism of the British Tertiary Volcanic Province. Scott. J. Geol. **18**, 49-107.

Tronnes, R. G., Takahashi, E., & Scarfe, C. M., 1988. Stability of K-richterite and phlogopite to 14 GPa. EOS **69**, 1510-1511.

Varne, R., 1976. On the origin of spinel lherzolite inclusions in basaltic rocks from Tasmania and elsewhere: J. Petrol. **18**, 1-23.

von Bargen, N, & Waff, H. S., 1986. Permeabilities, interfacial areas and curvatures of partially molten systems: results of numerical computations of equilibrium microstructures. J. Geophys. Res. **91-B9**, 9261-9276.

von Rad, U., Hinz, K., Sarnthein,M., & Seibold, E. (Eds.), 1982. Geology of the northwest African: Springer Verlag.

Wallace, M. E., & Green, D. H., 1988. An experimental determination of primary carbonatite magma composition. Nature, **335**, 343-346.

Ware, N. G., 1981. Computer programs and calibration with the PIBS technique for quantitive electron probe analysis using a lithium-drifted silicon detector. Computers and Geosciences, **7**, 167-184.

Wass, S. Y., & Rodgers, N. W., 1980. Mantle metasomatism - precursor to continental alkaline volcanism. Geochim. Cosmochim. Acta, **44**, 1811-143.

Wedepohl, K. H., 1983. Die chemische Zusammensetzung der basaltishen Gesteine der nordlichen Hessischen Senke und ihrer Umgebung. Geol. Jaharb. Hessen, **62**, 129-139.

Wedopohl, K. H., 1985. Origin of the Tertiary basaltic volcanism in the northern Hessian Depression: Contrib. Mineral. Petrol., **89**, 122-143.

Wellman, P., & McDougall, I., 1974. Cainozoic igneous activity in eastern Australia. Tectonophysics, **23**, 49-65.

Wells, P. R. A., 1977. Pyroxene thermometry in simple and complex systems. Contrib. Mineral. Petrol., **62**, 129-139.

Wilkinson, J. F. G., 1985. Undepleted mantle composition beneath Hawaii. Earth Planet. Sci. Lett., **75**, 129-138.

Winchell, H., 1947. Honolulu Series, Oahu, Hawaii. Geol. Soc. Am. Bull., **58**, 1-48.

Wright, T. L., 1984. Origin of Hawaiian tholeiites: a metasomatic model. J. Geophys. Res., **89-B5**, 3233-3252.

Wyllie, P. J., & Haung, W., 1975. Peridotite, kimberlite, and carbonatite explained in the system $CaO-MgO-SiO_2-CO_2$. Geology **3**, 621-625.

Yoder, H. S., 1976. Generation of basaltic magma. Nat. Acad. Sci., Washington, D.C.

Zharikov, V. A. & Litvin, Y. A., 1985. Experimental studies of

melting in the model ferriferous eclogitic system clinopyroxene-garnet at 40 kbars. Geologicky Zbornic - Geologica Carpathica, 36, 4, Bratislava, p. 387-396.

Zindler, A., Staudigel, H., & Batiza, R., 1984. Isotope and trace element geochemistry of young Pacific seamounts: implications for the scale of upper mantle heterogeneity. Earth Planet. Sci. Lett., **70**, 175-195.

Zindler, A., & Hart, S., 1986. Chemical geodynamics. An. Rev. Earth Planet Sci. **14**, 493-571.